

Tesi di dottorato internazionale in endocrinologia e malattie metaboliche, di Giuseppe Mangiameli, discussa presso l'Università Campus Bio-Medico di Roma in data 27/09/2016.
La disseminazione e la riproduzione di questo documento sono consentite per scopi di didattica e ricerca, a condizione che ne venga citata la fonte.



UNIVERSITA' CAMPUS BIO-MEDICO DI ROMA

FACOLTA' DIPARTIMENTALE DI MEDICINA E CHIRURGIA

INTERNATIONAL PhD

IN ENDOCRINOLOGY AND METABOLIC DISEASE

XXVIII CYCLE

Phd THESIS

NEW PERSPECTIVES, MANAGEMENT AND PROBLEMS

ASSOCIATED

WITH THYROID CANCER TREATMENT

Dr. Giuseppe Mangiameli

Chair: Professor Paolo Pozzilli

Co-Chair: Dottoressa Anna Crescenzi

2016

Tesi di dottorato internazionale in endocrinologia e malattie metaboliche, di Giuseppe Mangiameli, discussa presso l'Università Campus Bio-Medico di Roma in data 27/09/2016.
La disseminazione e la riproduzione di questo documento sono consentite per scopi di didattica e ricerca, a condizione che ne venga citata la fonte.

A Daniela

TABLE OF CONTENTS

SECTION I. NEW PERSPECTIVES OF DEVELOPMENT IN THYROID CANCER

GENERAL SECTION: THYROID CANCER

1.1 Classification.....	pag. 5
1.1.1 Papillary Carcinoma (PTC).....	pag. 5
1.1.2 Follicular Carcinoma (FTC).....	pag. 7
1.1.3 Anaplastic Carcinoma (ATC).....	pag. 9
1.1.4 Medullary Carcinoma (MTC).....	pag. 9
1.2 Incidence and risk factors for thyroid cancer.....	pag. 10
1.3 Diagnostic Criteria.....	pag. 14
1.4 Molecular pathways in thyroid cancer.....	pag. 15
1.4.1 MAPK pathway.....	pag.17
1.4.2 (PI3K)/AKT pathway.....	pag. 18
1.4.3 Additional genes mutated.....	pag. 18

SPECIAL SECTION: RAMAN SPECTROSCOPY

1.5 Raman spectroscopy.....	pag. 21
1.5.1 Raman spectroscopy technique.....	pag. 22
1.5.2 The role of Raman spectroscopy for cancer diagnosis.....	pag 24
1.5.3 Raman spectroscopy in thyroid cancer.....	pag. 31
1.5.4 Limitations of Raman spectroscopy.....	pag. 36
1.6 Clinical application of Raman spectroscopy for thyroid cancer diagnosis	
1.6.1 Materials and methods.....	pag. 39
1.6.2 Results.....	pag. 44

1.6.3 Conclusion.....pag. 59

SECTION II. MANAGEMENT AND PROBLEMS ASSOCIATED WITH THYROID CANCER TREATMENT

GENERAL SECTION: THYROID CANCER TREATMENT

2.1 Surgical treatment.....pag. 63

 2.1.1 Total thyroidectomy vs Lobectomy.....pag. 63

 2.1.2 Lymph node surgery.....pag. 66

2.2 Complication related with surgical treatment.....pag. 69

SPECIAL SECTION: POSTOPERATIVE HYPOCALCEMIA AND TERIPARATIDE

2.3 Postoperative hypocalcemia.....pag. 73

2.4 Management of Postoperative hypocalcemia.....pag. 74

2.5 Teriparatide for the prevention of post-surgical hypocalcemia: thypos trial

 2.5.1 Materials and methods.....pag. 75

 2.5.1.1 Screening.....pag. 76

 2.5.1.2 Patient enrollment.....pag. 77

 2.5.1.3 Sample size calculation and statistical analysis.....pag. 79

 2.5.2 Results: prospective phase II randomized open label trial.....pag. 79

 2.5.3 Conclusion.....pag. 83

ACKNOWLEDGEMENTS.....pag. 87

SECTION I. NEW PERSPECTIVES OF DEVELOPMENT IN THYROID CANCER

GENERAL SECTION: THYROID CANCER

1.1 Classification

Thyroid cancer is the most common malignant endocrine tumor, but represents only about 1% of all malignancies. Most primary thyroid cancers are epithelial tumors that originate from thyroid follicular cells. These cancers develop three main pathological types of carcinomas: papillary thyroid carcinoma (PTC), follicular thyroid carcinoma (FTC), and anaplastic thyroid carcinoma (ATC). Medullary thyroid carcinoma (MTC) arises from thyroid parafollicular (C) cells.

The main histologic types of thyroid carcinoma can be resumed:

1. Differentiated (PTC, FTC).
2. Medullary (MTC)
3. Anaplastic (ATC)

PTC and FTC are categorized as differentiated thyroid cancer (DTC) because of well differentiation and indolent tumor growth. PTC consists of 85-90% of all thyroid cancer cases, followed by FTC (5-10%) and MTC (about 2%). ATC accounts for less than 2% of thyroid cancers and typically arises in the elder patients.

1.1.1 Papillary thyroid carcinoma (PTC)

PTC is a major differentiated adenocarcinoma which consists of 90% of thyroid cancers and shows papillary proliferation pathologically. Most cases have excellent prognosis but approximately 10% of PTC patients undergo recurrences such as lymph node recurrence and lung metastasis. Selecting such high risk patients is the most important challenge as well as treatment of radioiodine refractory PTC. Clinicopathologically, age>45 years, large tumor size, extra thyroidal invasion, distant metastasis, vascular invasion and poor differentiated histology are well known detrimental prognostic factors.¹

PTC is usually gray-white color and shows a variety of gross appearance such as tumors with central scar and infiltrative borders, encapsulated tumor and lesional calcification (Figure 1A). Nearly half of PTCs have multifocal lesions and regional lymph node metastasis. These characteristics do not affect long-term survival.²

Most of PTCs shows papillary growth pattern but nuclear features are more important diagnostic hallmark which are common in almost all cases than such growth pattern itself (Figure 1B). The nuclear appearances of PTC are clear, ground glass, or Orphan-Annie eyed.³ These nuclei are larger than normal follicular nuclei and overlapping each other. The nuclei contain eosinophilic inclusions and have longitudinal grooves.⁴ These nuclear features are important characteristics of PTC but not specific. Indeed, chronic thyroiditis frequently shows similar intranuclear inclusions or nuclear grooves as well as follicular adenoma.⁵

Several subtypes are thought to be associated with either favorable or aggressive phenotype although it is still controversial. The most common variants are: follicular variant, tall cell variant, diffuse sclerosis variant, and solid variant.

A certain part of follicular variant of papillary carcinoma (FVPTC) was classified as FTC or follicular adenoma in the past. The nuclei of this variant rarely have all of the features of PTC (eg. rare nuclear groove). Accordingly, FVPTCs are often diagnosed as indeterminate cytology in contrast to high diagnostic accuracy of usual PTC. FVPTC is recognized by its follicular structure with papillary cytology, and composed of 2 subtypes; diffuse/invasive (infiltrative) and encapsulated type. FVPTC is associated with favorable prognosis especially if tumor is encapsulated.⁶ Diffuse/invasive subtype has similar clinical features to usual PTC. Diagnosis of encapsulated subtype is still under debate since this subtype shows no invasion or incomplete nuclear characteristics. This encapsulated subtype is slowly growing and conservative treatment may be warranted.⁷

Tall cell variant composes 10% of PTC, and have a 10-year mortality rate of up to 25%, less favorable prognosis than usual PTC. This variant is often associated with poor prognostic characteristics such as elder age, extra thyroidal invasion, and high mitotic rate. The tall cells are twice as tall as its width, and should occupy >50% of papillary carcinoma cells.⁵

The diffuse sclerosis variant is 3% of PTC, which infiltrates the entire thyroid gland and is associated with younger age.⁸ Presence of many psammoma bodies is one of hallmarks of this variant. Extensive calcification causes exceedingly firm tumor. Background thyroid of this variant shows chronic lymphatic thyroiditis with lymphocytic infiltration, resembling Hashimoto disease.⁹ This variant PTC often shows extra thyroidal extension and regional lymph node metastasis at diagnosis leading to decreased recurrence free survival although mortality is low.¹⁰ Solid variant PTC is diagnosed when solid growth represents more than 50% of tumor. This variant is commonly seen in children and often associated with secondary PTC patients after the Chernobyl nuclear accident.¹¹ Both lymphatic and venous invasion are frequently observed in this variant.¹² Some studies reported that the solid variant is associated with poor prognosis whereas others considered the prognosis of this variant is almost as good as usual PTC.^{13, 14}

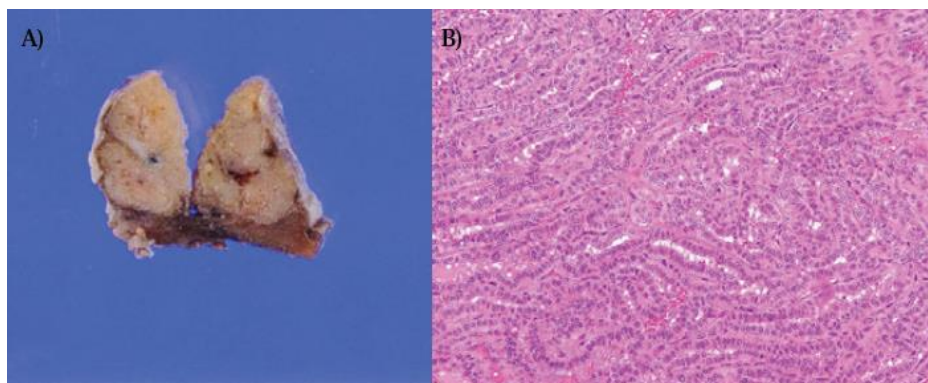


Figure 1. Typical image of papillary thyroid carcinoma
Macroscopic (A) (scale bar = 10 mm) and microscopic (B) (H&E, x200) features of PTC

1.1.2 Follicular thyroid carcinoma (FTC)

FTC represents 5-15% of thyroid cancer with follicular differentiation but no papillary nuclear characteristics.⁵ FTC is a solitary encapsulated tumor with gray-tan-pink color, usually focal hemorrhage. FTC is diagnosed by follicular cell invasion of the tumor capsule and/or blood vessels. Vascular invasion leads to worse prognosis than capsular infiltration alone.¹⁵ Majority of FTCs are minimally invasive with slight tumor capsular invasion alone (Figure 2). These minimally

invasive FTCs are similar appearance to follicular adenomas and rarely cause distant metastasis.¹⁶ Accordingly, a minimally invasive FTC is difficult to distinguish from a follicular adenoma in cytology or frozen section, and can be diagnosed only after thyroidectomy. Widely invasive FTC is much less common but ~80% of these tumors cause distant metastasis, leading to high mortality rate at around 20%.⁵ The poor prognostic factors are distant metastasis, age >45 years, large tumor size, extensive vascular invasion, extra thyroidal extension, and widely invasive tumors.¹⁷

Hürthle cell carcinoma (oxyphilic cell carcinoma) is presumed to be a variant of FTC but its prognosis is thought to be worse than usual FTC.^{18,19} A variant of papillary carcinoma is rare and have similar prognosis as FTC.²⁰ More than 75% follicular cells with oncocyctic characteristics are included in Hürthle cell tumor.²¹ Oxyphilic or oncocyctic cells are characterized by its polygonal shape, eosinophilic granular cytoplasm, hyperchromatic or vesicular nuclei with large nucleolus, and abundant mitochondria.

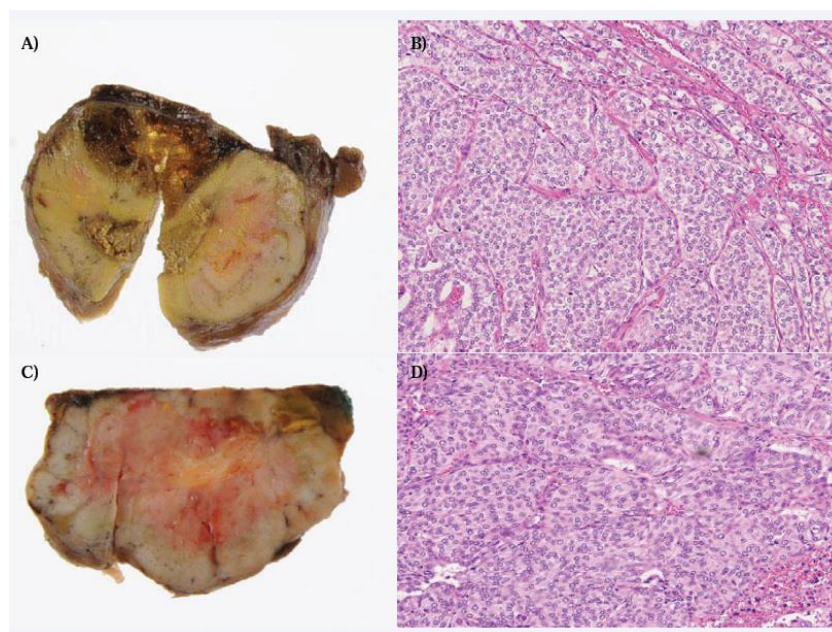


Figure 2. Typical images of follicular thyroid carcinoma

Macroscopic (A) (scale bar = 10 mm) and microscopic (B) (H&E, x200) images of minimally invasive (A and B) or widely invasive (C and D) FTC.

1.1.3 Anaplastic thyroid carcinoma (ATC)

ATC is extremely aggressive undifferentiated tumor, with almost 100% disease-specific mortality²², representing about 40% thyroid cancer deaths by only <2% of thyroid cancers. The median survival from diagnosis is around 6 months.²³ ATC extensively invades into surrounding structures, and distant metastases are observed at diagnosis in one-third of ATC patients. Peak age of patients is older than that of DTCs and >70% of patients are women.²⁴ Approximately 50% of ATC patients have prior or concurrent DTC. It is suggesting that ATC emerges as a result of de-differentiation of DTC. In contrast to DTC, ATC usually does not uptake iodine, leading to refractoriness against radioiodine treatment. Although clinically apparent ATCs are usually unresectable, intrathyroidal ATCs are surgically resectable and such radical resection offers better outcomes.²⁵ ATC shows extremely invasive large solid tumor with necrosis and hemorrhage (Figure 3). Large, pleomorphic giant cells resembling osteoclasts is one of hallmarks of ATC cells.²⁶ ATC is composed of spindle cells and squamoid cells.

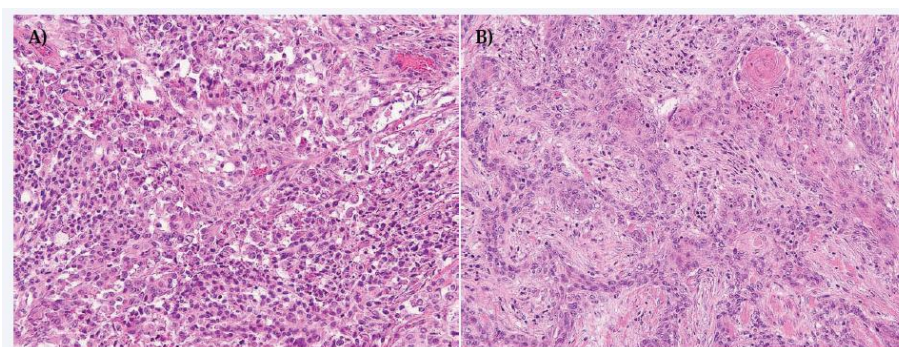


Figure 3. Anaplastic thyroid carcinoma

Microscopic images of 2 cases of ATC (H&E, x200).

1.1.4 Medullary thyroid carcinoma (MTC)

MTC represents less than 5% of thyroid carcinomas, which is neuroendocrine tumor originated from C cells of ultimobranchial body of neural crest and secretes calcitonin. Seventy to eighty percent of MTCs are sporadic while 20-30% of MTCs are familial. Familial MTCs are all autosomal dominant inheritance of germ line RET mutations and classified to 3 categories; multiple endocrine neoplasia 2A

(MEN2A), multiple endocrine neoplasia 2B (MEN2B), and familial medullary thyroid carcinoma (FMTC).²⁷ Peak age of familial MTC is younger (approximately 35 years) than that of sporadic MTC (40-60 years). The overall 5-year survival of patients with MTC is 86%. Poor prognostic factors include older age, advanced stage, the presence of lymph node metastasis at diagnosis, and somatic RET mutation.²⁸ Sporadic MTC is usually solitary whereas most of familial MTC exhibit bilateral, multicentric foci.

MTCs typically exhibit gray-tan color, firm, solid tumors and do not have a well-formed capsule. Tumor includes high concentration of C cells. MTC cells are round to oval, spindle, or polyhedral. Broad fibrovascular bands separate tumors into nodules (Figure 4). The nuclei are round to oval with salt-and-pepper nuclear chromatin. Amyloid deposits from calcitonin are frequently present in stroma. A background of C cell hyperplasia is observed in familial but not in sporadic MTCs.

29

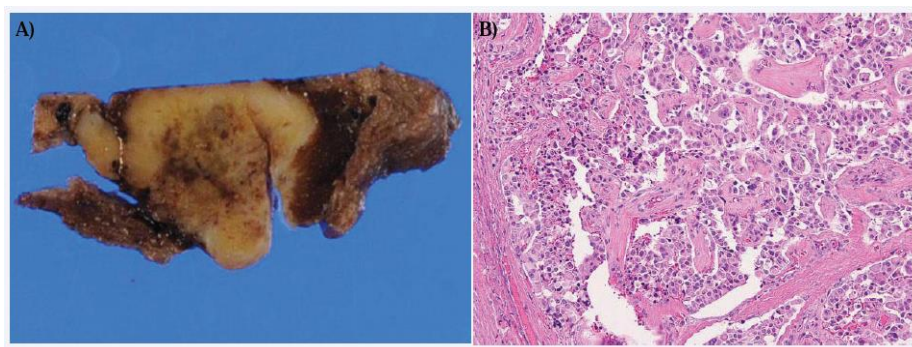


Figure 4. Medullary thyroid carcinoma

Macroscopic (A) (scale bar = 10 mm) and microscopic (B) (H&E, x200) features of MTC

1.2 Incidence and risk factors for thyroid cancer

The annual incidence of thyroid cancer varies considerably by geographic area, age and sex. An average of 58.629 patients per year were diagnosed with thyroid carcinoma from 2008 to 2012. Of these 58.629 patients, 89% had papillary

carcinoma, 5.1% had follicular carcinoma, 2.2% had Hurthle cell carcinoma, 1.7% had medullary carcinoma, and 0.8% had anaplastic carcinoma.³⁰

In 2016, It is estimated that 64,300 new cases of thyroid cancer were predicted to be diagnosed in 2016 compared with 37,200 in 2009 when the last ATA guidelines. In the same year approximately 1980 cancer deaths will occur among persons with thyroid carcinoma in the United States. Anaplastic carcinoma is almost uniformly lethal; however, most thyroid carcinoma deaths are from papillary, follicular and Hurthle cell carcinoma, which account from nearly 95% of all thyroid carcinoma cases.³¹

The yearly incidence has nearly tripled from 4.9 per 100,000 in 1975 to 14.3 per 100,000 in 2009. Almost the entire change has been attributed to an increase in the incidence of papillary thyroid cancer (PTC). Moreover, 25% of the new thyroid cancers diagnosed in 1988–1989 were ≤ 1 cm compared with 39% of the new thyroid cancer diagnoses in 2008–2009.³²

The reported escalating incidence during the last decades all over the globe is mainly due to an increase in micropapillary (<2 cm) histotype, while there is no substantial change in the incidence of the less common histological categories: follicular, medullary and anaplastic cancers.³³

This tumor shift (>5% per year in both men and women) may be due to the increasing use of neck ultrasonography or other imaging and early diagnosis and treatment³⁴, trends that are changing the initial treatment and follow-up for many patients with thyroid cancer.

A recent population-based study from Olmsted County reported the doubling of thyroid cancer incidence from 2000 to 2012 compared to the prior decade as entirely attributable to clinically occult cancers detected incidentally on imaging or pathology.³⁵ Another recent study estimated that over the past 2 decades, about one-half of all papillary thyroid cancers diagnosed in women, and 40% of those in men aged ≤ 50 years, were clinically irrelevant.³⁶

It is common experience in thyroid cancer referral centers that nearly 60%–80% of thyroid carcinomas detected nowadays are micropapillary thyroid carcinomas (<1 cm in size) carrying an excellent long-term prognosis.³⁷

However, increases across tumor size and stage, as well as for follicular carcinoma (a more aggressive subtype), suggest that some of the rise may be due to changes in environmental risk factors, such as obesity.^{38,39}

More recently, an increased incidence for all size of thyroid tumor has been reported in the USA. During 1997–2005, the annual percentage change (APC) for primary tumor <1.0 cm was 9.9 in man and 8.6 in women. A substantial increase was also observed for tumor >4 cm among men (1988–2005: APC 3.7) and women (1988–2005: APC 5.7).⁴⁰ These data suggested that increased diagnostic scrutiny is not the only explanation, and environmental influence should also be considered.

The only established environmental risk factor for thyroid carcinoma is exposure to ionizing radiation, and the risk, particularly of papillary carcinoma, is greater in subjects of younger age at exposure. An increased incidence of thyroid cancer in children and adolescents was observed in Ukraine, Belarus and certain regions of Russia as early as 4 years after the Chernobyl accident. The pre-Chernobyl incidence of thyroid cancer in Ukrainian children was very low (0.5–1.0 per 1 000 000 children). Following the explosion of the Chernobyl nuclear reactor in 1986, a dramatic increase in the incidence of benign and malignant thyroid tumors (80 times more) was observed in children born or conceived around the time of the accident in a wide area surrounding the reactor.⁴¹

In addition to environmental factors, genetic factors are involved in thyroid cancer predisposition.

As previously mentioned, the increased incidence of thyroid cancer diagnoses has been attributed, in part, to improved detection of small or subclinical thyroid nodules on thyroid ultrasonography and by other imaging techniques; however, increased incidence of thyroid tumors of all sizes has also been reported. The increased number of cases of papillary thyroid cancer is predominantly of follicular variant, RAS mutation positive tumors, suggesting a potential role for environmental (chemical/dietary) factors.⁴²

Aside from the well-characterized familial forms of medullary thyroid cancer, non-medullary thyroid cancer in a first-degree relative increases the risk 4-10 fold higher than in the general population.^{43,44} Familial non-medullary thyroid cancer is characterized by autosomal dominant inheritance with reduced penetrance, and has

been estimated to account for approximately 5-10% of all thyroid cancers.⁴⁵ Genetic linkage studies have mapped susceptibility loci to several regions including 1q21, 2q21, 8p23, 8q24, 9q22, 14q31, and 19p13.^{46,47, 48, 49,50, 51, 52.} Definitive germline genetic mutations underlying thyroid cancer predisposition remain yet to be identified within candidate genes in these regions. Thyroid tumor development likely involves a complex interplay between genetic predisposition and environmental risk factors.⁵³

The incidence of thyroid cancer is about three to four times higher among females than males worldwide, ranking the sixth most common malignancy diagnosed in women. By 2019, one study predicts that PTC will become the third most common cancer in women at a cost of \$19–21 billion in the United States.⁵⁴ Optimization of long term health outcomes and education about potential prognosis for individuals with thyroid neoplasms is critically important.

Among women, papillary thyroid cancer incidence rates are higher among Asians (10.96 per 100 000 woman-years) and lower among blacks (4.9 per 100 000 woman-years). Among men, papillary thyroid cancer incidence rates are higher among whites (3.58 per 100 000 woman-years) and lower among blacks (1.56 per 100 000 woman-years).⁵⁵

The incidence of follicular thyroid cancer in the USA is 0.82 per 100 000 person-years, with rates of 1.06 per 100 000 woman-years and 0.59 per 100 000 man-years. The incidence of follicular cancer does not vary substantially by race/ethnicity.⁵⁵ The incidence rates of medullary thyroid cancer (MTC) and anaplastic thyroid cancer (ATC) are 0.11 and 0.21 per 100 000 person years with no noted substantial differences by race/ethnicity and sex, respectively.⁵⁵

Thyroid cancer can occur at any age but it is rare in childhood. Most tumors are diagnosed during third to sixth decade of life. The age-adjusted death rate was 0.5 per 100 000 men and women per year, increasing from 0.1% under age 20%–30% in the seventh and the eighth decades.⁵⁶

Despite increasing incidence, the mortality from thyroid cancer has tended to decline over the last three decades. It is unclear how much of the decline in mortality is due to better diagnosis rather than to improved treatment of thyroid neoplasm.

The 5-year relative survival rates reported for patients with papillary and follicular carcinomas (stages I-II) are 98% and 90% respectively.⁵⁷

1.3 Diagnostic Criteria

Thyroid cancer presents as a thyroid nodule detected by palpation and more often by neck US. Thyroid nodules are a common clinical problem. While thyroid nodules are common (4%–50% depending on the diagnostic procedures and patients' age)⁵⁸, thyroid cancer is rare (~ 5% of all thyroid nodules). Epidemiologic studies have shown the prevalence of palpable thyroid nodules to be approximately 5% in women and 1% in men living in iodine-sufficient parts of the world.^{59,60}

Thyroid high-resolution ultrasound (US) is a widespread technique that is used as a first-line diagnostic procedure for detecting and characterizing nodular thyroid disease (I, A). The US can detect thyroid nodules in 19%–68% of randomly selected individuals, with higher frequencies in women and the elderly.^{61,62}

The clinical importance of thyroid nodules rests with the need to exclude thyroid cancer, which occurs in 7%–15% of cases depending on age, sex, radiation exposure history, family history, and other factors.^{63,64}

According to last guidelines published by ATA in 2016 a diagnostic thyroid/neck US should be performed in all patients with a suspected thyroid nodule, nodular goiter, or radiographic abnormality suggesting a thyroid nodule incidentally detected on another imaging study.⁶⁵

US features associated with malignancy are hypoechogenicity, microcalcifications, absence of peripheral halo, irregular borders, solid aspect, intranodular blood flow and shape (taller than wide). Each of these patterns taken individually is poorly predictive. When multiple patterns suggestive of malignancy are simultaneously present in a nodule, the specificity of US increases but the sensitivity becomes unacceptably low.^{66,67}

The pattern of sonographic features associated with a nodule confers a risk of malignancy, and combined with nodule size, guides FNA decision-making (see Recommendation 8 of ATA guidelines).^{68,69}

Fine needle aspiration cytology (FNAC) is an important technique that is used along with US for the diagnosis of thyroid nodules. FNA is the procedure of choice in the

evaluation of thyroid nodules, when clinically indicated. FNAC should be performed in any thyroid nodule >1 cm and in those <1 cm if there is any clinical (history of head and neck irradiation, family history of thyroid cancer, suspicious features at palpation, presence of cervical adenopathy) or ultrasonographic suspicion of malignancy. In the case of multinodular goiter, those with suspicious features at US should be submitted to FNAC. FNAC is a very sensitive tool for the differential diagnosis of benign and malignant nodules although there are limitations: inadequate samples and follicular neoplasia. In the event of inadequate samples, FNAC should be repeated, while in the case of follicular neoplasia, with normal thyroid stimulating hormone (TSH) and 'cold' appearance at thyroid scan, surgery should be considered.⁷⁰

The use of various immunohistochemical markers in cytologic samples to differentiate papillary thyroid carcinoma from other follicular derived lesions of thyroid has been explored during the last years but none of the markers appears to be specific enough to be employed as the diagnostic marker for the cytologic diagnosis of papillary thyroid carcinoma.⁷⁰ Recently, it has been reported that by molecular testing for thyroid nodules (BRAF, RAS, RET/PTC and PAX8/PPAR γ mutations), the presence of any mutation was a strong indicator of cancer because ~ 97% of mutation-positive nodules had malignant diagnosis at histology.^{71,72} Thyroid function test and thyroglobulin (Tg) measurement are of little help in the diagnosis of thyroid cancer. However, measurement of serum calcitonin (CT) is a reliable tool for the diagnosis of the few cases of MTC (5%–7% of all thyroid cancers) and has higher sensitivity compared with FNAC. For this reason, measurement of CT should be an integral part of the diagnostic evaluation of thyroid nodules.⁷⁰

1.4 Molecular pathways in thyroid cancer

Thyroid nodules are common, and the accurate diagnosis of cancer or benign disease is important for the effective clinical management of these patients. Molecular markers are a helpful diagnostic tool, particularly for cytologically indeterminate thyroid nodules. In the past few years, significant progress has been

made in developing molecular markers for clinical use in fine needle aspiration (FNA) specimens, including gene mutation panels and gene expression classifiers. With the availability of next generation sequencing technology, gene mutation panels can be expanded to interrogate multiple genes simultaneously and to provide yet more accurate diagnostic information. In addition, recently several new molecular markers in thyroid cancer have been identified that offer diagnostic, prognostic, and therapeutic information that could potentially be of value in guiding individualized management of patients with thyroid nodules.

From the 1990s, when pathogenesis of only approximately 25% of thyroid cancers was understood, to the present, when genes involved in the pathogenesis of greater than 90% of thyroid cancers have been described, much progress has been made in elucidating the molecular mechanisms underlying thyroid cancer (Fig. 5). This progress provides the basis upon which new diagnostic and prognostic markers, as well as new targeted therapies, have been developed.

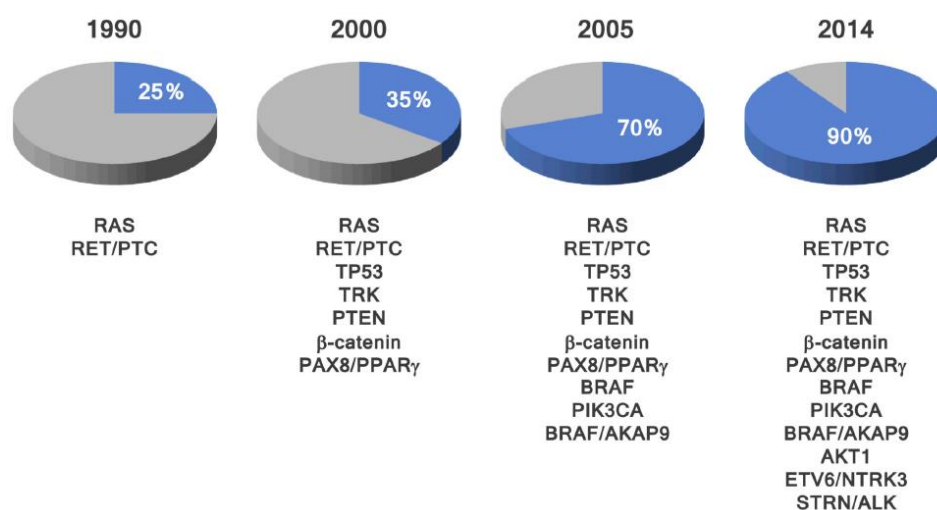


Figure 5. Progress in identifying mutational markers in thyroid cancer

The molecular pathogenesis of the majority of thyroid cancer involves dysregulation of the mitogen-activated protein kinase (MAPK) and phosphatidylinositol-3 kinase (PI3K)/AKT signaling pathways (Figure. 6).

1.4.1 MAPK pathway

The MAPK pathway is frequently activated in thyroid cancer through point mutations of the BRAF and RAS genes and RET/PTC and TRK rearrangements.^{73,74,75,76} Point mutation in BRAF is found in approximately 45% of papillary thyroid cancers.⁷⁷

BRAF is a serine-threonine kinase which, upon activation by RAS, activates MEK and leads to activation of downstream effectors of the MAPK pathway. In nearly all cases (98-99% of cases) activating point mutations of BRAF involve codon 600 and result in the V600E mutation, and in 1-2% of cases other BRAF mutations such as the K601E mutation, small in-frame insertions or deletions, or BRAF rearrangement can occur.^{78, 79}

RAS genes (HRAS, KRAS, and NRAS) are G proteins that signal to both the MAPK and PI3K/AKT pathways. Point mutations in the RAS genes typically occur in codons 12, 13, and 61, and are found in 40-50% of follicular carcinomas and in 10-20% of papillary thyroid carcinomas.^{80, 81, 82} RAS-mutated papillary thyroid carcinomas typically are of the follicular variant.^{83, 84} RAS mutations are also seen in 20-40% of follicular adenomas.^{85, 86, 87, 88} Whereas NRAS, HRAS and KRAS mutations are found in follicular-cell derived thyroid tumors, mutations in HRAS and KRAS also occur in medullary thyroid cancers.⁸⁹

The RET gene is a receptor tyrosine kinase that is expressed in thyroid C cells, but not in follicular cells. The RET gene can be activated by fusion with various partners that drive the expression of the 3' portion of the RET gene coding for the tyrosine kinase domain of the receptor, and provide the dimerization motif to lead to the constitutive activation of RET kinase. The most common rearrangement types are RET/PTC1 (formed by fusion of RET with the CCDC6 gene) and RET/PTC3 (formed by fusion of RET with the NCOA4 gene).^{90, 91} The RET/PTC1 and RET/PTC3 rearrangements are found in 10-20% of papillary thyroid carcinomas, and their incidence is progressively decreasing (Jung et al. 2013).⁹² These rearrangements are found at higher frequencies in children/young adults and in patients with a history of radiation exposure.^{93, 94} In addition to rearrangements

involving RET which are found in papillary thyroid tumors, the RET gene is commonly found to be mutated in medullary thyroid carcinomas, in both familial and sporadic cases.^{95, 96}

The PAX8/PPAR γ rearrangement, a fusion between a paired domain transcription factor and the peroxisome proliferator-activated receptor genes, is found in 30-40% of follicular carcinomas. The PAX8/PPAR γ rearrangement can also be seen, at lower prevalence, in the follicular variant of papillary thyroid carcinoma and in follicular adenomas.^{97, 98}

1.4.2 (PI3K)/AKT pathway

The importance of the PI3K/AKT pathway in thyroid tumorigenesis has been increasingly recognized in the last decade. The PI3K/AKT pathway can be activated by activating mutations in PIK3CA and AKT1 as well as by inactivation of PTEN, which negatively regulates this pathway (Figure. 6). Somatic mutations of PTEN have been reported in follicular thyroid tumors and anaplastic thyroid carcinoma, and germline mutations of PTEN can result in follicular thyroid tumors arising in patients with Cowden syndrome.^{99, 100} Activating mutations in PIK3CA typically occur at hotspots within exon 9 and exon 20 and have been reported in follicular thyroid carcinomas, poorly differentiated thyroid carcinomas, and anaplastic thyroid carcinomas.¹⁰¹ AKT1 mutations have been reported in metastatic thyroid cancer.¹⁰²

1.4.3 Additional genes mutated (TERT)

Additional genes mutated in thyroid cancer include TP53 and CTNNB1 (beta-catenin), ETV6/NTRK3, STRN/ALK, and TERT.

TP53 is a tumor suppressor that plays important roles in cell cycle regulation and DNA repair and CTNNB1 is involved in Wnt signaling. These genes tend to be mutated in more aggressive and advanced thyroid tumors.¹⁰³ In addition to these well characterized mutations, mutations in thyroid stimulating hormone receptor (TSHR) and GNAS have also been shown to play a role in thyroid tumorigenesis.

In addition to the *RET/PTC* and *PAX8/PPAR γ* rearrangements which are found in approximately 15% of thyroid tumors, many other gene fusions have been described such as rearrangements involving *NTRK* or *BRAF*. Fusion of *BRAF* with A kinase anchor protein 9 (*AKAP9*) is a rearrangement rarely found in sporadic thyroid cancer, although it also occurs at higher frequencies (up to 11%) in patients with a history of radiation exposure.¹⁰⁴ *NTRK1* is a receptor tyrosine kinase and when rearranged with one of 3 potential fusion partners, activates MAPK pathway signaling.^{105,106} *NTRK1* rearrangements are found in approximately 1-5% of papillary thyroid carcinomas and in higher frequencies in patients with radiation exposure. More recently, whole-transcriptome (RNA-Seq) analyses led to the discovery of novel gene fusions in thyroid cancer. RNA-Seq analysis of radiation-associated thyroid cancer identified a novel *ETV6-NTRK3* chromosomal rearrangement, which occurs in 2% of sporadic papillary thyroid cancers and 14.5% of radiation-associated tumors.¹⁰⁷ Another interesting gene fusion with therapeutic implications was recently identified by RNA-Seq analysis of aggressive forms of thyroid cancer. The fusion of the striatin (*STRN*) gene and anaplastic lymphoma kinase (*ALK*) gene were found in 9% of poorly differentiated thyroid cancers, 4% of anaplastic thyroid cancers, and 1.2% of well-differentiated papillary thyroid cancer.¹⁰⁸

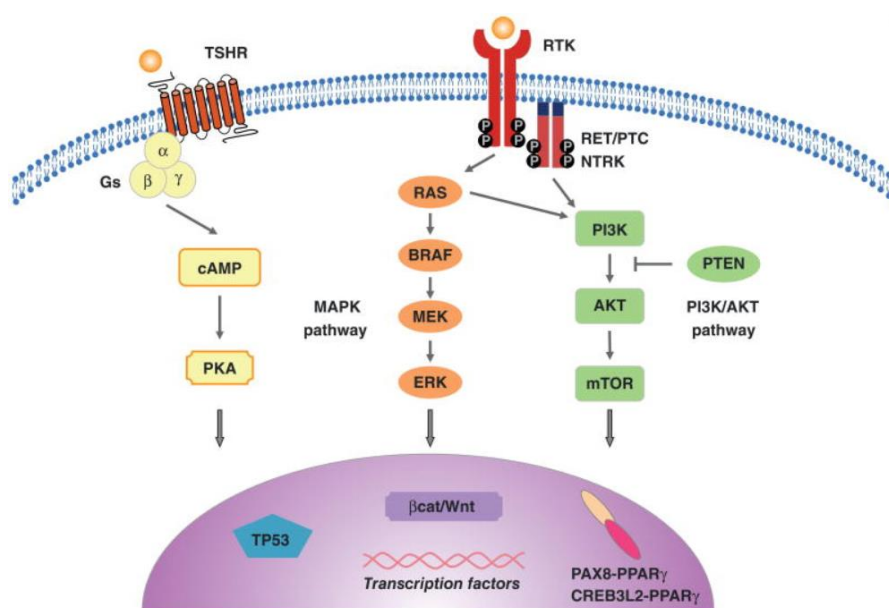


Figure 6. Molecular pathways in thyroid cancer

In addition to the above mentioned markers, another recently discovered molecular marker is mutation of the telomerase reverse transcriptase (TERT) promoter. Telomerase, a reverse transcriptase that maintains telomere length at the end of chromosomes, plays a key role in cellular immortality and tumorigenesis. Telomerase is usually absent in non-immortalized cells but is expressed at functionally significant levels in the vast majority of human cancer cells, enabling their replicative immortality.¹⁰⁹ The TERT gene encodes the reverse transcriptase component of the telomerase complex, and its overexpression in mouse models, such as in K5-Tert transgenic mice, leads to an increased incidence of cancer.^{110, 111} Telomerase is not expressed in most normal tissues, but is frequently activated in tumor cells.¹¹² Maintenance of telomere length, either through telomerase activation or a recombination based mechanism known as alternative lengthening of telomeres (ALT), is required for immortalization of cancer cells. Recently two mutations in the promoter of TERT (chr5:1295228C>T, termed C228T, and chr5:1295250C>T, termed C250T) were discovered in melanoma and were found to result in increased transcriptional activity of the promoter.^{113, 114} The C228T and C250T TERT promoter mutations were also detected in follicular cell-derived thyroid cancers but were absent in benign lesions and in medullary thyroid cancers.¹¹⁵ The C228T and C250T mutations have a significantly higher prevalence in aggressive thyroid tumors including widely invasive oncocytic carcinoma and anaplastic thyroid carcinoma.^{116, 117} Interestingly, TERT mutations in some studies were found to be more common in tumors with BRAF V600E mutation, which may suggest a possible synergistic interplay between MAPK pathway activation and telomerase activation to promote aggressive tumor behaviour.¹¹⁸ In a recent large study of 469 patients with a mean follow-up of 8 years the role of TERT promoter mutations was investigated. In this study TERT mutations were identified in 7,5% of papillary carcinomas, in 17,1% of follicular carcinomas, in 29% of poorly differentiated thyroid carcinoma and in 33,3% of anaplastic thyroid carcinomas. The authors conclude that TERT promoter mutations were found to be an independent risk factor for persistent disease, distant metastases, and disease-specific mortality for well-differentiated thyroid cancer.¹¹⁷

SPECIAL SECTION: RAMAN SPECTROSCOPY

1.5 Raman spectroscopy

Advanced in cancer diagnostic play a pivotal role in increasing early detection of cancer and improving the chances of successful treatment. Up to date, diagnostic pathways are complex and may involve many diagnostic tests such as X-ray, computed tomography, ultra-sound, and endoscopy, but currently histopathology remains the “gold standard” investigation. However, this method is invasive, requiring removal of tissue, often randomly and unnecessarily. Tissue fixation, sectioning and staining follow which can be costly and slow. Histological analysis is very subjective and is associated with considerable inter-observer disagreement.

119

Other diagnostic and screening methods may involve the use of ionising radiation as a precursor to histopathology, for example in breast cancer screening women undergo mammography to identify micro-calcification. Diagnostic methods which could potentially avoid the use of ionising radiation would have significant benefits. A minimally invasive, accurate, reproducible, rapid, non-destructive and cost effective tool is required.

In this setting, Raman spectroscopy (RS) is one of the promising techniques that may increase the reliability and decrease the diagnosis time by providing very specific molecular information from a tissue or a sensing system. Cells and tissues are characterized by a specific biochemical composition and molecular structure. In a similar way, each pathology or cellular abnormality is accompanied by biochemical and molecular changes. Optical and spectroscopic techniques that correlate the biochemical composition, molecular structure, and their variations with the diagnosis would provide powerful clinical tools.¹²⁰

Due to the fact that RS can provide molecular level information about the composition of a sample, the gradual biochemical changes from a healthy tissue to a tumor is reflected in a Raman spectrum. The observed spectral differences are attributed to the changes in the biomacromolecular composition of the tissues as it progresses to form tumor.

For these reasons Raman spectroscopy (RS) is beginning to gain recognition as a potential adjunct to histopathology due to the fact the method can overcome the limitations of current diagnostic techniques. Recent advances in RS have promoted it to a level at which in vivo trials are beginning to emerge. When used in combination with powerful multivariate algorithms the technique can potentially provide automated, objective and reproducible classification of pathology in clinically relevant time frames.¹²¹

1.5.1 Raman spectroscopy technique

Raman spectroscopy is a vibrational spectroscopic technique and it provides chemical information from a molecule or molecular structure. RS enables the elucidation of a tissue's biochemical fingerprint by measuring the molecular specific inelastic scattering of light. The physical mechanism behind Raman spectroscopy is inelastic light scattering of monochromatic laser radiation, which was experimentally discovered in the late 1920s.

All biomolecules, including proteins, lipids, nucleic acids, carbohydrates, and metabolites, are simultaneously probed within complex matrices without preparation, even under in-vivo conditions.

Primarily, RS requires the illumination of a tissue sample with a monochromatic laser and subsequent collection and analysis of the scattered light for intensity and wavelength. Photons in the incident laser light undergo inelastic collisions with molecules, causing an exchange of energy and therefore a change in frequency. The frequency change, known as the Raman shift, is specific to the species of molecule causing the scattering and can be defined as the difference between incoming and scattered photons. Larger shifts indicate that more energy is required to bring about a particular vibrational motion. The shift is independent of the wavelength of excitation, which means that the energy shift is constant for each separate molecular species. The intensity of the peak is directly proportional to the concentration of the sum of molecular constituents giving rise to that peak. Thus, the Raman spectrum is a direct function of the molecular composition of the interrogated volume within the tissue, giving us a complex molecular fingerprint. Since the Raman spectrum of a molecule is a 'fingerprint' and the bands on a spectrum have a narrow bandwidth,

a Raman spectrum from a molecular mixture can provide molecular level information about its chemical composition. As example, Figure 1 reports a Raman spectrum of oesophageal tissue measured using 830 nm excitation.

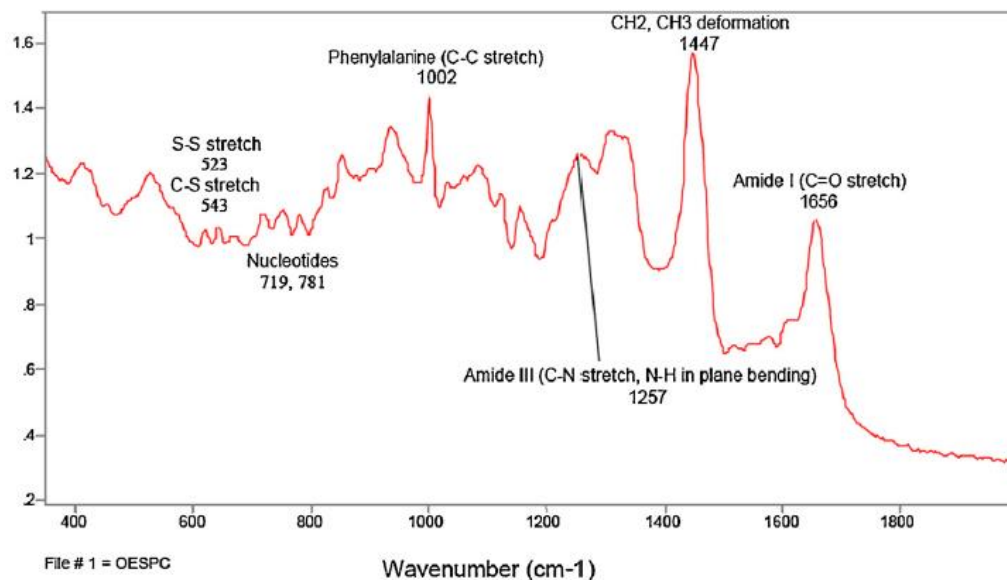


Fig.1. A Raman spectrum of oesophageal tissue measured using 830 nm excitation. Characteristic biochemical peaks have been labelled. Variations in peak height and position can be detected in tissue spectra and have been shown to indicate biochemical progression towards malignancy.

Fortunately, the majority of biological molecules are Raman active, each with their own fingerprint. As a result, RS is highly sensitive to subtle biochemical and molecular changes, which is vital in the differentiation of tissue samples. This property makes it potentially a very powerful diagnostic tool. As example of its high sensitivity, Figure 2 shows Raman spectral biochemical signatures of differing pathologies within a single oesophageal biopsy.

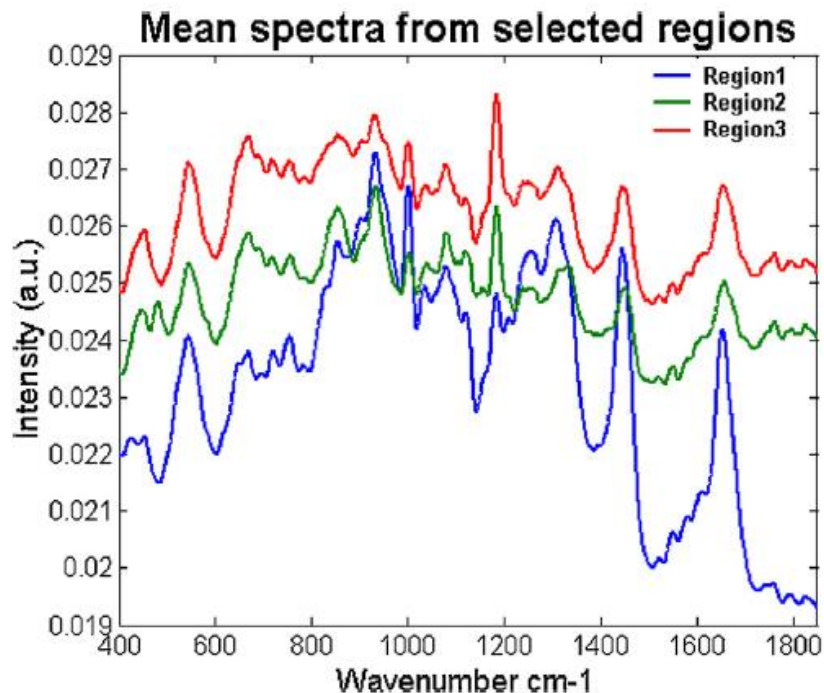


Fig.2. Raman spectral biochemical signatures of differing pathologies within a single oesophageal biopsy. Indicating the amount of information that can be obtained with Raman spectroscopy.

However, its inherently low scattering efficiency has hampered the use of RS until the development of powerful lasers and sensitive detectors. Over the past decade, progress in Raman spectroscopic instrumentation has increased in the sensitivity of its measurement capability to such an extent that the acquisition of high quality spectral data from biological tissue and samples is possible.

1.5.2 The role of Raman spectroscopy for cancer diagnosis

Almost all of the cancer diagnosis applications of technique focus on tissue examinations either *in vivo* or *ex vivo* by detecting a biomarker in a body fluid.

Up to date, the main developments are noted to be:

1. In vivo applications

In vivo, RS offers the potential for “optical biopsy” with important clinical benefits. For in vivo applications, it is ideal to use a fiber optic probe to guide the laser light to the target and collect Raman scattering. It can also be embedded into an endoscopy device.

Excisional tissue endoscopic biopsy carries risks of bleeding and visceral perforation, as well as removal of normal tissue unnecessarily. RS would obviate the need for this, thus reducing trauma to the patient, reducing clinician workload, and reducing secondary repeat procedures.

It will also decrease the rate of re-excisions of areas of dysplasia or malignancy by accurately defining resection margins.¹²² Raman spectroscopy (RS) is suitable for use with fibre-optic probes making it potentially ideal as a medical diagnostic tool for assessment of hollow organs such as esophagus^{123,124} bladder¹²⁵ and larynx.¹²⁶

One of the major fields of application of RS in endoscopy is the identification of Barrett's esophagus. Barrett's esophagus is a complication of chronic gastroesophageal reflux and considered as the predisposition for dysplasia. Therefore, its early detection may provide an opportunity for the prevention of cancer formation. The endoscopic examination of the suspicious regions is the current approach for the identification of these lesions. However, it is extremely difficult to identify these lesions with a white light endoscopy procedure. Therefore, the development of a fiber-optic based Raman probe is very important to increase the diagnosis accuracy of Barrett's esophagus. Recently, Bergholt et al. report the use of a fiberoptic embedded into an endoscopy device was used to collect Raman scattering with the guidance of wide field endoscopic, narrow-band and auto-fluorescence imaging. The Raman spectra from a total of 75 sites (42 healthy and 33 tumor sites) from 27 patients were acquired during the endoscopic examination. The study concluded that RS could provide valuable in vivo biochemical information for diagnosis.¹²⁷ Figure 3 reports a schematic diagram of the rapid multiplexing Raman spectroscopy technique during endoscopy.

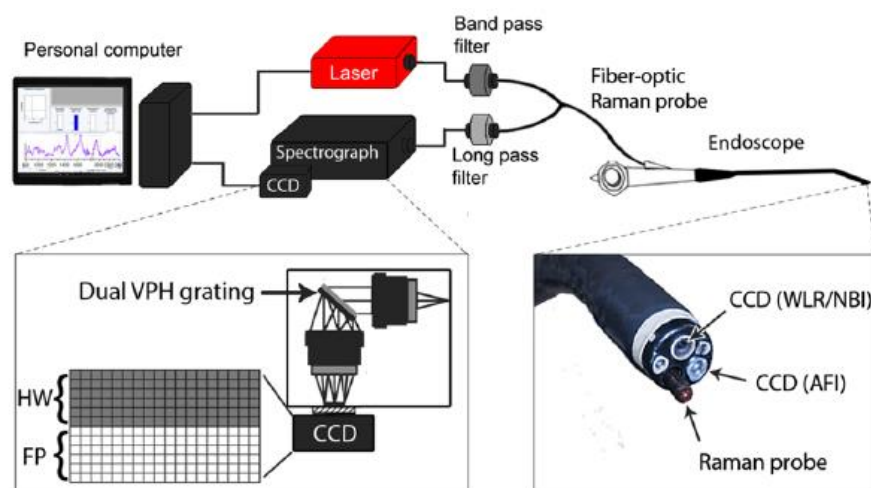


Figure 3.

Schematic diagram of the rapid multiplexing Raman spectroscopy technique for simultaneous acquisition of both the fingerprint (FP) and high wavenumber (HW) Raman spectra under trimodal endoscopic imaging [i.e., white light reflectance (WLR), narrowband imaging (NBI), autofluorescence imaging (AFI)] guidance. A customized dual-transmission VPH grating is incorporated into the Raman system for dispersion of FP and HW Raman spectra onto different vertical segments of a CCD

Furthermore, *in vivo* applications can provide real time and label-free biochemical information about the status of a lesion, which can be used to make diagnostic decision or to find the borders of a tumor during surgery. 128,129 ‘Optical biopsy’ can be a very vital tool during surgery to completely remove cancerous tissue during neurosurgery to prevent its recurrence as reported by Jermyn et al.¹³⁰ This can be extremely useful since the identification of the borders of a cancerous growth is very difficult with current imaging techniques. Figure 4 shows an example of handheld contact fiber optic probe for Raman spectroscopy used during neurosurgery.

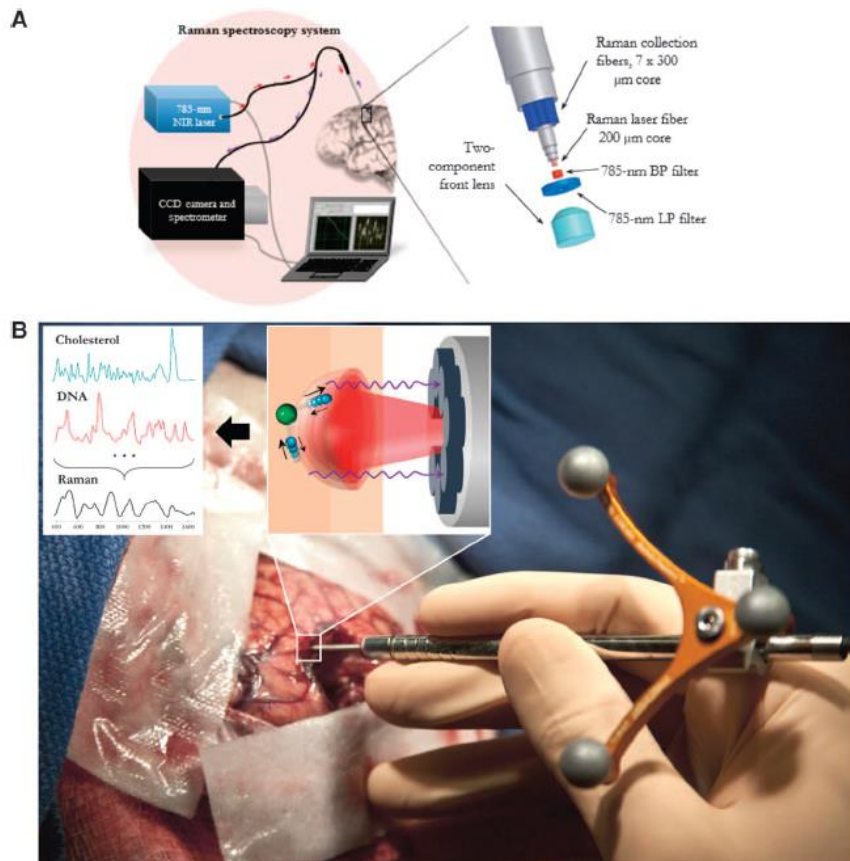


Figure 4.

(A) Experimental setup diagram with the 785-nm NIR laser and the high-resolution CCD spectroscopic detector used with the Raman fiber optic probe.

(B) The probe (Emvision, LLC) was used by authors to interrogate brain tissue during surgery.

2. Histopathology tools

In ex vivo applications, the tissue samples are either used directly or sliced to acquire Raman spectra in a similar way as tissue slices prepared for histopathological examination.

The majority of ex vivo studies has been performed on tissue sections. In large there has been a trend towards imaging/mapping approaches and so called 'histopathology tools' because they mimic the morphological appearance of current histopathology methods but include additional biochemically specific information.

Raman spectroscopy has demonstrated its potential in aiding histopathologists in the identification and objective classification of subtle biochemical changes related to carcinogenesis. There are several studies demonstrating the feasibility of the technique for the analysis of excised tissues directly without any preparation or sliced tissue sections.¹³¹

Recently, for example, Bergner¹³² reports the possibility of discrimination between oral cancer and healthy tissue based on water content determined by Raman Spectroscopy (see Figure 5).

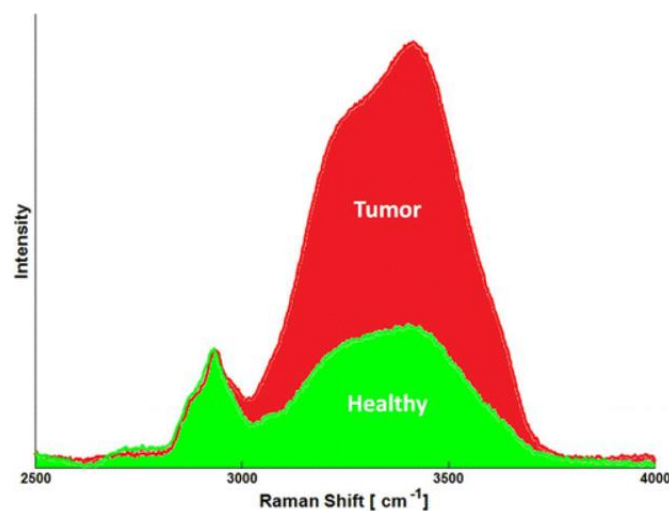


Figure 5 Discrimination between oral cancer and healthy tissue based on water content determined by Raman Spectroscopy.

Tumor-positive resection margins are a major problem in oral cancer surgery. The authors investigate the use of Raman spectroscopy to differentiate tumor from surrounding healthy tissue in oral squamous cell carcinoma. From 14 patients undergoing tongue resection for squamous cell carcinoma, the water content was determined at 170 locations on freshly excised tongue specimens using the Raman bands of the OH-stretching vibrations (3350–3550 cm^{-1}) and of the CH-stretching vibrations (2910–2965 cm^{-1}). The results were correlated with histopathological assessment of hematoxylin and eosin stained thin tissue sections obtained from the Raman measurement locations. The water content values from squamous cell

carcinoma measurements were significantly higher than from surrounding healthy tissue (p-value < 0.0001). Tumor tissue could be detected with a sensitivity of 99% and a specificity of 92% using a cutoff water content value of 69%. Because the Raman measurements are fast and can be carried out on freshly excised tissue without any tissue preparation, this finding signifies an important step toward the development of an intraoperative tool for tumor resection guidance with the aim of enabling oncological radical surgery and improvement of patient outcome.

3. Deep Raman tools for in vivo analysis in solid organs

'Deep Raman spectroscopy' is another application that is being developed for non-invasive diagnosis of solid organs that can be achieved from outside of the body. At this stage of development it can only be applied to specific applications where the Raman signature is very strong and distinct as there is a trade off with the intensity of the signature obtained from depth. This application has been tested in the study of calcification associated with breast cancer.^{133 134 135} The above mentioned studies report the possibility of utilising SORS for measuring calcification composition through varying thicknesses of tissues (2 to 10 mm), which is about one to two orders of magnitude deeper than has been possible with conventional Raman approaches (Figure 6). This result secures the first step in taking this technique forward for clinical applications seeking to use Raman spectroscopy as an adjunct to mammography for early diagnosis of breast cancer, by utilising both soft tissue and calcification signals. Non-invasive elucidation of calcification composition, and hence type, associated with benign or malignant lesions, could eliminate the requirement for biopsy in many patients.

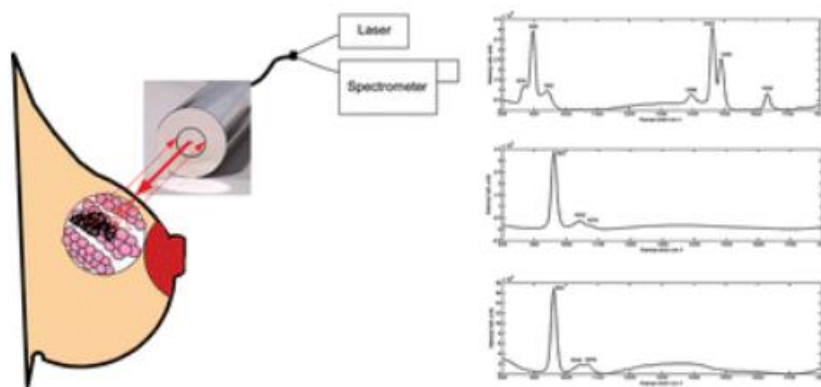


Figure 6. reports the first demonstration of spatially offset Raman spectroscopy (SORS) for potential in vivo breast analysis.

4. Detection of cancer biomarkers

The detection of cancer marker in body fluids for clinical decision-making is an exciting approach, which may allow screening to detect cancer formation as early as possible and simplify the early diagnosis process. An increased concentration of cancer markers can be detected in urine, saliva and blood. In a study, the detection of tumor suppressor p53 and cyclin-dependent kinase inhibitor p21 was demonstrated with a SERS-based immunoassay. The p53 and p21 quantifications in blood serum were performed from the two different Raman reporters (4MBA and DTNB). The authors claim excellent specificity, high sensitivity and very high reproducibility of the assay.¹³⁶

Another way that the technique can be utilized is the detection of cancer markers. A SERS based method for the quantitative determination of haptoglobin (Hp), a plasma glycoprotein and a prognostic ovarian cancer biomarker, was reported.¹³⁷ Several authors suggested that, increased adenosine concentration, usually related with tumor formation, can be used as biomarkers for cancer formation.¹³⁸

Finally, RS can provide rapid, reproducible, non-destructive measurement of disease specific tissue composition, which when combined with powerful mathematical algorithms allows objective classification. Numerous spectral

classification models are under development for both optical biopsy (probe) applications¹³⁹ and histology tool (mapping) applications. Initially, early studies focussed on differentiating normal tissue and advanced cancers. However, with developing technology and complex analytical methods, there has been a move towards diagnosis of neoplastic change at much earlier stages.

1.5.3 Raman spectroscopy in thyroid cancer

Up to date only two studies have investigated the role of Raman spectroscopy in thyroid cancer. The first one, performed by Harris et al.¹⁴⁰, aimed to investigate whether RS combined with advanced mathematical modeling (neural networks) could discriminate between 2 commercial thyroid cell lines; an human thyroid anaplastic carcinoma cell line (8305C) and a “normal” commercial cell line (Nthy-ori 3-1) obtained from the European Collection of Cell cultures (ECACC). Raman spectra were obtained using a Renishaw 'System 1000' Raman microscope while excitation was provided by a Sacher Lasertechnik Littrow external cavity laser set at 783 nm. Finally, detection of the Raman scattered light was performed with a Renishaw RenCam NIR enhanced CCD camera.

The authors obtained 52 spectra from the Nthy-ori 3-1 cells and 64 spectra from the 8305C cells.

Figure 7 and 8 report the typical Raman spectrum from the non-cancerous and cancerous thyroid cell lines.

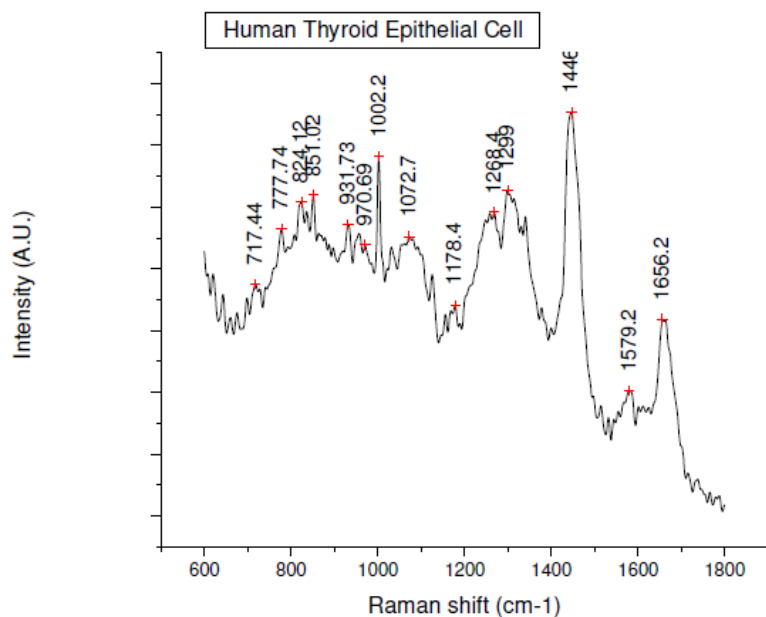


Figure 7: A typical Raman spectrum from the Human thyroid epithelial cell (Nthy-ori 3-1); a non-cancerous cell line.

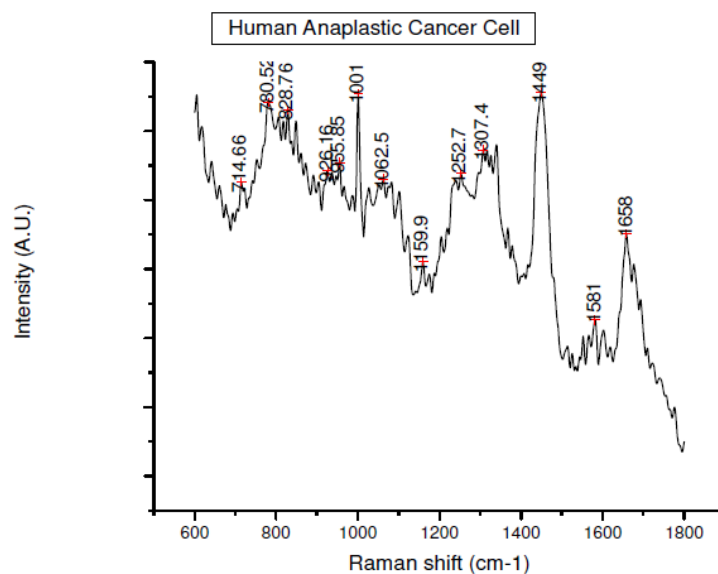


Figure 8: A typical Raman spectrum from a Human anaplastic thyroid cancer cell (8305C); a cancerous cell line.

In the study, the authors also report The PCA (Principal Component analysis) plot of non-cancerous and cancerous thyroid cell lines. This plot, reported in figure 9, is

not totally discriminatory even if it show a distinct clustering of normal and cancerous cell lines but the overlap is too great to be diagnostic.

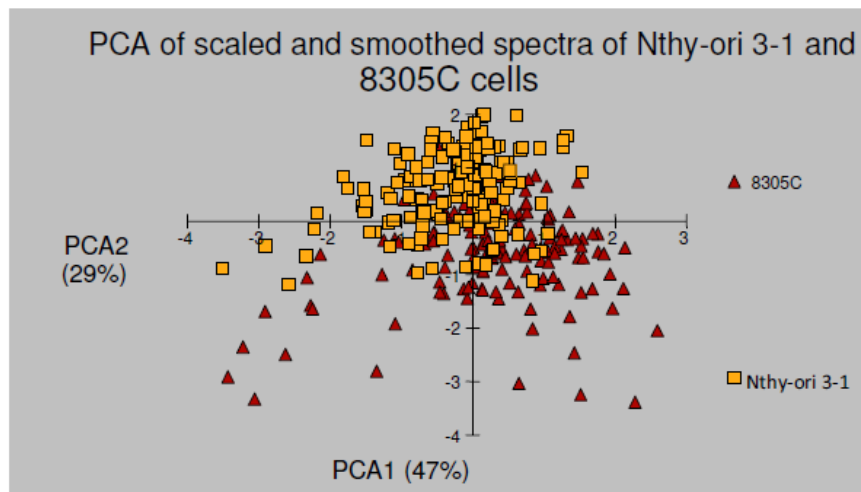


Figure 9: The results of PCA comparing the non-cancerous (Nthy-ori 3-1) and cancerous (8305C) cell lines from the Raman spectra results.

However the neural network result for the Raman data, provide a 95% sensitivity for the cancerous cell line and 92% sensitivity for normal cell line demonstrating that Raman spectroscopy, coupled with neural network analysis is able to discriminate between cancer and non-cancer cells in a simple model system with a high degree of accuracy.

Teixeira et al. report a thyroid tissue analysis through Raman spectroscopy in 2009.¹⁴¹ The objective of the above mentioned work was to study the biochemical alterations of tissues of the thyroid gland by means of molecular vibrations probed by FT-Raman spectroscopy. After the surgical procedure (thyroidectomy), a total of 27 fragments of the thyroid were collected from 18 patients, comprising the following histologic group: goitre adjacent tissue, goitre nodular region, follicular adenoma, follicular carcinoma and papillary carcinoma. The authors, through the discriminative linear analysis of the Raman spectra of the tissue, established (in percentages) the correct classification index among the groups.

For the groups goitre adjacent tissue versus goitre nodular region, a result of 58.3% of correct classification was obtained; this percentage was low, and it was not

possible to discriminate the FT-Raman spectra of these two groups. Figure 10 shows the median median between the spectra of the goitre adjacent tissue (black line) and the nodular region goitre (grey line). These spectral modifications were not significant enough to represent a relevant separation between them. The reported data justify the statement of Layfield et al.¹⁴² that adenomatous goitre is a hyperplasia, with no considerable cellular alterations; this also justifies the similarity between normal thyroid and adenomatous goitre, or adjacent and central tissues of a goitre injury.

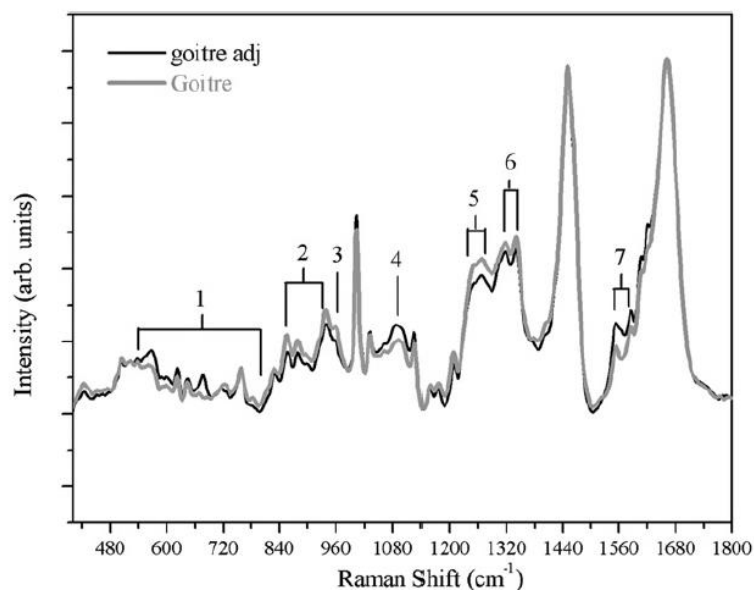


Figure 10 the median between the spectra of the goitre adjacent tissue (black line) and the nodular region goitre (grey line).

Interestingly the authors analyzed the difference between adenomatous goiter, follicular adenoma and follicular carcinoma. The relative median spectra were analyzed and reported in figure 11.

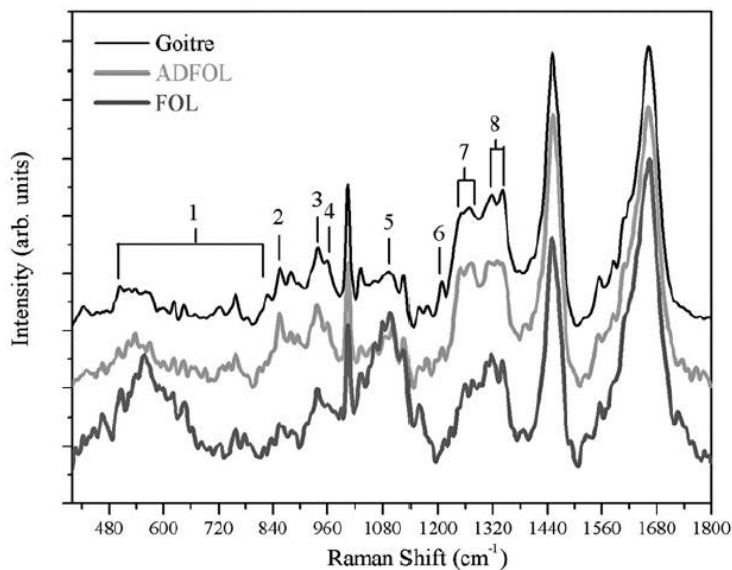


Figure 11

Median of the adenomatous goitre spectra (black line), follicular adenoma (grey line) and follicular carcinoma (dark grey line).

From the figure, it can be noted that some peaks appear in all three spectra; that is, the biochemical compositions are nearly the same in all three tissue types, although with different intensities among them. According the authors, these regions could be similar to those considered characteristic of the normal thyroidal tissue. However, there are also characteristic peaks for only one or two types of injuries, those being the modes of more relevance to differentiate the pathologies for they are exclusive and representative peaks of tissue alteration. Interestingly the authors invite to draw attention to the 1095 cm⁻¹ band which is characteristic of the follicular carcinoma and follicular adenoma tissues since it did not appear on the goitre nodular region. The follicular adenoma, on the other hand, has peaks with high intensity at 856, 937, and 960 cm⁻¹. The characteristic peaks for follicular carcinoma are from 500 to 840, 1095, 1258–1290, and 1315–1339 cm⁻¹.

Finally, the correct classification index reported between goitre (nodular region and periphery) and papillary carcinoma was 64.9%. However, relevant results were obtained in the analysis of the spectra in the benign tissues (goitre and follicular

adenoma) versus malignant tissues (papillary and follicular carcinomas) analysis, for which the percentage was 72.5%, which was considered very good. The median of the adenomatous goitre spectra (black line), papillary carcinoma (grey line) and follicular carcinoma (dark grey line) is reported in Figure 12.

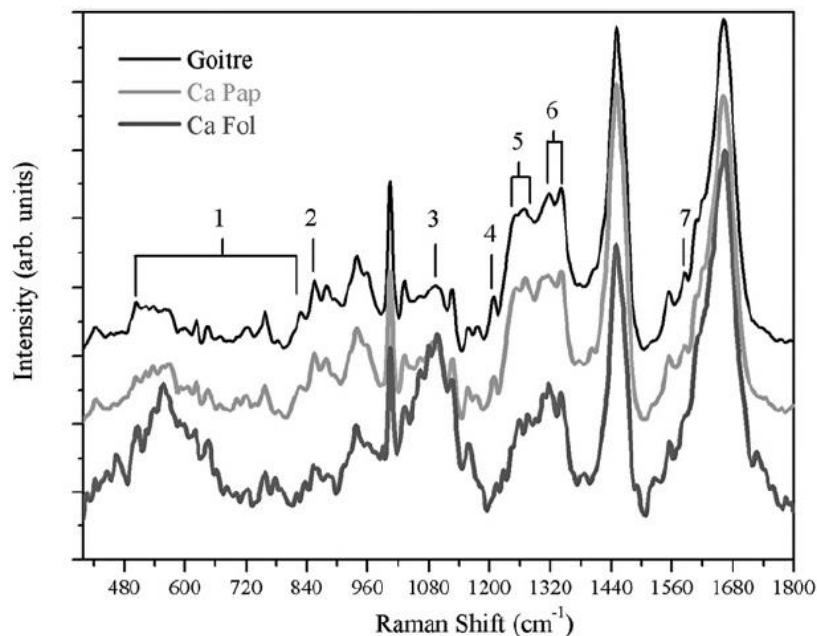


Figure 12: Median of the adenomatous goitre spectra (black line), papillary carcinoma (grey line) and follicular carcinoma (dark grey line).

1.5.4 Limitations of Raman spectroscopy

However, although Raman spectroscopy is a highly sophisticated technique with a well established ability to accurately discriminate neoplastic changes, there are several significant practical limitations.

First, the need for long (currently clinically unacceptable) acquisition times of greater than 1 s. A drawback of the technique is the long analysis time when spectral information is collected from an area other than points on a sample. The accuracy is clearly improved with longer acquisition times; also point measurement systems require accurate placement of the clinical probes with low throughput. The

alternative systems in particular fluorescence based techniques, allow larger areas to be interrogated.

Additional drawback is represented by the fact that interpretation and classification of Raman spectra requires complex multivariate algorithms. Thus, further developments in this field are aiding diagnostic models and it is hoped that advanced data processing techniques, for example support vector machines and random forests, may improve diagnostic accuracy, although validation of these models is required prior to clinical implementation. In addition, future developments in probe design and construction may improve signal to noise ratios. Systems must be robust enough to withstand day-to-day usage by clinical staff and decontamination and disinfection processes.

1.6 Clinical application of Raman spectroscopy for thyroid cancer diagnosis

The diagnosis of thyroid pathologies usually occurs in the following order: anamnesis, ultrasonography and laboratory exams. Recently, a fine needle aspiration (FNA) could be required, where the cells collected are cytologically analysed. From the FNA, if the suspected malignancy is confirmed, a surgical procedure (partial or total thyroidectomy) is advised so that, after the material is sent for histologic analysis (anatomical pathologic analysis), the medical diagnostic can be concluded. FNA is currently the most accepted procedure for diagnosing thyroid injuries, as it is a very useful and cost-effective tool. However, the sensitivity of this procedure for the thyroid is at times poor, with a high rate of false-negative results, and the variation ranges from 2% to 37%.¹⁴³ The differentiation of hyperplastic nodule (goitre), follicular adenoma or follicular carcinoma is difficult. The accuracy of the method is doubtful in these cases, and other alternatives and further methods are necessary to make the diagnosis more precise for such obscure injuries to the cytopathologic diagnosis. False-negative results occur due to an ordinary mistake in sampling, which may occur in small tumours and samples associated with inflammations and degenerative changes next to the thyroidal parenchyma. The cytopathologic diagnoses of follicular adenoma and follicular carcinoma are complicated due to the fact that they depend on the histologic access

to the capsular and vascular invasion perception. It is, therefore, vital to find new ways to detect the biochemical and cellular changes, in order to perfect the diagnosis and prognosis of thyroidal diseases. It is important to note that at times the incorrect diagnosis leads the patient to surgery without appropriate urgency and indication.

Considering the variations of the thyroid disease and the difficulty of the morphologic diagnosis, the necessity of further techniques to distinguish benign and malignant characteristics of the thyroid lesion is evident. It is known that these diseases, with no exception, are caused by biochemical changes in the cells and/or tissues. Thus, the current challenge of modern medicine is to find an analytic technique that investigates these alterations through minimally invasive and non-destructive methods. Few analytic methods fulfil these requirements and are sensitive enough to reveal details of the biochemical composition and structure.¹⁴⁴ Among the new techniques recently presented, optical biopsy by Raman spectroscopy is one of the most promising ones, due to the biochemical alterations that can be detected by the optical spectroscopy through the disease's characteristic spectral signs. Different aspects could be detected by the Raman spectroscopy method that can contribute and complement the clinic diagnosis of thyroidal pathologies.

The presented study aimed to investigate the biochemical alterations in thyroid tissues through Raman Spectroscopy of thyroid sample obtained from thyroid surgery.

In detail the aims of this research were:

1. To define the Raman spectra in PTC thyroid cancer as compared to normal thyroid tissue on surgical resected samples.
2. To evaluate different expression of Raman spectra in the different types of PTC thyroid neoplasm (classical Vs follicular) underwent to surgical resection.
3. To investigate the role of RS in define the surgical margin in resected thyroid cancer.

1.6.1 Materials and methods

1.6.1.1 Patients enrolment

This prospective monocentric study has been approved by the Ethical Committee of the University of Campus Bio-Medico (UCBM) (prot. 33.15 TS ComEt CBM), and all patients gave the written informed consent. Nine patients that received a diagnosis of PTC based on FNA at the Endocrinology Unit of UCBM were enrolled for this study. These patients underwent total thyroidectomy at the Surgical Unit of the same Institution.

Exclusion Criteria for enrolment of patients were:

- Under 18 years of age
- Pregnant or lactating females
- Major mental comorbidity
- Concomitant other malignancy or within previous 5 years
- Previous chemotherapy or radiotherapy;
- Concurrent anticancer systemic therapy
- Suspicious for difficult assessment of pathological staging (margin involved in section).

1.6.1.2 Thyroid tissue preparation

At the time of surgery the removed specimens were immediately submitted unfixed to the Pathology Unit in an appropriately labeled container. After completion of the gross examination of the specimen by the pathologist, resection margins were marked with black ink (Figure 14). A tissue slice of about 1x1x0.3 cm³ was then obtained, including both healthy and neoplastic areas, avoiding surgical margins, and the slice was frozen on a metallic cold-plate inside the cryostat. A 5 µm cryostatic section was cut and stained with Haematoxylin/Eosin, in order to confirm the presence of healthy and neoplastic tissue zones, as well as the transition area between them. Additional sections were cut at 20 and 30 µm of thickness, collected on separate slides and stored unstained at -20°C until the Raman evaluation (Figure 15). The surgical samples were subsequently fixed in buffered formalin and

embedded in paraffin for permanent sectioning. Diagnosis, grading and staging were performed, in agreement with the 7^oth edition of TNM. ¹⁴⁵

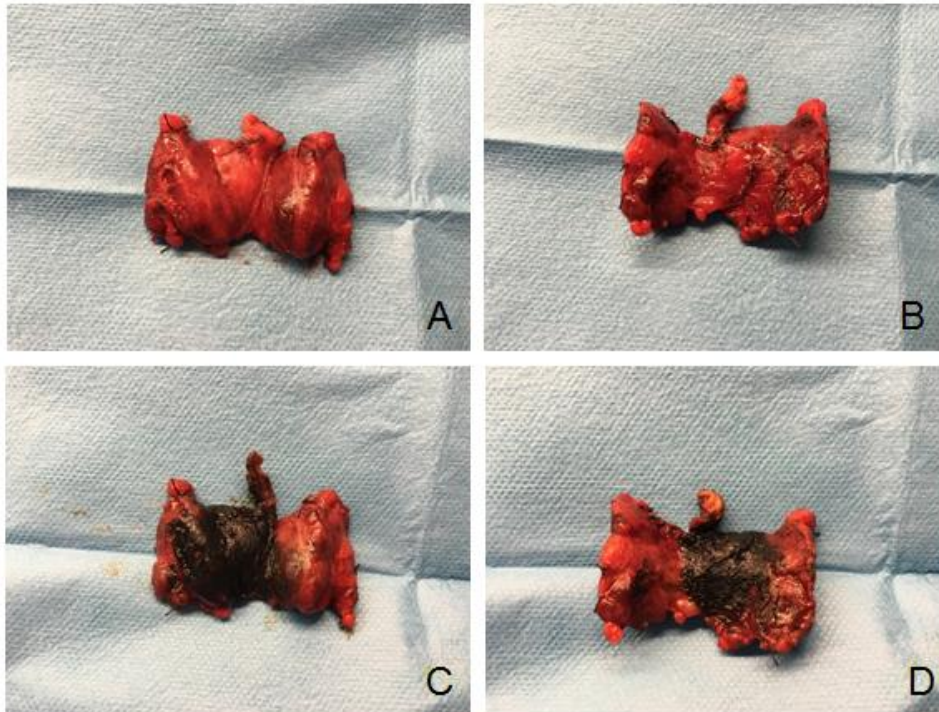


Figure 14. Thyroid tissue preparation of a PTC located in right lobe. A frontal view of surgical specimen. B posterior view of surgical specimen. Resection margins were marked with black ink in the front (C) and in the back (D).

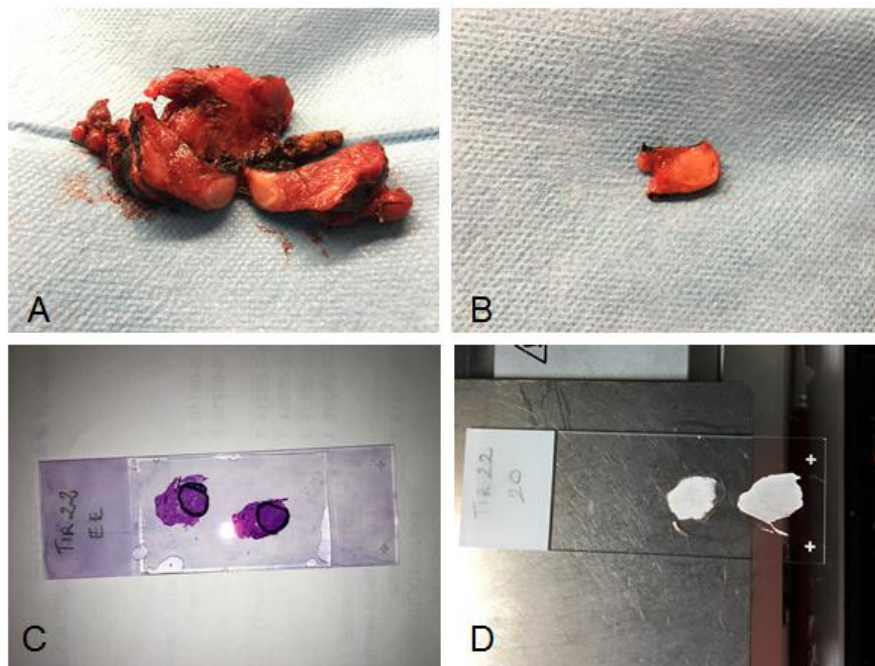


Figure 15. A. The PTC is located in the right lobe. B. A tissue slice of about 1x1x0.3 cm³ including both healthy and neoplastic areas. C. A section stained with Haematoxylin/Eosin D. Sections cut a 20 30 μ m of thickness for Raman evaluation.

1.6.1.3 Raman spectroscopy

Raman spectra were recorded using a Thermo Fisher Scientific DXRxi Raman microscope (RM) (Figure 16), at the following conditions: 532nm laser source; 200-3400 cm⁻¹ full range grating; 10x and 50x objectives; 25 μ m confocal pinhole, 5 (FWHM) cm⁻¹ spectral resolution. The indicated above RM instrument guarantees a fast change of experimental parameters, for better measurements procedure optimization, and does not require consumable reagents and staining treatments. As a first step, the collection of a number of mosaic images at low magnification (10x) using the RM has been carried out, providing the generic overview information on the tissue morphology and allowing one to individuate and evaluate regions of interest. After that, the region of interest was investigated collecting spectra at high magnification (50x).

Preliminary measurements were performed, in order to optimize the experimental parameters to provide a good S/N (signal-to-noise) ratio and to minimize tissue fluorescence. A 5th order polynomial correction was used to compensate the tissue fluorescence. A laser power of 8 mW measured at the sample has been applied as the best compromise between the signal quality and the undesired tissue burning. The exposure time was 0.8 sec, as a suitable compromise to achieve a good spectra quality and to shorten the overall acquisition time. At least 50 exposures were averaged to obtain a good signal-to-noise ratio. Laser spot size was about 700 nm (50x objective). Various Raman maps of tissue zone size from 100x100 μm^2 up to 1x1 mm^2 , collecting several thousands of spectra per map, were obtained. The background-subtracted Raman spectra were further normalized for the area under the curve for standardization of the tissue Raman intensities. No pre-treatment was performed on tissue samples before spectroscopic Raman examination. To assess intra-sample variability, multiple measurements were carried out at different regions within the same sample.



Figure 16: Thermo Fisher Scientific DXRxi Raman microscope (RM) used to analysed biological samples.

1.6.1.4 Analysis of Raman data

As a first step, Raman data were processed by ThermoScientific OMINCxi software with the statistical analysis “Multivariate Curve Resolution (MCR)” algorithm. Since we needed to analyze thousands of spectra composing a tissue map, powerful statistical methods to treat the data was necessary. MCR using constrained alternating least squares algorithms represents a powerful analysis capability for the quantitative analysis of hyperspectral image data.

The fluorescence background subtraction from each spectrum, a very useful and in case of biological tissues often strictly necessary option, with ThermoFisher™ DXRxi RIM it was not necessary to perform separately, since it was incorporated in the OMNIC spectra acquisition software. This subtraction was performed in real time during the spectra acquisition.

1.6.1.4 Dataset/casuistry

A number of thyroid tissue areas were histologically identified and diagnosed as healthy or pathological (Haematoxylin/Eosin staining of frozen samples) by an experienced pathologist (A.C.). By means of the RS imaging, 20 maps have been obtained from healthy and 20 from pathological areas. In Table 1, the experimental dataset is fully represented, showing the distribution of the tissue samples (healthy, PTC classical variant and PTC follicular variant) for each patient.

1.6.1.5 Statistical analysis

Statistical analysis was performed on average spectra of each map, corresponding to the 20 healthy tissue average spectra and the 20 PTC average spectra. The fingerprint region (FP) and the high wavenumber (HWN) range of Raman spectra, roughly 600÷1800 cm⁻¹ and 2800÷3100 cm⁻¹, respectively, were selected for statistical data analysis treatment. The remaining spectral range was not considered, as non-meaningful from the point of view of the contained biochemical

information. The collected Raman data were processed performing multivariate analysis, used for complex systems with high internal variability. Two principal statistical procedures were performed on the dataset: Principal Component Analysis (PCA) and Linear Discriminant Analysis (LDA).

At first, PCA was carried out in order to reduce the initial high dimensionality of the dataset and to verify whether, in a subset of dimensions, the variability of the different tissue typologies can reveal on its own differences among samples that could be considered diagnostic.

LDA was applied on the same components observed in PCA to verify if differences among the typologies do exist due to differences among the means of samples belonging to different tissue groups. Moreover, the implementation of the algorithm on principal components (PCs) let to optimize the process of classification on the basis of a reduced number of input variables. The LDA was performed using the leave-one-out cross validation method.

1.6.2 Results

In the period from January 2013 to May 2016, a total of 9 patients affected by PTC and submitted to thyroidectomy were enrolled. A total number of 40 maps was obtained, 20 maps have been obtained from healthy and 20 from pathological areas. In Table 1, the experimental dataset is fully represented, showing the distribution of the tissue samples (healthy, PTC classical variant and PTC follicular variant) for each patient.

Table 1. DATASET: Thyroid glands from 9 PTC patients

Case	Histological diagnosis: PTC	Number of healthy tissue maps	Number of pathological tissue maps	Total Raman maps	Total Raman spectra
1	classical	2	3	5	698
2	classical & follicular	2	3	5	799
3	classical	2	2	4	992
4	classical	2	2	4	618
5	follicular	1	1	2	1825
6	classical	4	3	7	6123
7	classical	2	2	4	239
8	follicular	3	2	5	881
9	classical	2	2	4	596
total		20	20		12771

Total number of MAPS: 40

Total number of spectra: 12 771

1.6.2.1 Statistical analysis

A) Discrimination between healthy and PTC tissue

The principal component analysis was performed on the matrix 40x1315 of the 40 average spectra in the range of $653\div 1723\text{ cm}^{-1}$ and $2828\div 3023\text{ cm}^{-1}$. Among all the calculated components, the first 20 ones represent almost the 100% of the total variance (the 20th PC corresponds to about 0.015%) and it is reasonable to affirm that the information about the hypothesized differences in composition is contained within the first 20 PCs, having most likely a larger contribution % to the variability. In order to observe whether any of PCs has diagnostic capability, a two sample *t*-test was applied, after having previously controlled the condition of validity of the equality assumption of the two group variances with respect to each PC by Fisher's test. The results of the *t*-test confirm that only for three PCs (PC2, PC4, PC8) a certain separation of the means of the healthy samples group with respect of the pathological one can be found (*p*-values of 0.007; 0.033; 0.035, respectively). Even if the test employed is robust with respect to the assumption of normality of the distribution underlying the samples (that is, are permitted deviations), the result is affected by the presence of outliers, invalidating the test in the case where the numerosity per group is not appropriate to the diversity between the distributions underlying the samples. The obtained result leads to the hypothesis that differences between tissue typologies exist, but can't be revealed by maximizing their respective variability, and truly none of the PCs has diagnostic capability.

The LDA algorithm was first applied on the 40x20 matrix obtained considering the scores of the 40 samples for the first 20 PCs. Various combinations of all or part of the PCs were tried in order to find the discriminant function with the simplest mathematical solution for the classification: the best result (f_1) was found using the first eight components plus the 10th, the 11th and the 20th. The result is shown in Fig. 17.

Having previously verified by Fisher's test that sample variances in the two groups are not significantly different ($F=0.376$; $df_N=18$; $df_D=14$), applying the two sample *t*-test to the sample scores on f_1 , a value of $t=-19.528$ is obtained for 22.037 degrees of freedom (Welch correction applied): as a result, the two groups shown in Fig. 17 are significantly different at a level of confidence of 0.001.

The employed leave-one-out cross-validation method classified the 100% of the samples correctly. It should be noticed that the groups are characterized by values ranging exclusively along the positive semi-axis (healthy samples) or the negative one (PTC samples).

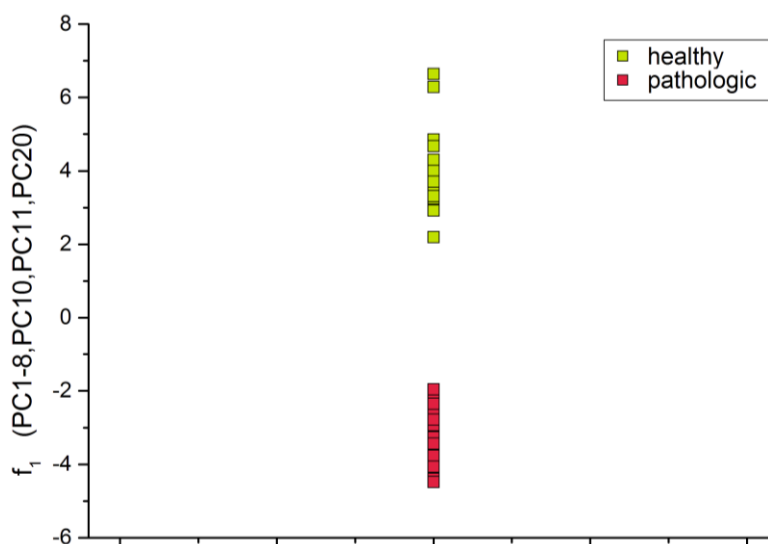


Figure 17: Projection of healthy and PTC samples along f_1 .

B) Discrimination between two PTC variants (classical and follicular)

The PCA was performed on a matrix 20x1315 of the 20 average spectra of PTC tissue samples in the $653\div 1723\text{ cm}^{-1}$ and $2828\div 3023\text{ cm}^{-1}$ ranges of spectra. The analysis of the values of the variance explained by each PC revealed that the first eighteen components explain almost the totality of the variance (the 18th PC represents <0.01%).

In this case, the values for F -test indicate that variances are not significantly different among the various PCs. The values of the t -test confirm that along none of the PCs means are significantly different (confidence level of 5%).

The LDA algorithm was applied also in this case and the result is the function f_2 (obtained combining the first fifteen PCs excluding the 6th). The result is shown in Fig. 18.

Having previously verified by the Fisher's test that sample variances in the two groups are not significantly different ($F=2.065; df_N=12; df_D=5$), applying the two samples t -test to the sample scores on f_1 a value $t=25.972$ is obtained for 13.84

degrees of freedom (Welch correction applied): as a result, the two groups shown in Fig. 18 are significantly different at a confidence level of 0.001. The leave-one-out cross-validation method employed classified the 89.5% of the samples correctly but also in this case the values of the two PTC variants are completely distinguished by the fact that range along opposite semiaxes (positive for classical variant and negative for follicular variant). This criterion on its own would lead to a completely correct classification of the samples.

Reassuming the results of this section, we can affirm that RS is able to discriminate between healthy and PTC tissues of thyroid with 100% of sensitivity, specificity and accuracy and to discriminate between classical and follicular variants of PTC with 92% of sensitivity, 83% of specificity and 89% of accuracy, by means of the leave-one-out cross-validated LDA.

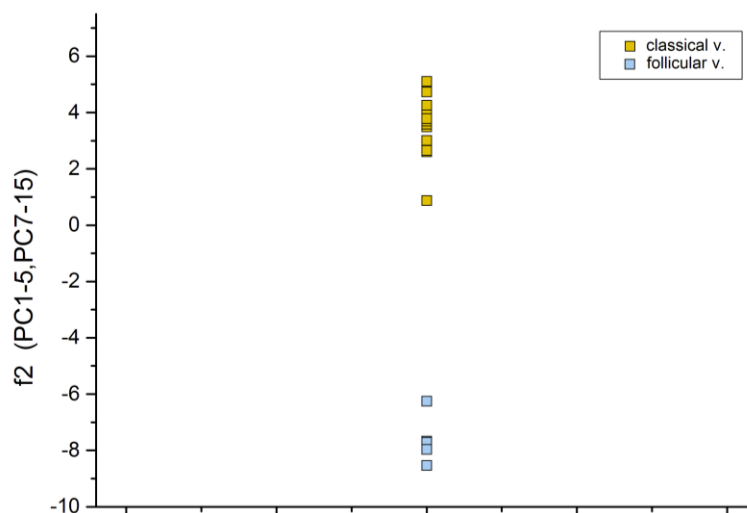


Figure 18: Projection of the samples of the two variants of PTC along f₂.

1.6.2.2 Biochemical profile study

A) Discrimination between healthy and PTC tissue

The spectra have been classified according to the tissue type (healthy and PTC) and obtained by averaging the corresponding maps, resulting in the 9 average PTC and the 9 average healthy spectra, corresponding to thyroid samples from 9 patients. In Fig. 19 (a,b), both sequences show the FP region of spectra.

It should be noticed that the spectra belonging to the same type of thyroid tissue (healthy or PTC), but belonging to different patients, are very similar to each other showing good intra- and inter- correlations, whereas comparison between healthy and PTC groups of spectra reveals significant differences.

An accurate assignment of the major thyroid Raman bands registered in our spectra and comparison with the literature data is given in Table 2. As regards thyroid tissue, the available Raman literature studies are not numerous.^{140, 146, 147} In this work, the applied RS technique allowed to detect for the first time some peculiar features, characteristic for thyroid tissue. The most remarkable difference between the corresponding spectra of healthy and PCT tissues consists in the presence of three intense bands at 1006, 1156 and 1520 cm^{-1} in the pathological tissue, attributable to carotenoids.^{145,148,149, 150}

Table 2. Peak positions and assignments of major Raman bands observed in thyroid healthy and PTC tissues.

Healthy tissue peak position (cm ⁻¹)	Classical PTC tissue peak position (cm ⁻¹)	Follicular PTC tissue peak position (cm ⁻¹)	Band attribution	Reference
673			tryptophan (ring breathing)	(146)
		717	membrane phospholipids head (C-N); adenine; lipids (CN ⁺ (CH ₃) ₃);	(146)
748	748	748	DNA	(146)
		851	proline&hydroxyproline (side chain vibration); tyrosine (ring breathing and Fermi doublet); glycogen;	(146,141)
919			proline; hydroxyproline; glycogen; lactic acid;	(146)
		957	carotenoids; phosphates $\nu_s(\text{PO}_4^{3-})$; cholesterol; quinoid ring in-plane deformation;	(146,141)
971	971		$\nu(\text{C-C})$ wagging	(146)
994			C-O ribose, C-C	(146)
1003	1003	1003	phenylalanine $\nu_s(\text{C-C})$	(146,147)
	1006	1006	Carotenoids	(146)
1031			phenylalanine($\delta(\text{C-H})$ and C-H in plane bending); protein (C-N stretching); carbohydrate residues of collagen;	(146,141)

1086	1084	1089	$\nu(\text{C-C})$ <i>gauche</i> ; $\nu_1(\text{CO}_3^{2-})$; $\nu_3(\text{PO}_4^{3-})$; $\nu(\text{PO}^{2-})$; $\nu(\text{C-C})$ skeletal of acyl backbone in lipid (<i>gauche</i> conform.);	(146,141)
1128	1128	1128	proteins (C-N stretching); carbohydrates (C-O stretching); ceramides; acyl backbone in lipid (trans conform., $\nu(\text{C-C})$);	(146-147)
1156	1156	1156	protein (stretching C-C and C-N)	(146)
1156	1156	1156	Carotenoids	(146)
1172	1172	1172	$\delta(\text{C-H})$, tyrosine	(146)
	1205		$\nu(\text{C-C}_6\text{H}_5)$; tryptophan; phenylalanine; adenine and tyrosine (ring breathing); amide III;	(141)
1225			amide III (β sheet structure)	(146)
1234			a concerted ring mode	(146)
1239			amide III	(146,141)
	1264	1264	lipids	(146)
1307	1307	1307	lipid and collagen (twisting, bending, wagging)	(146)
1337	1337	1337	C-H deformation (protein); amide III; glycine and proline side chain (CH_2 wagging vibrations); adenine and guanine (ring breathing modes);	(146)
1360	1360	1360	tryptophan	(146)
1393	1393	1393	CH rocking	(146)
1424			lipid (CH_2 scissoring); deoxyribose (B, Z-marker);	(146)
	1440/1442	1440/1442	CH, CH_2 and CH_3 deformation; cholesterol; triglycerides (fatty acids);	(146)

			lipids (CH ₂ scissoring and CH ₃ bending); collagen;	
1445			collagen ($\delta(\text{CH}_2)$, $\delta(\text{CH}_3)$ and CH ₂ CH ₃ bending); phospholipids ($\delta(\text{CH}_2)$, $\delta(\text{CH}_3)$ and CH ₂ CH ₃ bending); methylene (bending);	(146)
1450	1448/1452/1464	1448	CH ₂ CH ₃ , CH ₂ and CH deformation; $\nu(\text{C-H})$; $\delta(\text{CH}_2)$; methyl groups bending; methylene deformation; proteins ($\delta(\text{CH})$ and $\delta(\text{CH}_2)$);	(146)
1498		1498	(C-C) stretching in benzenoid ring	(146)
	1516/1518	1516/1518	β -carotene $\nu(\text{C-C})$; carotenoid (C-C and conjugated C=C stretching); porphyrin $\nu(\text{C=C})$;	(146)
	1520	1520	(-C=C-) carotenoids	(146)
1545			C ₆ -H deformation; tryptophan;	(146)
1552			tryptophan $\nu(\text{C=C})$; porphyrin $\nu(\text{C=C})$;	(146)
1557		1557	tryptophan; porphyrin $\nu(\text{C=C})$; amide II ($\nu(\text{CN})$ and $\delta(\text{NH})$); COO ⁻ (tyrosine, amide II);	(146)
1584	1584	1584	phenylalanine $\delta(\text{C-C})$; (C-C) olefinic stretching; hydroxyproline; acetoacetate; riboflavin; lipids;	(146-147)
1602		1602	phenylalanine $\delta(\text{C-C})$	(146)
1638	1640		water (intermolecular bending and very weak and broad ν_2)	(146)

1660	1660	1660	v(C-C) cis; (C-C) groups in unsaturated fatty acids; fatty acids; lipids; ceramide backbone; amide I;	(146)
	2852	2852	v _s (CH ₂); lipids; fatty acids;	(146)
2879			lipids and proteins (CH ₂ and CH)	(146)
	2888	2888	lipids and proteins (CH ₂ asymmetric stretching)	(146)
2931	2931	2931	CH ₂ asymmetric stretching	(146)
2936		2936	chain end CH ₃ symmetric band	(146)
	2960	2960	out-of-plane chain end antisymmetric CH ₃ stretching	(146)
	3010	3010	unsaturated =CH stretching	(146)

Indeed, the comparison between Fig. 19 a (healthy) and Fig. 19 b (PTC) sequences of spectra provides clear evidence that PTC tissue hosts a significant presence of carotenoid bands, which is otherwise just trace-like in healthy tissue. The less intense Raman band at 956 cm⁻¹ (4th carotenoid peak) was not distinguishable in our spectra, due to its low intensity (only about 10% of the 1156 cm⁻¹ band intensity). The 1006 cm⁻¹ band is a mixed Raman peak, with contribution of carotenoids and phenylalanine v_s (C-C) (at 1003 cm⁻¹) (see Table 2). In Figure 20 the sequence of average Raman spectra collected upon normal tissue and PTC tissue are reported together.

In addition, the HWN region of spectra depicts a broad band centered at 2900 cm⁻¹ (not shown here). This band is generally assigned to proteins, lipids and fatty acids normal modes. In our case, the intensity of this band in the PTC spectra is approximately 3-4 times higher than the intensity of bands belonging to the FP region, while for the healthy tissue, the HWN/FP intensity ratio is about 1.3-1.5.

The ratio of HWN PTC/HWN healthy is approximately 2.5. Therefore, another characteristic of PTC is a much more intense band at 2900 cm^{-1} .

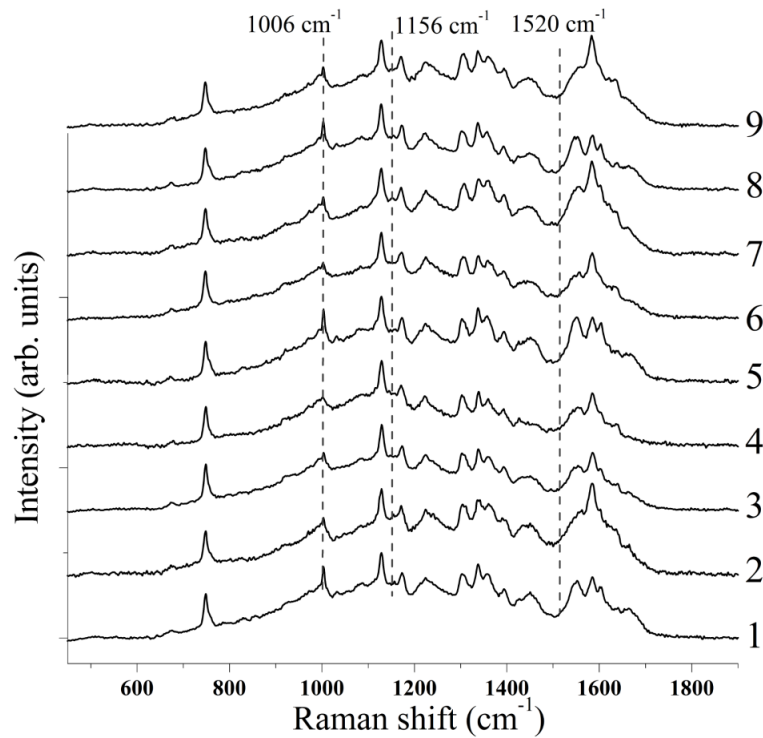


Figure 19 a: Sequence of average Raman spectra collected upon healthy thyroid tissue

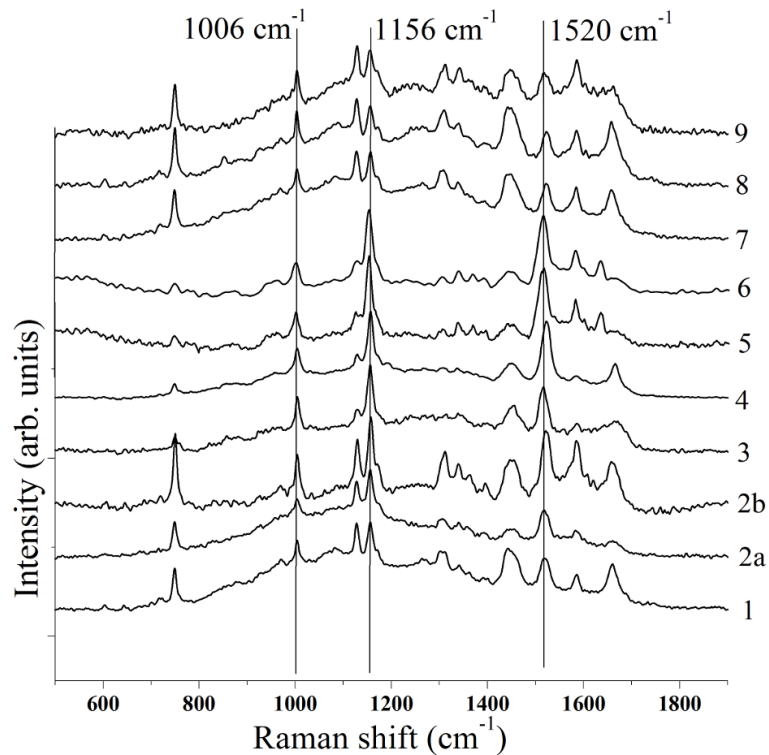


Figure 19 b: Sequence of average Raman spectra collected upon PTC tissue.

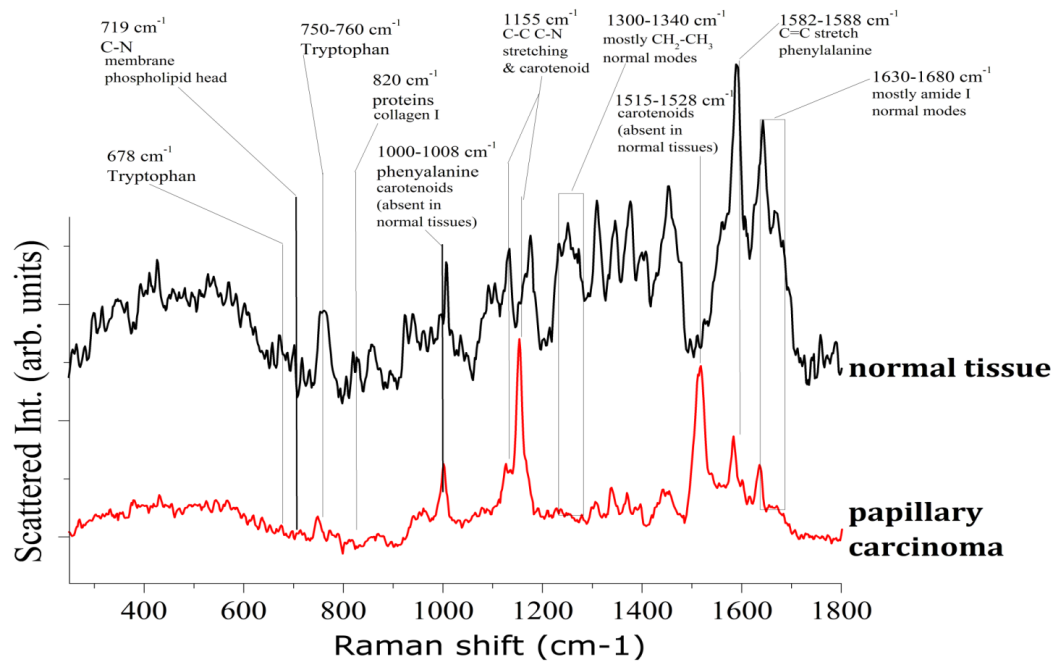


Figure 20. Sequence of average Raman spectra collected upon normal tissue and PTC tissue.

B) Discrimination between two PTC variants (classical and follicular)

Interestingly the comparison between sequences of spectra obtained by two variants of PTC (classical and follicular) shows an intense correspondence with the exceptions of two bands.

Figure 21 provides clear evidence that classical PTC hosts a more intense Raman band at 1300-1340 cm^{-1} and at 1630-1680 cm^{-1} than follicular variant of PTC.

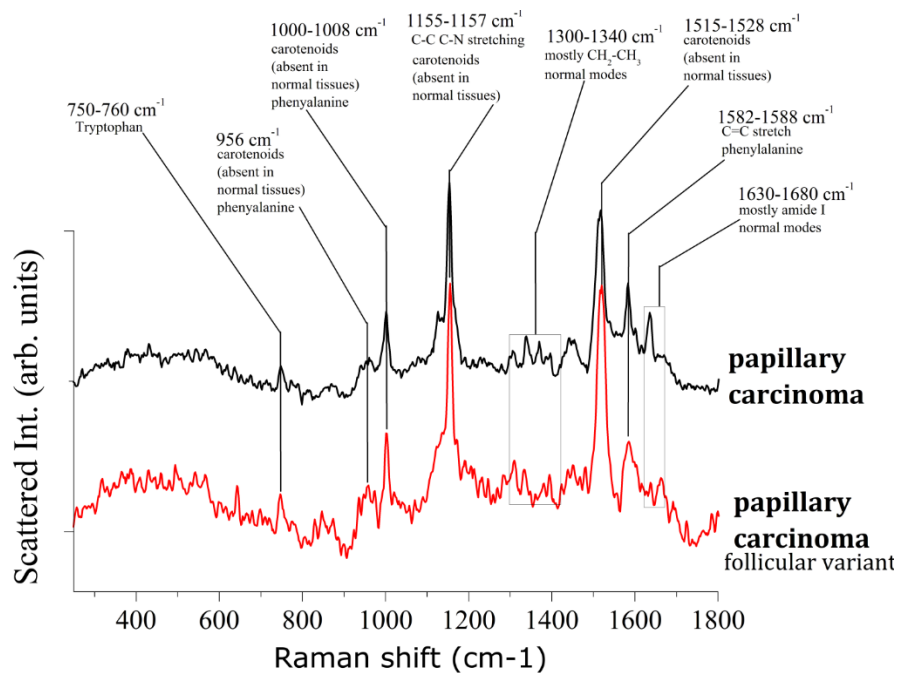


Figure 21. Sequence of average Raman spectra collected upon classical papillary PTC and follicular variant of PTC.

1.6.2.3 RS imaging

Discrimination between healthy and PTC tissue

The Raman spectra collected upon a selected area provide intrinsic biochemical information that can be used for diagnosis. Selecting specific wavelengths, Raman imaging lets one to obtain different graphic results for the maps of the two tissue typologies. An example of such maps (20 μm pixel step and 400x300 μm^2 area) in false colors referred to the band at 1156 cm^{-1} is shown in Figure 22. In Fig. 22 (a), the results obtained for healthy tissue (left part – Raman biochemical map, right part – dark field optical image) are presented. The healthy tissue is in blue, while some insignificant amount of carotenoids is represented by the yellow-green colors. In Fig. 22 (b), the PTC tissue is shown (left part – Raman biochemical map, right part – dark field optical image). As can be clearly observed, the considerable

presence of carotenoids in PTC tissue was detected (false colors in green-yellow-red represent the corresponding increasing intensity of carotenoids).

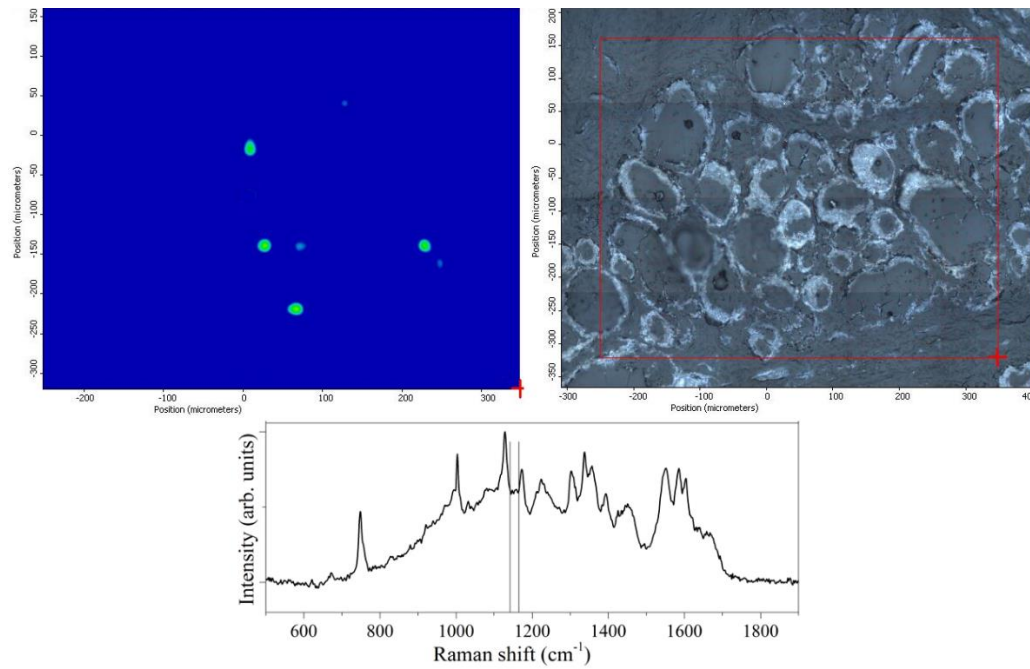


Figure 22 a. Typical example of Raman chemigram maps (1156 cm⁻¹ band reference) for thyroid tissues: healthy tissue (left part – Raman map, right part – dark field optical image),

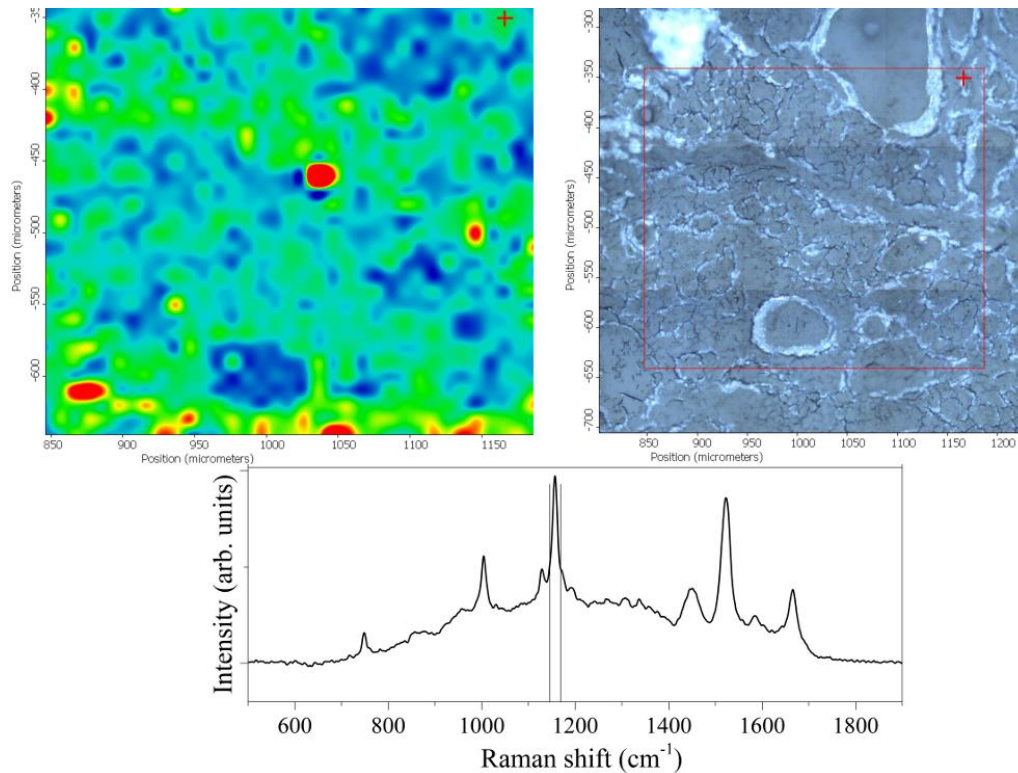


Figure 22 b. Typical example of Raman chemigram maps (1156 cm^{-1} band reference) for thyroid tissues: (PTC tissue (left part – Raman map, right part – dark field optical image). The average reference spectra are shown below.

In Fig. 23, the mixed (healthy-PTC) zone of tissue was mapped. In the PTC zone, the papillary structures can be distinguished. As can be seen, the applied RS technique allows one to distinguish between healthy and pathologic tissue. This is important for tumor margins precise identification during excision surgery for tumors with extra-capsular extension. More information on the “border-line” healthy-PTC can be obtained decreasing the pixel step size.

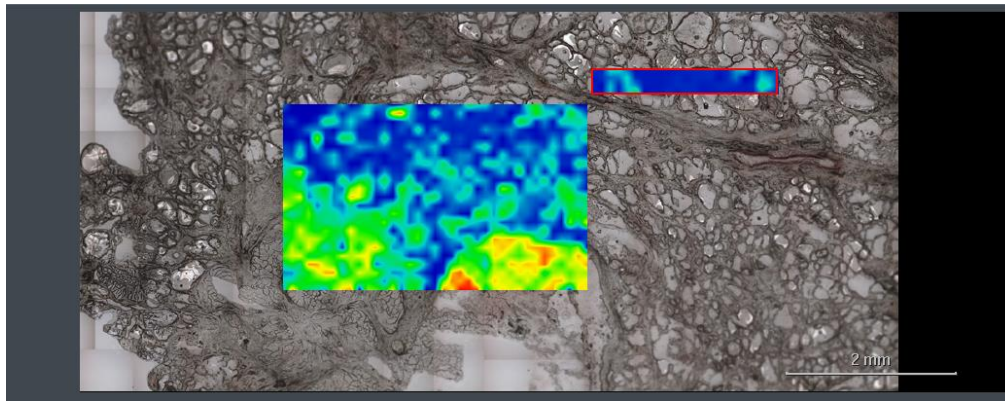


Figure 23. Raman map of Thyroid tissue, evidencing papillary structures of papillary carcinoma (green-yellow-red). Healthy tissue corresponds to blue zone.

1.6.3 Conclusion

Our results have demonstrated the feasibility and reproducibility of RS to discriminate normal thyroid tissue from PTC, and between classical and follicular variants of PTC, on the basis of their biochemical fingerprints.

Based on the experimental results obtained in this work, we can attest the significant carotenoids presence in the PTC tissues with respect to the healthy tissue, in which their absence or minimal and localized presence was detected (see Fig. 19-20). To our knowledge, this is the first experimental evidence of carotenoids presence in the neoplastic thyroid tissue.

Papillary thyroid carcinoma has been extensively investigated with multiplatform molecular analysis and the area of unknown genomic alteration has been reduced substantially from 25% to less than 4%.¹⁵¹ Detailed study of the genomic background, however, though instrumental in better understanding the oncogenetic and biochemical pathways of cancer, is still not sufficient to fully investigate the mechanisms that lead to neoplastic transformation, which, in turn, would lead to the identification of more accurate diagnostic, prognostic and predictive makers. For example, BRAFV600E gene mutation that is considered a driver of molecular alteration in classic PTC, has been recognized in over 70% of benign nevus without neoplastic progression.¹⁵² Spectroscopy methods applied in clinics should provide the best possible sensitivity, specificity and accuracy in order to minimize false

definitions. Ideally, a new method should be performed as *in situ* analysis encompassing the assessment of multiple cellular constituents and allowing paired morphological and biochemical analysis. RS is among the few available methods fulfilling the above requirements.

In our study, we considered the FP and the HWN range of thyroid Raman spectra, both presenting changes while passing from healthy to PTC areas and, therefore, both important for diagnostic utility, as confirmed also by authors for cervical tissue.¹⁵³

RS has the ability to identify specific tumor expression molecules and molecular species involved in tumorigenesis and progression. For instance, Talari et al.¹⁴⁵ claimed the 956, 1006, 1156-1157, 1524-1528 cm^{-1} Raman peaks as “carotenoids absent in normal tissue”. Puppels et al.¹⁵⁴ investigated carotenoids located in human lymphocyte subpopulations and natural killer cells, evidencing a high carotenoids concentration in the CD4+ lymphocytes, and proposed to investigate the possible mechanisms behind the protective role of carotenoids against the development of cancers. The increased intensities at 1159 and 1527 cm^{-1} , assigned to carotenoids have been identified also in the Raman spectra of brain tumors¹⁴⁵ and neurinomas.¹⁵⁵ Talari et al.¹⁴⁵ suggested that carotenoids can be used as Raman biomarkers in breast cancer pathology.

Resonance Raman is among the best ways to study the properties of carotenoids in complex media, such as, for example, binding sites of biological macromolecules in living organisms.¹⁵⁶ In this case, i.e. when the wavelength of the excitation laser is in the range of electronic absorption band of molecule of interest, resonance Raman intensities may be enhanced up to 6 orders of magnitude, as compared to normal Raman scattering.¹⁵⁷ In the present work, the enhancement of carotenoid Raman bands was obtained, using 532 nm laser wavelength, which lies in the range of carotenoids UV/Vis absorption region.¹⁵⁸

The coupled histopathological and Raman biochemical observations performed in this work highlighted that carotenoids are mainly present in cellular areas of PTC, so that their presence seems to be related to the neoplastic thyrocytes within the tumor tissue. Our study suggests that these characteristics could be used as Raman biomarkers in the PTC pathology. However, the mechanism underlying potential

oncogenic effects of carotenoids is still unknown, since very little is known about the biochemical content of neoplastic cells especially what regards lipids, lipoproteins and lipophilic substances that are commonly lost in routinely processed histological samples. Among human tissues, different normal cells are able to utilize carotenoids, i.e. beta-carotene is reported as a local supply of vitamin A in the skin and melanocytes.¹⁵⁹ However, physiological mechanism for carotenoids uptake in normal thyrocytes is not reported, and our results raise the hypothesis of a carotenoid-related pathway for the PTC oncogenesis. This hypothesis needs for validation but underlines the presence of carotenoids in neoplastic thyrocytes, as previously described for other organs.

In conclusion, we performed the RS investigation and biochemical mapping of healthy thyroid tissue and of PTC (classical and follicular variants). The obtained results demonstrate the great potential of RS to support histopathological evaluation, increasing the reliability of cancer diagnostics. Based on the results of multivariate statistical algorithms, based on leave-one-out cross-validated LDA, we can affirm that RS is able to discriminate between healthy and PTC tissues of thyroid with 100% of sensitivity, specificity and accuracy and to discriminate between classical and follicular variants of PTC with 92% of sensitivity, 83% of specificity and 89% of accuracy. The achieved diagnostic accuracy, sensitivity and specificity are compatible with the clinical use, both for the PTC diagnosis and what regards the differentiation between classical and follicular variants of PTC, the latter being a significant challenging point for thyroid nodules evaluation.

Only a few literature studies report RS investigations of thyroid tissue and neoplasia.^{141,147} The particularity of our RS analysis is that for the first time it is performed on tissue sections and combined with microscopic assessment of the analyzed areas. The method is very cost-effective, being the cryostatic tissue sections observed without any additional staining or treatment. Our results represent a major advance in imaging of thyroid tissues, leading to subsequent clinical application of the RS diagnostics. As a potential clinical tool to support cancer diagnosis, RS should improve clinical accuracy in decision-making and reduce inter-observer variability.

This study is the first demonstration of particular features of the spectroscopic

fingerprint of the PTC tissues presenting the significant carotenoids presence with respect to the healthy tissue. Our investigation suggests that carotenoids could be used as Raman biomarker for the PTC pathology. With this regard, combination of the histological and Raman microscopy analysis approaches should open a new way to integrative findings with wide implications for basic pathobiology, tumor classification schemes, and therapeutic strategies.

Several future perspectives can derive from these preliminary results:

1. The development of a RS optical biopsy system to investigate thyroid tissue alterations. This innovative diagnostic device should be represented by a needle containing the RS fibers to explore in vivo thyroid nodules and to perform a non-destructive in vivo optical biopsy.
2. The development of intraoperative technology which may able to classify cell populations in real time, making it an ideal guide for surgical resection and decision making. Raman-based probe could be used, for example, to define surgical margin during thyroid surgery, to evaluated nodes involvement allowing to perform the correct modality of lymphadenectomy, to evaluated the presence of surgical residual after thyroidectomy.

SECTION II. MANAGEMENT AND PROBLEMS ASSOCIATED WITH THYROID CANCER TREATMENT

GENERAL SECTION: THYROID CANCER TREATMENT

2.1 Surgical treatment

The mainstay of therapy for differentiated thyroid cancer is surgery. Although when initially attempted, thyroidectomy was associated with high rates of mortality, improvements in anaesthetic and surgical technique have resulted in thyroid surgery being extremely safe. Death following thyroid surgery is reported in <0.5% of cases. In contrast, rates of injury to the recurrent laryngeal nerve and parathyroid glands are more common (2% nerve palsy and 6% need for calcium supplements at follow up).¹⁶⁰ These complications, while not life threatening, result in voice change (and occasionally tracheostomy in cases of bilateral recurrent laryngeal nerve injury) and the need for long term calcium supplementation. The initial surgical approach to thyroid cancer was radical. Total thyroidectomy and bilateral radical neck dissection achieved macroscopic disease clearance at a cost. In particular, the cervical lymphadenectomy was associated with significant functional and cosmetic impact. The recognition that histology could predict the biological behaviour of tumors was made in the mid-20th century. Good outcomes were described for patients with differentiated lesions of follicular cell origin (papillary carcinoma/follicular carcinoma/ Hurthle cell carcinoma) in comparison with medullary or anaplastic carcinoma.¹⁶¹ This observation led to a significant change in surgical approach, with a move away from aggressive neck surgery in patients with differentiated thyroid cancer.

2.1.1 Total thyroidectomy vs Lobectomy

The most important aim of primary surgery is to achieve complete macroscopic disease clearance and to minimize the chance that ipsilateral thyroid bed surgery will ever be required again. This requires a thyroid lobectomy as a minimum (other than for the occasional patient with isolated isthmic disease). An extra capsular thyroidectomy with preservation of the recurrent laryngeal nerve and parathyroid

glands should be the standard. This will achieve disease clearance and minimize the risk of thyroid bed recurrence. A second aim of primary surgery is to render the patient suitable for adjuvant radioactive iodine by removing all thyroid tissue.

Selected patients are suitable for thyroid lobectomy rather than total thyroidectomy. While preserving excellent oncological outcomes, this approach has significant potential benefits. Rates of recurrent laryngeal nerve injury, hypocalcaemia, and tracheostomy are significantly lower following such unilateral surgery. The ideal candidate for such an approach is a young patient with uninodular disease limited to the thyroid. The risk of permanent post-operative hypocalcaemia and tracheostomy is more or less 0% following thyroid lobectomy. Recurrent nerve injury is most commonly a temporary palsy, but is permanent in around 2% of cases. Operating on one side rather than both is, unsurprisingly, associated with lower rates of morbidity.¹⁶² However, these patients, by definition, have a residual lobe following treatment. They are not suitable for radioactive iodine and require monitoring of the contralateral lobe in the post-operative period by ultrasound. In the long term, 5–10% of such patients will require completion thyroidectomy at some point during follow up. This is mainly due to the development of nodular disease in the residual lobe. Such disease is malignant approximately half of the time.¹⁶³

A number of factors make the decision of which primary procedure to offer complex. Many expert authors report extremely low complication rates following total thyroidectomy. In contrast, reports from a community setting suggest that complication rates are significantly higher for the majority of patients who are operated on outside centers of excellence.^{164 165} Following initial therapy, the tumor marker thyroglobulin can be used during follow up to detect recurrence. This tumor marker is produced both from native thyroid tissue and persistent disease. Therefore, it is less useful in patients who have had thyroid lobectomy. Due to high rates of multifocal disease within the thyroid, most authors do not recommend thyroid lobectomy if there are nodules in the contralateral lobe, even if they appear benign. This is particularly relevant in areas with a high incidence of multinodular thyroid disease and is an issue increasingly encountered due to improvements in

ultrasound imaging, which now detect nodular disease in over 50% of otherwise healthy individuals.¹⁶⁶

When making a decision about primary thyroid surgery, the clinician must consider a number of factors. Risk stratification should be performed for each patient and used as a guide to selection of therapy. Tumor factors are critical, and total thyroidectomy remains the treatment of choice for those high-risk patients who will be candidates for adjuvant radioactive iodine. When performed well, it provides excellent oncological outcomes safely. It facilitates radioactive iodine if required, allows optimal follow up using thyroglobulin as a tumor marker, and addresses concerns about multifocal disease within the gland.

ATA guidelines, in recommendation 35, suggests that the initial surgical procedure should include a near-total or total thyroidectomy for patients with thyroid cancer >4 cm, or with gross extra-thyroidal extension (clinical T4), or clinically apparent metastatic disease to nodes (clinical N1) or distant sites (clinical M1) while thyroid lobectomy alone should be performed for patients with thyroid cancer <1 cm without extrathyroidal extension and cN0.⁶⁵

For patients with thyroid cancer >1 cm and <4 cm without extrathyroidal extension, and without clinical evidence of any lymph node metastases (cN0), the initial surgical procedure can be either a bilateral procedure (neartotal or total thyroidectomy) or a unilateral procedure (lobectomy). Thyroid lobectomy alone may be sufficient initial treatment for low-risk papillary and follicular carcinomas; however, the treatment team may choose total thyroidectomy to enable RAI therapy or to enhance follow-up based upon disease features and/or patient preferences.

Finally disease management teams of patients affected by differentiated thyroid cancer should decide the surgical strategy by balancing tumor, clinician, and patient factors. An individualized plan can be tailored for each patient using a risk-adapted approach to optimize outcome on a case by case basis (see Figure 24).

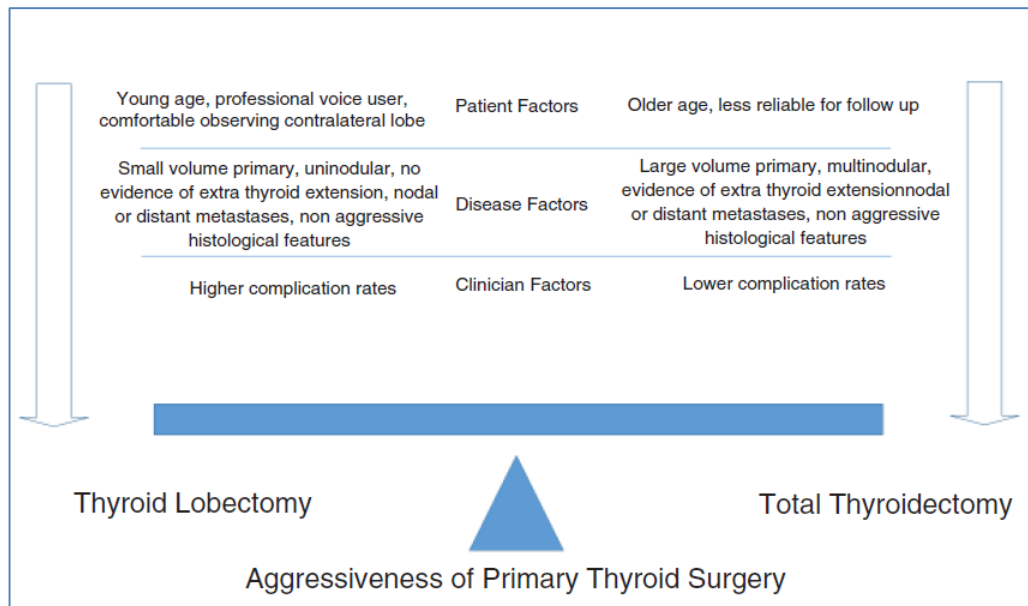


Figure 24. An individualized approach to selecting the aggressiveness of primary thyroid surgery. Treated by Nixon I. *The Surgical Approach to Differentiated Thyroid Cancer*. F1000Research 2015, 4(F1000 Faculty Rev):1366 Last updated: 15 FEB 2016.

2.1.2 Lymph node surgery

Differentiated thyroid cancer and in particular papillary thyroid cancer commonly metastasizes to the neck. The most common site of metastasis is the central neck (levels VI and VII), which surrounds the thyroid gland. The second echelon of lymph nodes is the lateral neck (most commonly levels III and IV). As mentioned above, radical neck dissection was considered the treatment of choice at one point.¹⁶⁷ This was an operation that was relatively quick, safe, and resulted in macroscopic disease clearance. However, it was associated with high rates of morbidity. A vogue for a much less aggressive “berry picking” approach to the removal of macroscopically involved neck nodes has largely been abandoned due to unacceptably high recurrence rates. As experience in neck surgery has improved, a compartment oriented neck dissection is recommended by most authors as the operation of choice for patients with evidence of neck disease.¹⁶⁸

Critically, the surgeon must ensure the neck has been properly evaluated prior to embarking on surgery. Ultrasound is a reliable way of assessing the lateral neck and is also the investigation of choice for the thyroid. If lateral nodal disease is encountered, imaging of the central neck may be considered using CT or MRI. Cross sectional imaging is preferable to ultrasound in assessing the central neck, particularly the mediastinal component (level VII), which is poorly visualized using ultrasound.

Those patients considered N1a or N1b (metastatic disease in the central or lateral neck respectively) following investigation should have surgery planned to remove all involved levels, and any other levels considered at risk (therapeutic neck dissection). So, those patients with disease in the central neck alone should have a central neck dissection (almost always with a total thyroidectomy as radioactive iodine is likely to be indicated).

Those patients with lateral neck involvement should have clearance of levels II-V, which are at the highest risk of metastatic involvement.¹⁶⁹ Involvement of the neck above the accessory nerve and in the submental/submandibular region (level I) is uncommon, so these levels are routinely spared. In addition, differentiated thyroid cancer rarely presents with aggressive nodal disease and extra nodal extension. Therefore, in almost all patients, the sternocleidomastoid muscle, internal jugular vein, and accessory nerve can be spared. This significantly limits the morbidity of surgery and has become the standard of care for patients with lateral neck disease. In contrast, the approach to the clinically negative neck is highly controversial. The reasons for the controversy are multiple, and again, without prospective evidence may never be resolved.

There are authors who recommend prophylactic lateral neck dissection (surgery without pre-operative evidence of involved nodes).¹⁷⁰ However, they are in the minority and the vast majority do not consider the morbidity of lateral neck surgery worth the "benefit".¹⁷¹

Despite this, if one chooses to dissect the apparently uninvolved lateral neck, metastatic disease will often be found on histology. This disease rarely manifests and if it does it can safely be salvaged at a later date. In addition, entering the lateral neck requires an extended incision and places structures at risk that are not routinely

encountered in thyroid and central neck surgery (accessory nerve, marginal mandibular nerve, carotid sheath and thoracic duct).

In contrast, when performing a thyroidectomy, the central neck is, by definition, entered. The recurrent laryngeal nerves and parathyroid glands are encountered during the dissection and revision central neck surgery carries higher risks than primary procedures.

Authors who argue for prophylactic central neck surgery highlight the fact that the central neck is exposed during primary thyroid surgery. They also cite high rates of occult histopathological metastases and that such metastases “upstage” patients when identified, which gives the treating team an effective way of further risk stratifying patients to rationalize the approach to adjuvant radioactive iodine. There is some evidence that excision of the involved nodes in the central neck results in lower post-operative thyroglobulin levels, which may result in lower recurrence rates. No author has ever proven that prophylactic central neck dissection results in improved survival, as almost no patient without metastatic disease dies during follow up.

In contrast, those authors who do not support prophylactic surgery highlight the higher surgical morbidity of the procedure versus thyroidectomy alone, and the fact that patients who have observation rather than central neck dissection have extremely good outcomes with low rates of recurrence and extremely low rates of death. With such good outcomes enjoyed by this group of low-risk patients, the need for radioactive iodine is questionable. In addition, the approach to a central neck dissection is probably variable. Prophylactic central neck surgery involves removing tissue that lies between the recurrent laryngeal nerves. However, those centers with experience of re-operative central neck surgery find high rates of disease in areas not normally included in prophylactic surgery, such as dorsal to the recurrent laryngeal nerve or low at the thoracic inlet, which are high-risk areas for dissection and hence not included in the primary surgical field.¹⁷²

The controversy has resulted in ambiguity in international guidelines. Such documents recommend an individualization of approach dependant on risk factors for involvement.

The recommendations reported in 2015 American Thyroid Association guidelines can be resumed as follows⁶⁵:

- Therapeutic lateral neck compartmental lymph node dissection should be performed for patients with biopsy-proven metastatic lateral cervical lymphadenopathy. (Strong recommendation, Moderate-quality evidence)
- Therapeutic central-compartment (level VI) neck dissection for patients with clinically involved central nodes should accompany total thyroidectomy to provide clearance of disease from the central neck. (Strong recommendation, Moderate-quality evidence)
- Prophylactic central-compartment neck dissection (ipsilateral or bilateral) should be considered in patients with papillary thyroid carcinoma with clinically uninvolved central neck lymph nodes (cN0) who have advanced primary tumors (T3 or T4) or clinically involved lateral neck nodes (cN1b), or if the information will be used to plan further steps in therapy. (Weak recommendation, Low-quality evidence)
- Thyroidectomy without prophylactic central neck dissection is appropriate for small (T1 or T2), noninvasive, clinically node-negative PTC (cN0) and for most follicular cancers. (Strong recommendation, Moderate-quality evidence)

2.2 Complication related with surgical treatment

The most common complications related with surgical treatment are: recurrent laryngeal nerve injury, postoperative hypocalcemia and postoperative haemorrhage.

The risks of total thyroidectomy are significantly greater than that for thyroid lobectomy, with a recent meta-analysis suggesting a pooled relative risk (RR) significantly greater for all complications, including recurrent laryngeal nerve

injury (transient RR= 1.7, permanent RR= 1.9), hypocalcemia (transient RR= 10.7, permanent RR= 3.2), and hemorrhage/ hematoma (RR= 2.6).¹⁷³

Surgeon experience likely influences the risks of thyroidectomy, with higher volume surgeons having lower complication rates.^{174 175}

In a recent review of 27 articles and 25,000 patients, the average incidence of temporary or permanent vocal fold paralysis after surgery was 9.8%, with a wide range from 2.3% to 26%, in part related to the timing and method of laryngeal examination.¹⁷⁶ The Scandinavian quality register reported a vocal fold paralysis rate of 4.3% nerves at risk, based on 3660 thyroid operations performed in 2008 in 26 endocrine surgical units from Sweden and Denmark.^{177, 178} Further, the detection of vocal fold paralysis doubled when patients were submitted to routine laryngeal exam after surgery as compared to laryngoscopy performed only in patients with persistent and severe voice changes.

The 3rd British Association of Endocrine and Thyroid Surgeons (BAETS) audit reported a 2.5% rate of RLN palsy and 4.9% incidence of voice changes in a sample of 10,814 cases of thyroid surgery. For first-time surgery, the reported incidence of RLN palsy was 1.4% after lobectomy and 3.7% after total thyroidectomy. These figures increased to 5.4% and 6.9%, respectively, in revision surgery.¹⁷⁹ Such data are derived from self-reporting by selected surgeons and as such might be too optimistic for extrapolation to the overall practice of thyroid surgery.¹⁸⁰ Administrators of these 2 national databases deem the rates of temporary and permanent RLN paralysis to be severely underestimated, due to lack of routine laryngeal exam.

RLN injury rates are lower when the nerve is routinely visualized in comparison with surgeries in which the nerve is simply avoided.¹⁸¹ Studies with or without intraoperative nerve monitoring demonstrate similar patient outcomes with regard to nerve injury rates,¹⁸² but studies likely have been underpowered to detect statistically significant differences (413,424).^{183,184} A recent systematic meta-analysis of 20 randomized and nonrandomized prospective and retrospective studies suggested no statistically significant benefit of intraoperative neuromonitoring compared to visualization alone during thyroidectomy for the

outcomes of overall, transient, or permanent RLN palsy when analysed per nerve at risk or per patient.¹⁸⁵

Correlation between vocal symptoms and actual vocal cord function is poor given the potential for variation in paralytic cord position, degree of partial nerve function, and contralateral cord function/ compensation; therefore, vocal symptoms may be absent in patients with vocal cord paralysis.

Vocal fold immobility symptoms vary widely and may range from minimal or no symptoms to acute airway distress. For example, in a recent study of 98 patients with unilateral vocal fold immobility, the voice was judged to be normal in 20% of subjects and improved to normal in an additional 8%. Therefore, nearly one-third of patients with unilateral vocal fold immobility were, or later became, asymptomatic.¹⁸⁶ In contrast, bilateral vocal fold immobility is typically associated with profound and immediate respiratory distress, may require tracheotomy, and if initially not recognized and treated promptly, can be associated with anoxic brain injury and death.¹⁸⁷

Voice changes may also occur after thyroid surgery through a variety of mechanisms, including those that are non-neural and without vocal fold immobility. In several large studies of patients without vocal fold immobility, subjective voice complaints occurred in 30% to 87% of patients.^{188 189 190}

With a reported incidence of 1.6% to 50%,¹⁹¹ postoperative hypocalcemia is the most common and sometimes the most severe complication observed after total thyroidectomy. Therefore patients must undergo close postoperative observation and frequent laboratory evaluations. The reasons for postoperative hypoparathyroidism are devascularization of parathyroid glands during surgery owing to the close proximity of the thyroid capsule, the accidental removal of 1 or more parathyroid gland(s), destruction of the parathyroid glands as a result of lymphadenectomy along the recurrent laryngeal nerve (RLN), or hypoparathyroidism due to hematoma formation.¹⁹²¹⁹³

2015 ATA guidelines recommended that “the parathyroid glands and their blood supply should be preserved during thyroid surgery”.⁶⁵

Typically, parathyroid gland preservation is optimized by gland identification via meticulous dissection.¹⁹⁴¹⁹⁵ If the parathyroid(s) cannot be located, the surgeon

should attempt to dissect on the thyroid capsule and ligate the inferior thyroid artery very close to the thyroid, since the majority of parathyroid glands receive their blood supply from this vessel. There are exceptions to this rule; for example, superior glands in particular may receive blood supply from the superior thyroid artery. If the parathyroid glands are inadvertently or unavoidably removed (e.g., they are intrathyroidal, or require removal during a central lymph node dissection) or devascularized, confirmation of cancer-free parathyroid tissue should be performed, and then the glands can be autotransplanted into the strap or sternocleidomastoid muscles. It is important to inspect the thyroidectomy and/or central lymphadenectomy specimen when removed and before sending it to pathology to look for parathyroid glands that can be rescued.

SPECIAL SECTION: POSTOPERATIVE HYPOCALCEMIA AND TERIPARATIDE

2.3 Postoperative hypocalcemia

Hypoparathyroidism is a rare disease characterized by hypocalcemia and absent or deficient parathyroid hormone.¹⁹⁶ Hypoparathyroidism and hypocalcaemia have been described as postoperative complications since the early descriptions of thyroid surgery from the days of Kocher and Billroth.¹⁹⁷ Postsurgical hypoparathyroidism is usually due to inadvertent or unavoidable removal or damage to the parathyroid glands and/or their blood supply. A recent meta-analysis has estimated the prevalence of postoperative hypocalcemia from 19% to 38%.¹⁹⁸ In particular, transient hypoparathyroidism after neck surgery (often called “stunning” of the glands) is relatively common, ranging from 6.9% to 46%.^{199,200, 201,202} However, Its true prevalence is probably underestimated for many reasons: lack of clear definitions of hypocalcemia, variety of laboratory ranges for normocalcemia and reference values, timing of blood sampling in the postoperative period and short or incomplete follow-up.²⁰³ Decreased serum calcium, secondary to hypoparathyroidism, may present clinically with muscle cramps, perioral and peripheral paresthesias, carpedal spasm or tetany, and/or confusion.²⁰⁴ Moreover, hypocalcemia can lead to delayed repolarization of the heart with increased risk of torsades de pointes.²⁰⁵ Symptomatic patients often require extended hospitalizations following thyroid surgery with increased healthcare costs.²⁰⁶

Predicting the risk of developing hypoparathyroidism is a challenge for the best care offered to patients. In particular, some studies indicate that iPTH levels measured shortly after surgery have a high predictive value: iPTH levels below the normal range (<10 pg/mL) at 4 and 6 hours after the operation correctly predicted postoperative hypocalcemia.^{207, 208} Indeed, Grodski et al, have concluded that iPTH levels <10 pg/mL, at 4 hours after total thyroidectomy, had the best precision to predict hypocalcemia (defined as serum adjusted level <8 mg/dL) 24 hours after surgery, with a positive predictive value of 90%, sensitivity 94% and specificity 100% with overall accuracy 98%.²⁰⁹ Instead, chronic complete hypoparathyroidism is relatively rare. The diagnosis of chronic hypoparathyroidism requires that

features of hypoparathyroidism persist for at least 6 months after surgery. Surgical centers with experienced endocrine surgeons and a high case volume report rates of post thyroid surgical permanent hypoparathyroidism of 0.9-1.6%.^{210,211, 212} iPTH measured shortly after surgery and/or serum adjusted calcium level may be useful also to predict the onset of persistent hypoparathyroidism. In particular, Asari et al have shown that a iPTH level of ≤ 15 pg/mL, or postoperative serum calcium level of ≤ 1.9 mmol/L (≤ 7.6 mg/dL), on postoperative day 2, increased the risk of postoperative hypoparathyroidism²¹³; Gao L et al. have demonstrated that iPTH levels < 7 ng/L on the first day after surgery, might be associated with persistent hypoparathyroidism.²¹⁴

2.4 Management of Postoperative hypocalcemia

In hypoparathyroidism, symptomatic hypocalcemia (carpal or pedal spasm, seizures, broncho- or laryngospasm) can be a medical emergency requiring acute intravenous administration of calcium. Although the actual value of the corrected serum calcium level is often regarded as a threshold for acute management (ie, 1.9 mmol/L [7.5 mg/dL]),^{215,216,217} symptoms generally dictate the decision to administer acute therapy. Intravenous calcium gluconate should be used. Calcium chloride should be avoided because it is irritating and potentially sclerosing to veins.²¹⁸

According to the diagnostic, therapeutic and healthcare management protocols in thyroid surgery approved by the I Consensus Conference proposed by the Italian Association of Endocrine Surgery Units the symptomatic hypocalcaemia should be treated with calcium gluconate (2 vials in Saline 250 cc. 2 or 3 times a day e.v) and oral calcium carbonate (2-3 g) in divided doses + calcitriol 0.50-1.5 mcg. According to the same Consensus Conference the treatment of chemical hypocalcemia (≤ 8 mg/dl) is oral calcium carbonate (2-3 gr) in divided doses and calcitriol 0.50-1.5 mcg to continue after discharge day independent of clinical symptoms.²¹⁹

2.5 Teriparatide for the prevention of post-surgical hypocalcemia: thypos trial

Teriparatide (PTH 1-34) is a synthetic human recombinant form of parathyroid hormone. It is an effective anabolic agent²²⁰ and, in 2002, it was approved as a treatment for severe osteoporosis.²²¹ PTH 1-34 has been successfully tested in permanent chronic hypoparathyroidism. In particular, Winer et al have demonstrated that the administration of once-daily PTH(1-34) can restore normocalcemia for 12 hours,²²² whereas twice-daily administrations or pump infusion is able to reduce the required total daily dose of calcium and bone turnover markers with restoring normocalcemia in a pediatric population.^{223,224} Recently, it has been also clearly demonstrated that replacement therapy using twice-daily 20-mcg subcutaneous injection of PTH(1-34) was able to maintain serum calcium and phosphate levels and to improve quality of life in adults subjects with post-surgical hypoparathyroidism, with no serious side effects.²²⁵

A very recent pilot study has also shown that teriparatide therapy, in patients with post-thyroidectomy hypoparathyroidism, can both control symptomatic hypocalcemia and reduced the duration of hospitalization. The authors have shown that teriparatide was safe, rapidly eliminated hypocalcemic symptoms, and likely reduced the duration of hospitalization.²²⁶

Up to now, no data are available on the effect of teriparatide as a primary prevention for post-surgical hypocalcemia. In this setting was born the study reported below. The aim of this Prospective Phase II Randomized Open Label Trial was to evaluate whether teriparatide can prevent post-surgical hypocalcemia in high risk subjects after thyroid surgery. We also investigated the effect of teriparatide on the duration of hospitalization.

2.5.1 Materials and methods

This is a Monocentric Prospective Phase II Randomized Open Label Trial (Teriparatide for **HY**popalcemia in **PO**st-surgical Subjects: Thypos Trial). All investigations were conducted in accordance with the Declaration of Helsinki. The study was approved by our local Ethical Committee and all the patients signed an

informed consent statement allowing their anonymized information to be used for data analysis. Patient's records were anonymized and de-identified prior to analysis. ISRCTN registry (reference number: ISRC TN74486450).

2.5.1.1 Screening

At Surgical ward, at University Campus Bio-Medico (Rome), preoperatively, all patients with formal surgical indication for thyroidectomy (thyroid cancer or Grave's disease or multinodular goiter) were screened for the study. During the screening visit, we have evaluated patients' baseline status and clinical history. Physical examination was performed and height and body weight (body mass index kg/m²), were recorded. At 8.00 AM, in a fasting state, a blood sample was drawn and calcium, phosphate, albumin, magnesium, iPTH, 25 OH vitamin D, kidney and liver function were measured.

Exclusion criteria were:

- Age younger than 18 years
- Pregnancy
- Renal failure (glomerular filtration rate < 30 mL/min)
- Hypersensitivity to the active substance or excipients
- Any prior parathyroid pathology
- Preexisting hypercalcemia
- Metabolic bone disease other than osteoporosis
- Ongoing therapy for osteoporosis
- Administration of calcitonin, systemic corticosteroids, estrogens, raloxifene, fluoride, lithium, loop or thiazide diuretics, aromatase inhibitors or other drugs that could interfere with calcium metabolism in the last 12 months

- History of skeletal malignancies (primary or metastatic)
- Active or recent urolithiasis
- Unexplained elevation of serum alkaline phosphatase levels
- Prior radiation therapy involving the skeleton
- Serum magnesium levels below the lower limits or above the upper limits of normal

All the screened patients (seventy-two subjects) underwent total thyroidectomy. All surgical procedures were performed by two experienced endocrine surgeons working at the Neck and Chest Surgery department, University Campus Bio-Medico (Rome). Total thyroidectomy was defined as total bilateral extracapsular thyroidectomy. Operative time was registered and surgical procedures lasted from 70 to 90 minutes. iPTH was measured at 4 hours after the end of the surgical procedure. Every surgical procedure was performed between 8.00 AM and 10.00 AM.

2.5.1.2 Patient enrollment

Twenty-six subjects with iPTH levels at 4 hours after thyroidectomy ≤ 10 pg/ml were enrolled in the present study and they were randomized (1:1) to receive treatment with teriparatide (treatment group) or following the standard clinical care (“wait and see”). A blocked randomization scheme was generated by a software algorithm (“blockrand” package for R). A nurse was educated to the subcutaneous abdominal administration of 20 mcg of teriparatide using an injection pen (Forsteo® Eli Lilly Nederland B.V.). The first administration was done immediately after the randomization. Subsequent administrations were done every 12 hours until discharge. Therefore, subjects belonging to the treatment group received 4 subcutaneous administrations of teriparatide according to the mean duration of hospitalization after surgery (2 days).

At 8.00 AM on postoperative days 1 and 2, in a fasting state, a blood sample was drawn and calcium, phosphate, albumin, magnesium, were measured. iPTH was

measured by an immunochemiluminometric assay using the automatic analyzer Modular E170 (Roche Diagnostics, Indianapolis, Ind, USA). Normal serum iPTH levels ranged between 10 and 65 pg/ml. Serum calcium was measured by automated techniques. Serum calcium was adjusted for albumin by the following formula: $(0.8 [4.0 - \text{patient's albumin}] + \text{serum calcium})$.²²⁷ Serum phosphate, magnesium and creatinine were also measured by automated techniques.

A clinical evaluation and ECG were performed in order to exclude signs or symptoms of hypocalcemia. In the presence of any sign or symptom of hypocalcemia, a new blood sample was drawn in order to confirm the hypocalcemic state. Hypocalcemia was defined as a serum calcium concentration <8.0 mg/dL in at least one measurement. The presence and type of symptoms of hypocalcemia was registered by a surgeon or by a nurse, together with the evaluation of Chvostek and Trousseau's signs, twice a day, from the day of surgery to hospital discharge. Hypocalcemic patients received supplementation therapy, even if asymptomatic. Supplementation therapy included 1g every 12 hours of oral calcium (Metocal 1250 mg tablets, Artropharm A.P.S.; 1 tablet contains 500 mg of elemental calcium) and 0.25 mcg every 12 hours of 1,25(OH)vitamin D (calcitriol [Rocaltrol] 0.25 mcg tablets; Roche SpA, Milan, Italy). If symptoms persisted following oral therapy or in the presence of electrocardiographic abnormalities or calcium concentration <7 mg/dL, intravenous calcium gluconate was administered. Supplementation therapy was adjusted on the basis of serum calcium measurements. If a patient belonging the treatment group developed hypocalcemia, teriparatide was stopped and calcium and vitamin D supplementation therapy was started.

At the discharge, all the subjects were prescribed 2 g per day of oral calcium together with 0.5 mcg per day of 1,25(OH)vitamin D. In order to balance the treatment with calcium and vitamin D after the discharge, measurement of blood calcium, phosphate and albumin was scheduled every week for 1 month, for each subject. In particular, if serum adjusted calcium remained stable above the 8.0 mg/dL without any symptoms, calcium supplement was reduced by 1000 mg decrements until the potential withdrawal was reached. If calcium supplementation

was stopped, calcitriol was reduced by 0.25 mcg (weekly) decrements until the potential withdrawal was reached maintaining stable serum calcium.

2.5.1.3 Sample size calculation and statistical analysis

Previous studies have shown that measurement of iPTH levels < 10 pg/ml at 4 hours after thyroidectomy has a positive predictive value of 90%²⁰⁹, sensitivity 94% and specificity 100% with an overall accuracy of 98% in predicting hypocalcemia.²⁰⁷ Estimating an incidence of hypocalcemia of 90% in the control group and a 30% incidence of hypocalcemia in the group treated with teriparatide, a sample size needed to achieve 80% statistical power at two side significance level of 0.05 is of 11 subjects per each group.

The two groups were compared using descriptive statistics, differences were evaluated using the t-test for independent groups or the chi-square test, as appropriate. The variation of serum calcium concentration over time in the two groups was analyzed using ANOVA for repeated measures including a time group interaction. The risk of developing hypocalcemia in the treatment group compared to the control group was estimated by calculating the relative risk with 95% confidence intervals. Finally, longitudinal changes in serum calcium concentration and dose of calcium and vitamin D supplementation were evaluated using ANOVA for repeated measures.

2.5.2 Results: prospective phase II randomized open label trial

Twenty-six subjects were recruited for this study (6 males, 20 females, mean age 53.4, SD 17.0). Baseline patient characteristics for both groups are summarized in Table 1. No differences among the factors known to negatively affect calcium balance after thyroidectomy were found between the two groups (Table 1).

	CONTROL GROUP (n=13)	TREATMENT GROUP (n=13)	P-value
M (%)	25	18	1
Age (yrs)	51.1 (19.7)	55.9 (13.8)	0.506
BMI (Kg/m²)	26.1 (4.1)	25 (4.5)	0.529
Adjusted serum calcium (mg/dl)	9.1 (0.3)	9.1 (0.4)	0.925
Serum Phosphate (mg/dl)	3.4 (0.5)	3.2 (0.7)	0.457
Basal iPTH (pg/ml)	57.9 (20.4)	61.1 (24)	0.74
25 (OH)Vitamin D (ng/ml)	22.9 (7)	24.3 (5.9)	0.596
Serum creatinine (mg/dl)	0.7 (0.2)	0.7 (0.1)	0.953
Magnesium (mg/dl)	1.9 (0.3)	1.9 (0.2)	0.847
PTH at 4 hours (pg/ml)	6 (3.7)	6.5 (3.1)	0.701

Table 1: baseline patient characteristics

Biochemical and clinical evaluation

Overall, the incidence of hypocalcemia was 3/13 in treatment group and 11/13 in the control group (P = 0.006) (Figure 1). At day one, we observed one hypocalcemic event in the treatment group and two events in control group. The relative risk for hypocalcemia in the treatment group compared to the control group was 0.26 (95% CI: 0.09 -- 0.723).

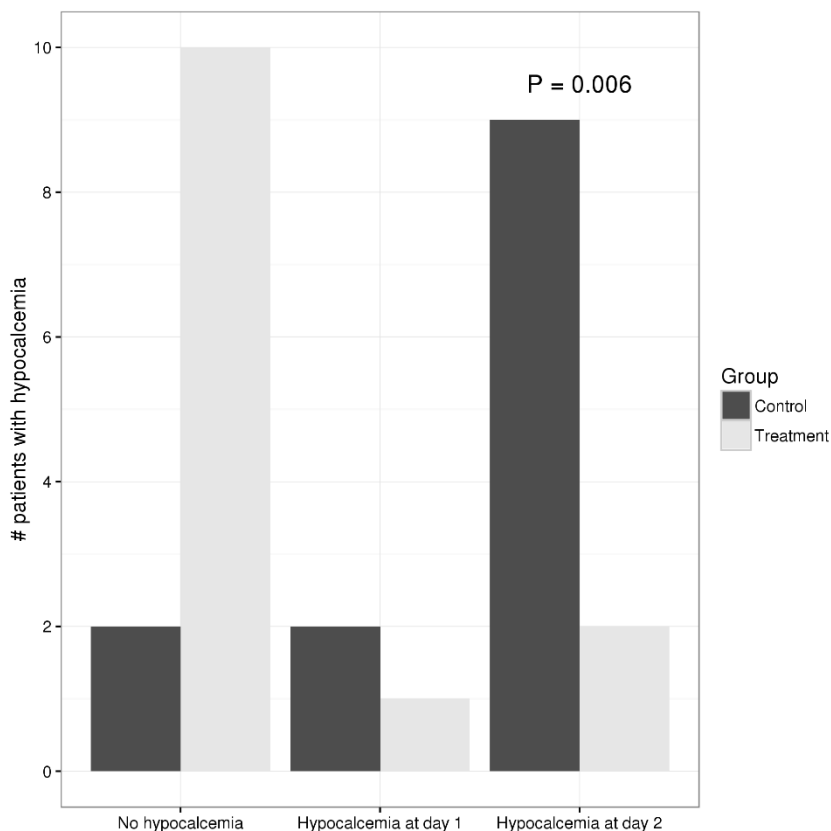


Figure 1: Biochemical and clinical evaluation at day 1 and day 2.

In the treatment group, mean serum adjusted calcium concentration on post-operative days 1 and 2 were 8.8 mg/dl and 8.3 mg/dl, respectively. The corresponding figures in the control group were 8.2 mg/dl ($P = 0.006$ vs. treatment group) and 7.6 mg/dl ($P = 0.001$ vs. treatment group) (ANOVA for repeated measures $P = 0.006$) (Figure 2).

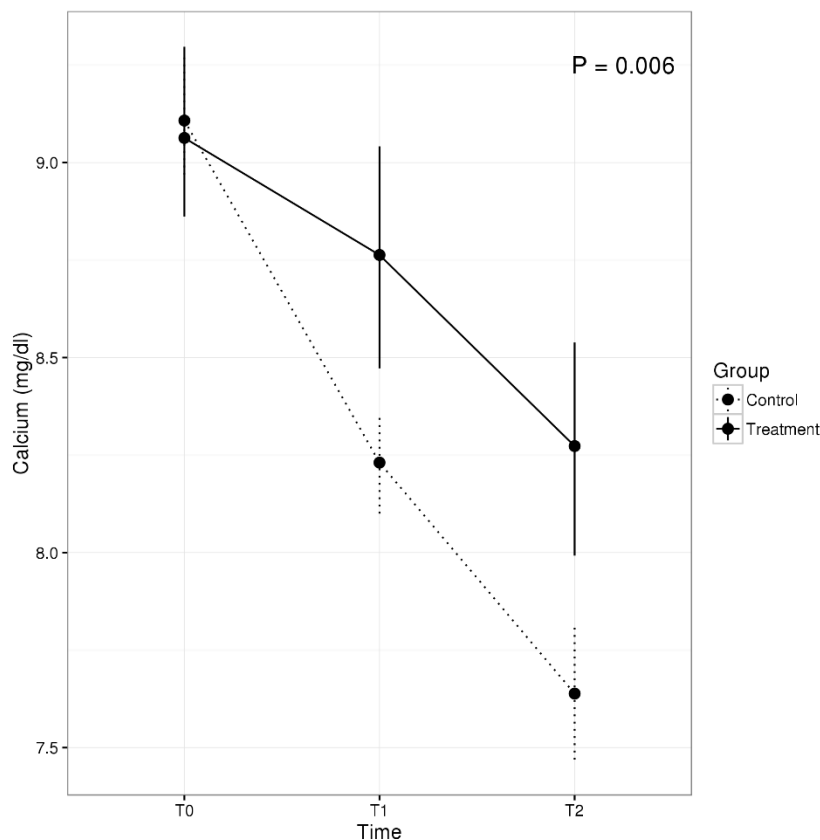


Figure 2: Mean serum adjusted calcium concentration on post-operative days 1 and 2 for control and treatment group.

Two out of three hypocalcemic subjects belonging to the treatment group experienced minor signs or symptoms of hypocalcemia such as perioral tingling with positive Chvostek's sign that disappeared after calcium/vitamin D administration.

In the control group, all the subjects with hypocalcemia (11/13) experienced minor symptoms such as perioral tingling with positive Chvostek's sign. In only 3 subjects, Trousseau's sign and carpopedal spasms were both positive. Oral calcium and calcitriol administration led to full resolution of symptoms. No subject required intravenous calcium administration.

The median duration of hospitalization was 3 days (IQR: 1) in control subjects and 2 days (IQR: 0) in treated subjects ($P = 0.012$). At hospital discharge, patients treated with teriparatide had a median calcium level of 8.5 mg/dL (SD: 0.5) while control subjects had a median calcium level of 7.8 mg/dL (SD: 0.4) ($P < 0.001$).

Safety data

No serious adverse events occurred during the study period. Only 2 subjects experienced nausea. According to the study protocol, 3 subjects discontinued teriparatide treatment due to hypocalcemia onset. No other adverse events requiring discontinuation of teriparatide treatment were observed.

2.5.3 Conclusion

We have demonstrated that teriparatide may prevent the onset of post-surgical hypocalcemia in subjects with high risk of hypocalcemia after thyroidectomy.

It has been estimated that hypocalcemia may occur in approximately 15% and 85% of hospitalized and critically ill patients, respectively.²²⁸ In particular, in postoperative subjects, reduced oral intake, nutritional compromise, and hemodilution due to infusion of intravenous fluids could explain transient hypocalcemia, which is often asymptomatic and mild.²²⁹ Instead, subjects who undergo neck surgery such as thyroidectomy can experience severe hypocalcemia due to the devascularization of parathyroid tissue and/or inadvertent gland removal.²³⁰

It has been well established that the most common form of transient or permanent hypoparathyroidism is post-surgical. Moreover, neck exploration for thyroid cancer, Graves' disease, large multinodular goiter, together with poor surgeon's experience, vitamin D deficiency, age and rate of PTH decline may represent important factors that will negatively affect the calcium and phosphate balance.²³¹

As shown in Table 1, our study population was homogeneous relative to the potential risk factors for hypocalcemia: in fact, at baseline, the above-mentioned parameters did not significantly differ between treatment and control groups. In particular plasma vitamin D was similar in the two groups thus avoiding the risk of a pre- and post-surgical different stimulation of PTH secretion. This hypothesis is confirmed by iPTH level at 4 hours after thyroidectomy, that did not show any significant difference between the two groups, but as far as all the subjects enrolled

in our study had blood vitamin D levels lower than normal, the doubt of an altered calcium balance may still arise. As a matter of fact, low vitamin D represents a deficient substrate that, in turn, may reduce the conversion of vitamin D into calcitriol even under the effect of supplemental exogenous PTH. Although a recent paper by Raffaelli et al have clearly shown that vitamin D deficiency is not a risk factor for post-surgical hypocalcemia²³² we cannot exclude that the achievement of normal pre-surgical plasma values of vitamin D could have changed the rates of hypocalcemia onset in both groups. On the other hand we must observe that teriparatide-treated patients showed higher values of post-surgical plasma calcium than controls thus suggesting that exogenous PTH may enhance 25(OH) vitamin D conversion into calcitriol even in a condition of vitamin D deficiency. Moreover, PTH may have increased plasma calcium independently of calcitriol by directly acting on distal tubular reabsorption of calcium and maybe on bone resorption.

Before January 2015, the only therapies that had been approved by the US Food and Drug Administration (FDA) for hypoparathyroidism (from any cause) were calcium and magnesium supplements variably associated with an active forms of vitamin D (calcitriol). In the last 15 years, several authors have described the ability of PTH(1-34)²³³ and PTH(1-84)^{234,235} to restore and maintain normocalcemia together with improving the quality of life²³⁶ in subjects with chronic hypoparathyroidism. These evidence have led to the FDA approval for the use of recombinant PTH (1-84) in hypoparathyroidism. Although there are authors that have investigate the safety and efficacy of PTH treatment for the management of chronic hypoparathyroidism, poor and low quality data are available for the therapy of acute hypocalcemia. Severe hypocalcemia may lead to cardiac arrhythmias and tetany with an increase of morbidity rate and duration of hospitalization. Raffaelli et al have demonstrated that the most important determinant of acute hypocalcemia is a post-surgical iPTH decline higher than 50% with respect to baseline values 20. Therefore, early PTH administration after neck surgery appears to be an etiological approach to acute post-surgical hypocalcemia. Recently, Shah et al have shown in a small open label trial that teriparatide administration to hypocalcemic hospitalized patients following thyroidectomy is safe and it can rapidly eliminate symptoms linked to low calcium levels; furthermore, this treatment has been associated with

reduced duration of hospitalization (Shah). Our results allow going further in the treatment of post-surgical hypocalcemia. In fact in our study teriparatide was administered if iPTH went under 10 pg/ml at 4 hours after surgery thus configuring an etiological therapy rather than a rescue treatment for acute hypocalcemia. Teriparatide allowed a good control of hypocalcemia in treated patients, while standard clinical care (“wait and see”) was not able to achieve a similar result in the control group. Moreover our patients had been taking teriparatide every 12 hours only for the duration of hospital staying (2-3 days), while patients in Shah’s study were on teriparatide for at least 1 week, with the option of continuing it for up to 3 weeks. While our data do not allow us to draw any definitive conclusion, it may be hypothesized that by rapidly counteracting iPTH post-surgical fall with teriparatide, the stress on parathyroid glands is lower as calcium homeostasis is exogenously maintained. Therefore, a less urgent “functioning request” can give enough time for a more physiological recovery to the sub-ischemic parathyroid gland. Whatever the case, the difference in therapeutic schedules between our study and Shah’s study represent an undeniable economic advantage as a shorter period of teriparatide administration leads to a significant reduction in the overall costs and particularly it may positively counterbalance the expenses for teriparatide purchase with a shorter hospital stay.

Finally, we were able to confirm that teriparatide treatment is safe and well tolerated. Two patients treated with teriparatide experienced minor symptoms of hypocalcemia such as perioral tingling and Chvostek’s sign compared to 11 out of 13 subjects in the control group. Moreover, in control group severe symptoms and signs of hypocalcemia such as Trousseau’s sign and carpopedal spasms have been recorded.

This study has some important limitations. First of all, it is lacking of placebo controlled group. As far as symptoms, but not signs, of hypocalcemia may be emphasized by individual perception, the presence of a placebo group could have given a better definition of their entity. Secondly, we enrolled a small group of patients in this study and even though we reached the pre-calculated sample size it cannot be excluded that different results can be obtained from a larger population.

Third, we did not measure PTH at 30 days after discharge and, therefore, we do not have any data on parathyroid glands functional recovery even though the lower need of calcium supplements in teriparatide-treated patients seems to suggest an endogenous PTH production.

In summary, to our knowledge this is the first study that has evaluated that PTH (1-34) treatment may prevent hypocalcemia in subjects at high risk of post-surgical hypocalcemia. Teriparatide might be associated both with a reduction of hospitalization duration and with a lower need of calcium carbonate supplements after the discharge. Larger and more robust randomized placebo controlled trials are needed in order to confirm our findings.

ACKNOWLEDGEMENTS

I am grateful to Professor Paolo Pozzilli for the opportunity to perform this research project: only with this kind of mentor is possible to obtain these results; to Drs. Anna Crescenzi and Chiara Taffon for their assistance in sampling and review the first section; to Dr. Andrea Palermo for his help in project the second section.

REFERENCES

-
- 1 DeLellis RA, Lloyd RV, Heitz PU. Pathology and Genetics: Tumors of Endocrine Organs. WHO classification of Tumors. IARC Press, Lyon 2004.
 - 2 Shaha AR1, Loree TR, Shah JP. Prognostic factors and risk group analysis in follicular carcinoma of the thyroid. *Surgery*. 1995; 118: 1131-1136.
 - 3 Hapke MR, Dehner LP. The optically clear nucleus. A reliable sign of papillary carcinoma of the thyroid? *Am J Surg Pathol*. 1979; 3: 31-38.
 - 4 Scopa CD1, Melachrinou M, Saradopolou C, Merino MJ. The significance of the grooved nucleus in thyroid lesions. *Mod Pathol*. 1993; 6: 691-694.
 - 5 DeLellis RA, Lloyd RV, Heitz PU. Pathology and Genetics: Tumors of Endocrine Organs. WHO classification of Tumors. IARC Press, Lyon 2004.
 - 6 Tielens ET, Sherman SI, Hruban RH, Ladenson PW. Follicular variant of papillary thyroid carcinoma. A clinicopathologic study. *Cancer*. 1994; 73: 424-431.
 - 7 Liu J, Singh B, Tallini G, Carlson DL, Katabi N, Shaha A, et al. Follicular variant of papillary thyroid carcinoma: a clinicopathologic study of a problematic entity. *Cancer*. 2006; 107: 1255-1264.
 - 8 Sherman SI. Thyroid carcinoma. *Lancet*. 2003; 361: 501-511.
 - 9 Chan JK, Tsui MS, Tse CH. Diffuse sclerosing variant of papillary carcinoma of the thyroid: a histological and immunohistochemical study of three cases. *Histopathology*. 1987; 11: 191-201.
 - 10 Fukushima M, Ito Y, Hirokawa M, Akasu H, Shimizu K, Miyauchi A. Clinicopathologic characteristics and prognosis of diffuse sclerosing variant of papillary thyroid carcinoma in Japan: an 18-year experience at a single institution. *World J Surg* 2009; 33: 958-962.
 - 11 Nikiforov Y, Gnepp DR, Fagin JA. Thyroid lesions in children and adolescents after the Chernobyl disaster: implications for the study of radiation tumorigenesis. *J Clin Endocrinol Metab*. 1996; 81: 9-14.
 - 12 Nikiforov Y, Gnepp DR. Pediatric thyroid cancer after the Chernobyl disaster. Pathomorphologic study of 84 cases (1991-1992) from the Republic of Belarus. *Cancer* 1994; 74: 748-766.
 - 13 Collini P, Mattavelli F, Pellegrinelli A, Barisella M, Ferrari A, Massimino M. Papillary carcinoma of the thyroid gland of childhood and adolescence: Morphologic subtypes, biologic behavior and prognosis: a clinicopathologic study of 42 sporadic

cases treated at a single institution during a 30-year period. *Am J Surg Pathol* 2006; 30: 1420- 1426.

14 Nikiforov YE, Erickson LA, Nikiforova MN, Caudill CM, Lloyd RV. Solid variant of papillary thyroid carcinoma: incidence, clinical-pathologic characteristics, molecular analysis, and biologic behavior. *Am J Surg Pathol*. 2001; 25: 1478-1484.

15 Van Heerden JA, Hay ID, Goellner JR, Salomao D, Ebersold JR, Bergstralh EJ, et al. Follicular thyroid carcinoma with capsular invasion alone: a nonthreatening malignancy. *Surgery*. 1992; 112: 1130-1136

16 LiVolsi VA, Asa SL. The demise of follicular carcinoma of the thyroid gland. *Thyroid*. 1994; 4: 233-236.

17 Ito Y, Hirokawa M, Higashiyama T, Takamura Y, Miya A, Kobayashi K, et al. Prognosis and prognostic factors of follicular carcinoma in Japan: importance of postoperative pathological examination. *World J Surg*. 2007; 31: 1417-1424.

18 Lopez-Penabad L, Chiu AC, Hoff AO, Schultz P, Gaztambide S, Ordoñez NG, et al. Prognostic factors in patients with Hürthle cell neoplasms of the thyroid. *Cancer*. 2003; 97: 1186-1194.

19 Sugino K, Ito K, Mimura T, Kameyama K, Iwasaki H, Ito K. Hürthle cell tumor of the thyroid: analysis of 188 cases. *World J Surg*. 2001; 25: 1160-1163

20 Herrera MF, Hay ID, Wu PS, Goellner JR, Ryan JJ, Ebersold JR, et al. Hürthle cell (oxyphilic) papillary thyroid carcinoma: a variant with more aggressive biologic behavior. *World J Surg*. 1992; 16: 669-674

21 Stojadinovic A, Ghossein RA, Hoos A, Urist MJ, Spiro RH, Shah JP, et al. Hürthle cell carcinoma: a critical histopathologic appraisal. *J Clin Oncol*. 2001; 19: 2616-2625.

22 Are C, Shaha AR. Anaplastic thyroid carcinoma: biology, pathogenesis, prognostic factors, and treatment approaches. *Ann Surg Oncol*. 2006; 13: 453-464.

23 Untch BR, Olson JA Jr. Anaplastic thyroid carcinoma, thyroid lymphoma, and metastasis to thyroid. *Surg Oncol Clin N Am*. 2006; 15: 661-679, x.

24 Kebebew E, Greenspan FS, Clark OH, Woeber KA, McMillan A. Anaplastic thyroid carcinoma. Treatment outcome and prognostic factors. *Cancer*. 2005; 103: 1330-1335

25 Sugitani I, Hasegawa Y, Sugasawa M, Tori M, Higashiyama T, Miyazaki M, et al. Super-radical surgery for anaplastic thyroid carcinoma: a large cohort study using the Anaplastic Thyroid Carcinoma Research Consortium of Japan database. *Head Neck*. 2014; 36: 328-333

26 Gaffey MJ, Lack EE, Christ ML, Weiss LM. Anaplastic thyroid carcinoma with osteoclast-like giant cells. A clinicopathologic, immunohistochemical, and ultrastructural study. *Am J Surg Pathol* 1991; 15:160-168.

27 Giuffrida D, Gharib H. Current diagnosis and management of medullary thyroid carcinoma. *Ann Oncol.* 1998; 9: 695-701.

28 Elisei R, Cosci B, Romei C, Bottici V, Renzini G, Molinaro E, et al. Prognostic significance of somatic RET oncogene mutations in sporadic medullary thyroid cancer: a 10-year follow-up study. *J Clin Endocrinol Metab.* 2008; 93: 682-687.

29 Etit D, Faquin WC, Gaz R, Randolph G, DeLellis RA, Pilch BZ. Histopathologic and clinical features of medullary microcarcinoma and C-cell hyperplasia in prophylactic thyroidectomies for medullary carcinoma: a study of 42 cases. *Arch Pathol Lab Med* 2008; 132: 1767- 1773.

30 NCCN Clinical Practice Guidelines in Oncology (NCCN Guidelines). Version 2.2015, NCCN.org

31 Siegel RL, Miller KD, Jemal A. Cancer statistics, 2016. *CA Cancer J Clin.* 2016 Jan;66(1):7-30. doi: 10.3322/caac.21332. Epub 2016 Jan 7.

32 Davies L, Welch HG 2014 Current thyroid cancer trends in the United States. *JAMA Otolaryngol Head Neck Surg* 140:317–322.

33 Howlader N, Noone AM, Krapcho M (eds) et al. SEER Cancer Statistics Review, 1975–2008. Bethesda, MD: National Cancer Institute 2011 http://seer.cancer.gov/csr/1975_2008/ based on November 2010 SEER data submission, posted to the SEER web site.

34 Leenhardt L, Bernier MO, Boin-Pineau MH, Conte DB, Mare´chaud R, Niccoli-Sire P, Nocaudie M, Orgiazzi J, Schlumberger M, We´meau JL, Cherie-Challine L, De Vathaire F 2004 Advances in diagnostic practices affect thyroid cancer incidence in France. *Eur J Endocrinol* 150:133–139

35 Brito JP, Al Nofal A, Montori V, Hay ID, Morris JC III 2015 The impact of subclinical disease and mechanism of detection on the rise in thyroid cancer incidence: a population-based study in Olmsted County, Minnesota during 1935 through 2012. *Thyroid* 25:999–1007.

36 O’Grady TJ, Gates MA, Boscoe FP. Thyroid cancer incidence attributable to overdiagnosis in the United States 1981-2011. *Int J Cancer.* 2015;137:2664-2673.

37 Leenhardt L, Bernier MO, Boin-Pineau MH et al. Advances in diagnostic practices affect thyroid cancer incidence in France. *Eur J Endocrinol* 2004; 150: 133–139.

38 Aschebrook-Kilfoy B, Grogan RH, Ward MH, Kaplan E, Devesa SS. Follicular thyroid cancer incidence patterns in the United States, 1980-2009. *Thyroid.* 2013;23:1015- 1021.

39 Schmid D, Ricci C, Behrens G, Leitzmann MF. Adiposity and risk of thyroid cancer: a systematic review and meta-analysis [published online ahead of print September 14, 2015]. *Obes Rev*. doi: 10.1111/obr.12321.

38 Aschebrook-Kilfoy B, Ward MH, Sabra MM et al. Thyroid cancer incidence patterns in the United States by histologic type, 1992–2006. *Thyroid* 2011; 21:125–134.

40 Chen AY, Jemal A, Ward EM. Increasing incidence of differentiated thyroid cancer in the United States, 1988–2005. *Cancer* 2009; 115: 3801–3807.

41 Tronko MD, Bogdanova TI, Komissarenko IV et al. Thyroid carcinoma in children and adolescents in Ukraine after the Chernobyl nuclear accident: statistical data and clinicomorphologic characteristics. *Cancer* 1999; 86: 149–156.

42 Jung CK, Little MP, Lubin JH, Brenner AV, Wells SA Jr, Sigurdson AJ, Nikiforov YE. The increase in thyroid cancer incidence during the last four decades is accompanied by a high frequency of BRAF mutations and a sharp increase in RAS mutations. *J Clin Endocrinol Metab*. 2013jc20132503.

43 Frich L, Glatte E, Akslen LA. Familial occurrence of nonmedullary thyroid cancer: a population based study of 5673 first-degree relatives of thyroid cancer patients from Norway. *Cancer Epidemiol Biomarkers Prev*. 2001; 10:113–117. [PubMed: 11219767]

44 Hemminki K, Eng C, Chen B. Familial risks for nonmedullary thyroid cancer. *J Clin Endocrinol Metab*. 2005; 90:5747–5753. [PubMed: 16030170]

45 Mazeh H, Sippel RS. Familial nonmedullary thyroid carcinoma. *Thyroid*. 2013; 23:1049–1056. [PubMed: 23734600]

46 Bignell GR, Canzian F, Shayeghi M, Stark M, Shugart YY, Biggs P, Mangion J, Hamoudi R, Rosenblatt J, Buu P, et al. Familial nontoxic multinodular thyroid goiter locus maps to chromosome 14q but does not account for familial nonmedullary thyroid cancer. *Am J Hum Genet*. 1997; 61:1123–1130. [PubMed: 9345104]

47 Canzian F, Amati P, Harach HR, Kraimps JL, Lesueur F, Barbier J, Levillain P, Romeo G, Bonneau D. A gene predisposing to familial thyroid tumors with cell oxyphilia maps to chromosome 19p13.2. *Am J Hum Genet*. 1998; 63:1743–1748. [PubMed: 9837827]

48 Malchoff CD, Sarfarazi M, Tendler B, Forouhar F, Whalen G, Joshi V, Arnold A, Malchoff DM. Papillary thyroid carcinoma associated with papillary renal neoplasia: genetic linkage analysis of a distinct heritable tumor syndrome. *J Clin Endocrinol Metab*. 2000; 85:1758–1764.[PubMed: 10843148]

49 McKay JD, Lesueur F, Jonard L, Pastore A, Williamson J, Hoffman L, Burgess J, Duffield A, Papotti M, Stark M, et al. Localization of a susceptibility gene for familial nonmedullary thyroid carcinoma to chromosome 2q21. *Am J Hum Genet.* 2001; 69:440–446. [PubMed: 11438887]

50 Cavaco BM, Batista PF, Martins C, Banito A, do Rosario F, Limbert E, Sobrinho LG, Leite V. Familial non-medullary thyroid carcinoma (FNMTC): analysis of fPTC/PRN, NMTC1, MNG1 and TCO susceptibility loci and identification of somatic BRAF and RAS mutations. *Endocr Relat Cancer.* 2008; 15:207–215. [PubMed: 18310288]

51 He H, Nagy R, Liyanarachchi S, Jiao H, Li W, Suster S, Kere J, de la Chapelle A. A susceptibility locus for papillary thyroid carcinoma on chromosome 8q24. *Cancer Res.* 2009; 69:625–631. [PubMed: 19147577]

52 Tomaz RA, Sousa I, Silva JG, Santos C, Teixeira MR, Leite V, Cavaco BM. FOXE1 polymorphisms are associated with familial and sporadic nonmedullary thyroid cancer susceptibility. *Clin Endocrinol (Oxf).* 2012; 77:926–933. [PubMed: 22882326]

53 Susan J. Hsiao and Yuri E. Nikiforov. Molecular Approaches to Thyroid Cancer Diagnosis. *Endocr Relat Cancer.* 2014 October ; 21(5): T301–T313. doi:10.1530/ERC-14-0166.

55 Aschebrook-Kilfoy B, Grogan RH, Ward MH, Kaplan E, Devesa SS. Follicular thyroid cancer incidence patterns in the United States, 1980-2009. *Thyroid.* 2013;23:1015- 1021.

56 Howlader N, Noone AM, Krapcho M (eds) et al. SEER Cancer Statistics Review, 1975–2008. Bethesda, MD: National Cancer Institute 2011 http://seer.cancer.gov/csr/1975_2008/ based on November 2010 SEER data submission, posted to the SEER web site.

57 Hundahl SA1, Fleming ID, Fremgen AM, Menck HR. A National Cancer Data Base report on 53,856 cases of thyroid carcinoma treated in the U.S., 1985-1995 [see comments]. *Cancer.* 1998 Dec 15;83(12):2638-48.

58 Dean DS, Gharib H. Epidemiology of Thyroid Nodules. *Best Pract Res Clin Endocrinol Metab* 2008; 22: 901–911

59 Vander JB, Gaston EA, Dawber TR 1968 The significance of nontoxic thyroid nodules. Final report of a 15- year study of the incidence of thyroid malignancy. *Ann Intern Med* 69:537–540.

60 Tunbridge WM, Evered DC, Hall R, Appleton D, Brewis M, Clark F, Evans JG, Young E, Bird T, Smith PA 1977 The spectrum of thyroid disease in a community: the Whickham survey. *Clin Endocrinol (Oxf)* 7:481–493.

61 Tan GH, Gharib H 1997 Thyroid incidentalomas: management approaches to nonpalpable nodules discovered incidentally on thyroid imaging. *Ann Intern Med* 126: 226–231.

62 Guth S, Theune U, Aberle J, Galach A, Bamberger CM 2009 Very high prevalence of thyroid nodules detected by high frequency (13 MHz) ultrasound examination. *Eur J Clin Invest* 39:699–706.

63 Hegedus L 2004 Clinical practice. The thyroid nodule. *N Engl J Med* 351:1764–1771.

64 Mandel SJ 2004A 64-year-old woman with a thyroid nodule. *JAMA* 292:2632–2642

65 Haugen BR, Alexander EK, Bible KC, Doherty GM, Mandel SJ, Nikiforov YE, Pacini F, Randolph GW, Sawka AM, Schlumberger M, Schuff KG, Sherman SI, Sosa JA, Steward DL, Tuttle RM, Wartofsky L. 2015 American Thyroid Association Management Guidelines for Adult Patients with Thyroid Nodules and Differentiated Thyroid Cancer: The American Thyroid Association Guidelines Task Force on Thyroid Nodules and Differentiated Thyroid Cancer. *Thyroid*. 2016 Jan;26(1):1-133. doi: 10.1089/thy.2015.0020.

66 Pacini F, Schlumberger M, Dralle H et al. European Thyroid Cancer Taskforce. European consensus for the management of patients with differentiated thyroid carcinoma of the follicular epithelium. *Eur J Endocrinol* 2006; 154: 787–80

67 American Thyroid Association (ATA) Guidelines Taskforce on Thyroid Nodules and Differentiated Thyroid Cancer. Cooper DS, Doherty GM, Haugen BR et al. Revised American Thyroid Association management guidelines for patients with thyroid nodules and differentiated thyroid cancer. *Thyroid* 2009; 19: 1167–1214.

68 Smith-Bindman R, Lebda P, Feldstein VA, Sellami D, Goldstein RB, Brasic N, Jin C, Kornak J 2013 Risk of thyroid cancer based on thyroid ultrasound imaging characteristics: results of a population-based study. *JAMA Intern Med* 173:1788–1796.

69 Brito JP, Gionfriddo MR, Al NA, Boehmer KR, Leppin AL, Reading C, Callstrom M, Elraiyah TA, Prokop LJ, Stan MN, Murad MH, Morris JC, Montori VM 2014 The accuracy of thyroid nodule ultrasound to predict thyroid cancer: systematic review and meta-analysis. *J Clin Endocrinol Metab* 99:1253–1263.

70 F. Pacini, M. G. Castagna, L. Brillì & G. Pentheroudakis, on behalf of the ESMO Guidelines Working Group. Thyroid cancer: ESMO Clinical Practice Guidelines for diagnosis, treatment and follow-up. *Annals of Oncology* 23 (Supplement 7): vii110–vii119, 2012.

71 Nikiforov YE, Steward DL, Robinson-Smith TM et al. Molecular testing for mutations in improving the fine-needle aspiration diagnosis of thyroid nodules. *J Clin Endocrinol Metab* 2009; 94: 2092–2098

72 Cantara S, Capezzone M, Marchisotta S et al. Impact of proto-oncogene mutation detection in cytological specimens from thyroid nodules improves the diagnostic accuracy of cytology. *J Clin Endocrinol Metab* 2010; 95: 1365–1369.

73 Kimura ET, Nikiforova MN, Zhu Z, Knauf JA, Nikiforov YE, Fagin JA. High prevalence of BRAF mutations in thyroid cancer: genetic evidence for constitutive activation of the RET/PTC-RASBRAF signaling pathway in papillary thyroid carcinoma. *Cancer Res.* 2003; 63:1454–1457. [PubMed: 12670889]

74 Soares P, Trovisco V, Rocha AS, Lima J, Castro P, Preto A, Maximo V, Botelho T, Seruca R, Sobrinho-Simoes M. BRAF mutations and RET/PTC rearrangements are alternative events in the etiopathogenesis of PTC. *Oncogene.* 2003; 22:4578–4580. [PubMed: 12881714]

75 Frattini M, Ferrario C, Bressan P, Balestra D, De Cecco L, Mondellini P, Bongarzone I, Collini P, Gariboldi M, Pilotti S, et al. Alternative mutations of BRAF, RET and NTRK1 are associated with similar but distinct gene expression patterns in papillary thyroid cancer. *Oncogene.* 2004; 23:7436–7440. [PubMed: 15273715]

76 Adeniran AJ, Zhu Z, Gandhi M, Steward DL, Fidler JP, Giordano TJ, Biddinger PW, Nikiforov YE. Correlation between genetic alterations and microscopic features, clinical manifestations, and prognostic characteristics of thyroid papillary carcinomas. *Am J Surg Pathol.* 2006; 30:216–222. [PubMed: 16434896]

77 Cohen Y, Xing M, Mambo E, Guo Z, Wu G, Trink B, Beller U, Westra WH, Ladenson PW, Sidransky D. BRAF mutation in papillary thyroid carcinoma. *J Natl Cancer Inst.* 2003; 95:625–627. [PubMed: 12697856]

78 Chiosea S, Nikiforova M, Zuo H, Ogilvie J, Gandhi M, Seethala RR, Otori NP, Nikiforov Y. A novel complex BRAF mutation detected in a solid variant of papillary thyroid carcinoma. *Endocr Pathol.* 2009; 20:122–126. [PubMed: 19370421]

79 Ciampi R, Nikiforov YE. Alterations of the BRAF gene in thyroid tumors. *Endocr Pathol.* 2005; 16:163–172. [PubMed: 16299399]

80 Lemoine NR, Mayall ES, Wyllie FS, Williams ED, Goyns M, Stringer B, Wynford-Thomas D. High frequency of ras oncogene activation in all stages of human thyroid tumorigenesis. *Oncogene.* 1989; 4:159–164. [PubMed: 2648253]

81 Namba H, Rubin SA, Fagin JA. Point mutations of ras oncogenes are an early event in thyroid tumorigenesis. *Mol Endocrinol.* 1990; 4:1474–1479. [PubMed: 2283998]

82 Suarez HG, du Villard JA, Severino M, Caillou B, Schlumberger M, Tubiana M, Parmentier C, Monier R. Presence of mutations in all three ras genes in human thyroid tumors. *Oncogene.* 1990; 5:565–570. [PubMed: 2183158]

83 Zhu Z, Gandhi M, Nikiforova MN, Fischer AH, Nikiforov YE. Molecular profile and clinicalpathologic features of the follicular variant of papillary thyroid carcinoma. An unusually high prevalence of ras mutations. *Am J Clin Pathol.* 2003; 120:71–77. [PubMed: 12866375]

84 Adeniran AJ, Zhu Z, Gandhi M, Steward DL, Fidler JP, Giordano TJ, Biddinger PW, Nikiforov YE. Correlation between genetic alterations and microscopic features, clinical manifestations, and prognostic characteristics of thyroid papillary carcinomas. *Am J Surg Pathol.* 2006; 30:216–222. [PubMed: 16434896]

85 Lemoine NR, Mayall ES, Wyllie FS, Williams ED, Goyns M, Stringer B, Wynford-Thomas D. High frequency of ras oncogene activation in all stages of human thyroid tumorigenesis. *Oncogene.* 1989; 4:159–164. [PubMed: 2648253]

86 Namba H, Rubin SA, Fagin JA. Point mutations of ras oncogenes are an early event in thyroid tumorigenesis. *Mol Endocrinol.* 1990; 4:1474–1479. [PubMed: 2283998]

87 Suarez HG, du Villard JA, Severino M, Caillou B, Schlumberger M, Tubiana M, Parmentier C, Monier R. Presence of mutations in all three ras genes in human thyroid tumors. *Oncogene.* 1990; 5:565–570. [PubMed: 2183158]

88 Motoi N, Sakamoto A, Yamochi T, Horiuchi H, Motoi T, Machinami R. Role of ras mutation in the progression of thyroid carcinoma of follicular epithelial origin. *Pathol Res Pract.* 2000; 196:1–7. [PubMed: 10674266]

89 Agrawal N, Jiao Y, Sausen M, Leary R, Bettegowda C, Roberts NJ, Bhan S, Ho AS, Khan Z, Bishop J, et al. Exomic sequencing of medullary thyroid cancer reveals dominant and mutually exclusive oncogenic mutations in RET and RAS. *J Clin Endocrinol Metab.* 2013; 98:E364–369. [PubMed: 23264394]

90 Grieco M, Santoro M, Berlingieri MT, Melillo RM, Donghi R, Bongarzone I, Pierotti MA, Della Porta G, Fusco A, Vecchio G. PTC is a novel rearranged form of the ret proto-oncogene and is frequently detected in vivo in human thyroid papillary carcinomas. *Cell.* 1990; 60:557–563.[PubMed: 2406025]

91 Santoro M, Dathan NA, Berlingieri MT, Bongarzone I, Paulin C, Grieco M, Pierotti MA, Vecchio G, Fusco A. Molecular characterization of RET/PTC3; a novel rearranged version of the RETprotooncogene in a human thyroid papillary carcinoma. *Oncogene.* 1994; 9:509–516. [PubMed: 8290261]

92 Jung CK, Little MP, Lubin JH, Brenner AV, Wells SA Jr, Sigurdson AJ, Nikiforov YE. The increase in thyroid cancer incidence during the last four decades is accompanied by a high frequency of BRAF mutations and a sharp increase in RAS mutations. *J Clin Endocrinol Metab.* 2013 jc20132503.

93 Rabes HM, Demidchik EP, Sidorow JD, Lengfelder E, Beimfohr C, Hoelzel D, Klugbauer S. Pattern of radiation-induced RET and NTRK1 rearrangements in 191 post-chernobyl papillary thyroid carcinomas: biological, phenotypic, and clinical implications. *Clin Cancer Res.* 2000; 6:1093–1103. [PubMed: 10741739]

94 Fenton CL, Lukes Y, Nicholson D, Dinauer CA, Francis GL, Tuttle RM. The ret/PTC mutations are common in sporadic papillary thyroid carcinoma of children and young adults. *J Clin Endocrinol Metab.* 2000; 85:1170–1175. [PubMed: 10720057]

95 de Groot JW, Links TP, Plukker JT, Lips CJ, Hofstra RM. RET as a diagnostic and therapeutic target in sporadic and hereditary endocrine tumors. *Endocr Rev.* 2006; 27:535–560. [PubMed: 16849421]

96 Kloos RT, Eng C, Evans DB, Francis GL, Gagel RF, Gharib H, Moley JF, Pacini F, Ringel MD, Schlumberger M, et al. Medullary thyroid cancer: management guidelines of the American Thyroid Association. *Thyroid.* 2009; 19:565–612. [PubMed: 19469690]

97 French CA, Alexander EK, Cibas ES, Nose V, Laguette J, Faquin W, Garber J, Moore F Jr, Fletcher JA, Larsen PR, et al. Genetic and biological subgroups of low-stage follicular thyroid cancer. *Am J Pathol.* 2003; 162:1053–1060. [PubMed: 12651598]

98 Dwight T, Thoppe SR, Foukakis T, Lui WO, Wallin G, Hoog A, Frisk T, Larsson C, Zedenius J. Involvement of the PAX8/peroxisome proliferator-activated receptor gamma rearrangement in follicular thyroid tumors. *J Clin Endocrinol Metab.* 2003; 88:4440–4445. [PubMed: 12970322]

99 Dahia PL, Marsh DJ, Zheng Z, Zedenius J, Komminoth P, Frisk T, Wallin G, Parsons R, Longy M, Larsson C, et al. Somatic deletions and mutations in the Cowden disease gene, PTEN, in sporadic thyroid tumors. *Cancer Res.* 1997; 57:4710–4713. [PubMed: 9354427]

100 Gustafson S, Zbuk KM, Scacheri C, Eng C. Cowden syndrome. *Semin Oncol.* 2007; 34:428–434. [PubMed: 17920899]

101 Garcia-Rostan G, Costa AM, Pereira-Castro I, Salvatore G, Hernandez R, Hermsem MJ, Herrero A, Fusco A, Cameselle-Teijeiro J, Santoro M. Mutation of the PIK3CA gene in anaplastic thyroid cancer. *Cancer Res.* 2005; 65:10199–10207. [PubMed: 16288007]

102 Ricarte-Filho JC, Ryder M, Chitale DA, Rivera M, Heguy A, Ladanyi M, Janakiraman M, Solit D, Knauf JA, Tuttle RM, et al. Mutational profile of advanced primary and metastatic radioactive iodine-refractory thyroid cancers reveals distinct pathogenetic roles for BRAF, PIK3CA, and AKT1. *Cancer Res.* 2009; 69:4885–4893. [PubMed: 19487299]

103 Garcia-Rostan G, Camp RL, Herrero A, Carcangiu ML, Rimm DL, Tallini G. Beta-catenin dysregulation in thyroid neoplasms: down-regulation, aberrant nuclear expression, and CTNNB1

exon 3 mutations are markers for aggressive tumor phenotypes and poor prognosis. *Am J Pathol.* 2001; 158:987–996. [PubMed: 11238046]

104 Ciampi R, Nikiforov YE. Alterations of the BRAF gene in thyroid tumors. *Endocr Pathol.* 2005; 16:163–172. [PubMed: 16299399]

105 Bongarzone I, Vigneri P, Mariani L, Collini P, Pilotti S, Pierotti MA. RET/NTRK1 rearrangements in thyroid gland tumors of the papillary carcinoma family: correlation with clinicopathological features. *Clin Cancer Res.* 1998; 4:223–228. [PubMed: 9516975]

106 Musholt TJ, Musholt PB, Khaladj N, Schulz D, Scheumann GF, Klempnauer J. Prognostic significance of RET and NTRK1 rearrangements in sporadic papillary thyroid carcinoma. *Surgery.* 2000; 128:984–993. [PubMed: 11114633]

107 Leeman-Neill RJ, Brenner AV, Little MP, Bogdanova TI, Hatch M, Zurnadzy LY, Mabuchi K, Tronko MD, Nikiforov YE. RET/PTC and PAX8/PPARgamma chromosomal rearrangements in post-Chernobyl thyroid cancer and their association with iodine-131 radiation dose and other characteristics. *Cancer.* 2013a; 119:1792–1799. [PubMed: 23436219]

108 Kelly LM, Barila G, Liu P, Evdokimova VN, Trivedi S, Panebianco F, Gandhi M, Carty SE, Hodak SP, Luo J, et al. Identification of the transforming STRN-ALK fusion as a potential therapeutic target in the aggressive forms of thyroid cancer. *PNAS.* 2014. Published online before print on February 3, 2014. doi: 2010.1073/pnas.1321937111.

109 Hanahan D, Weinberg RA. Hallmarks of cancer: the next generation. *Cell.* 2011; 144: 646-674.

110 Blasco MA. Telomeres and human disease: ageing, cancer and beyond. *Nat Rev Genet.* 2005; 6: 611-622.

111 Gonzales-Suarez E, Flores JM, Blasco MA. Cooperation between p53 mutation and high telomerase transgenic expression in spontaneous cancer development. *Mol Cell Biol.* 2002; 22: 7291-7301.

112 Shay JW, Bacchetti S. A survey of telomerase activity in human cancer. *Eur J Cancer.* 1997; 33:787– 791. [PubMed: 9282118]

113 Horn S, Figl A, Rachakonda PS, Fischer C, Sucker A, Gast A, Kadel S, Moll I, Nagore E, Hemminki K, et al. TERT promoter mutations in familial and sporadic melanoma. *Science.* 2013; 339:959– 961. [PubMed: 23348503]

114 Huang FW, Hodis E, Xu MJ, Kryukov GV, Chin L, Garraway LA. Highly recurrent TERT promoter mutations in human melanoma. *Science.* 2013; 339:957–959. [PubMed: 23348506]

115 Liu T, Wang N, Cao J, Sofiadis A, Dinets A, Zedenius J, Larsson C, Xu D. The age- and shorter telomere-dependent TERT promoter mutation in follicular thyroid cell-derived carcinomas. *Oncogene*. 2013

116 Liu X, Bishop J, Shan Y, Pai S, Liu D, Murugan AK, Sun H, El-Naggar AK, Xing M. Highly prevalent TERT promoter mutations in aggressive thyroid cancers. *Endocr Relat Cancer*. 2013b; 20:603–610. [PubMed: 23766237]

117 Melo M, Rocha AG, Vinagre J, Batista R, Peixoto J, Tavares C, Celestino R, Almeida A, Salgado C, Eloy C, et al. TERT promoter mutations are a major indicator of poor outcome in differentiated thyroid carcinomas. *J Clin Endocrinol Metab*. 2014 jc20133734.

118 Landa I, Ganly I, Chan TA, Mitsutake N, Matsuse M, Ibrahimasic T, Ghossein RA, Fagin JA. Frequent somatic TERT promoter mutations in thyroid cancer: higher prevalence in advanced forms of the disease. *J Clin Endocrinol Metab*. 2013; 98:E1562–1566. [PubMed: 23833040]

119 Montgomery E, Bronner MP, Goldblum JR, Greenson JK, HaberMM, Hart J, et al. Reproducibility of the diagnosis of dysplasia in Barrett esophagus: a reaffirmation. *Human Pathology* 2001;32:368—78.

120 Krafft C, Popp J. Raman4Clinics: the prospects of Raman-based methods for clinical application

121 Kallaway C, Max Almond L, Barr H, Wood J, Hutchings J, Kendall C, Stone N. Advances in the clinical application of Raman spectroscopy for cancer diagnostics. *Photodiagnosis and Photodynamic Therapy* (2013) 10, 207—219

122 Hanlon EB, Manoharan R, Koo T-W, Shafer KE, Motz JT, Fitzmaurice M, et al. Prospects for in vivo Raman spectroscopy. *Physics in Medicine and Biology* 2000;45. R1—R59.

123 Kendall C, Stone N, Shepherd N, Geboes K, Warren B, Ben-nett R, et al. Raman spectroscopy: elucidation of biochemical changes in carcinogenesis of oesophagus. *Journal of Pathology* 2003;200:602—9

124 Shetty G, Kendall C, Shepherd N, Stone N, Barr H. Raman spectroscopy: elucidation of biochemical changes in carcinogenesis of oesophagus. *British Journal of Cancer* 2006;94(10):1460—4. May 22.

125 Crow P, Molekowsky A, Stone N, Uff J, Wilson B, Wong KeeSong LM. Assessment of fiberoptic near-infrared Raman spectroscopy for diagnosis of bladder and prostate cancer. *Urology* 2005;65(June (6)):1126—30.

126 Stone N, Stavroulaki P, Kendall C, Birchall M, Barr H. Raman spectroscopy for early detection of laryngeal malignancy: preliminary results. *Laryngoscope* 2000;110(10 (Pt 1)):1756—63. October.

127 Bergholt MS, Zheng W, Huang Z. Development of a multiplexing fingerprint and high wavenumber Raman spectroscopy technique for real-time in vivo tissue Raman measurements at endoscopy. *J. Biomed. Opt.* 18(3), 030502–030502 (2013).

128 Karabeber H, Huang R, Iacono P et al. Guiding brain tumor resection using surface-enhanced Raman scattering nanoparticles and a hand-held Raman scanner. *ACS Nano* 8(10), 9755–9766 (2014).

129 Kong K, Zaabar F, Rakha E, Ellis I, Koloydenko A, Notingher I. Towards intra-operative diagnosis of tumours during breast conserving surgery by selective-sampling Raman micro-spectroscopy. *Phys. Med. Biol.* 59(20), 6141 (2014).

130 M. Jermyn, K. Mok, J. Mercier, J. Desroches, J. Pichette, K. Saint-Arnaud, L. Bernstein, M.-C. Guiot, K. Petrecca, F. Leblond, Intraoperative brain cancer detection with Raman spectroscopy in humans. *Sci. Transl. Med.* 7, 274ra19 (2015).

131 Barroso EM, Smits RWH, Bakker Schut T et al. Discrimination between oral cancer and healthy tissue based on water content determined by Raman spectroscopy. *Anal. Chem.* 87(4), 2419–2426 (2015).

132 Bergner N, Bocklitz T, Romeike BF et al. Identification of primary tumors of brain metastases by Raman imaging and support vector machines. *Chemometrics Intellig. Lab. Syst.* 117 224–232 (2012).

133 Baker R, Matousek P, Ronayne KL, Parker AW, Rogers K, Stone N. Depth profiling of calcifications in breast tissue using picosecond Kerr-gated Raman spectroscopy. *Analyst* 2007;132:48–53.

134 Stone N, Baker R, Rogers K, Parker AW, Matousek P. Future possibilities in the diagnosis of breast cancer by subsurface probing of calcifications with spatially offset Raman spectroscopy (SORS). *Analyst* 2007;132:899–905

135 Stone N, Matousek P. Advanced transmission raman spectroscopy: a promising tool for breast disease diagnosis. *Cancer Research* 2008;68:4424–30.

136 Wu L, Wang Z, Zong S et al. Simultaneous evaluation of p53 and p21 expression level for early cancer diagnosis using SERS technique. *Analyst* 138(12), 3450–3456 (2013).

137 Perumal J, Balasundaram G, Mahyuddin AP, Choolani M, Olivo M. SERS-based quantitative detection of ovarian cancer prognostic factor haptoglobin. *Int. J. Nanomed.* 10 1831 (2015).

138 Zhang J-Q, Wang Y-S, He Y et al. Determination of urinary adenosine using resonance light scattering of gold nanoparticles modified structure-switching aptamer. *Anal. Biochem.* 397(2), 212–217 (2010).

139 Kendall C, Day J, Hutchings J, Smith B, Shepherd N, Barr H, et al. Evaluation of Raman probe for oesophageal cancer diagnosis. *Analyst* 2010;135:30 38—41

140 Harris AT, Garg M, Yang XB, Fisher SE, Kirkham J, Smith DA, Martin-Hirsch DP and High AS. Raman spectroscopy and advanced mathematical modelling in the discrimination of human thyroid cell lines. *Head & Neck Oncology* 2009, 1:38

141 Teixeira CSB, Bitar RA, Martinho HS, Santos ABO, Kulcsar MAV, Friguglietti CUM, da Costa RB, Arisawa EAL and Martina AA. Thyroid tissue analysis through Raman spectroscopy
Analyst, 2009, 134, 2361–2370 | 2361.

142 L. J. Layfield, T. Wax and C. Jones, *Cancer Cytopathol.*, 2003, 99, 217–222.

143 P. Rout and S. Shariff, *Cytopathology*, 1999, 10, 171–179.

144 R. A. Bitar, H. S. Martinho, C. J. T. Criollo, L. N. Z. Ramalho, M. M. Netto and A. A. Martin, *J. Biomed. Opt.*, 2006, 11, 054001.

145 Edge SB, Byrd DR, Compton CC, Fritz AG, Greene FL, Trotti A, editors. *AJCC cancer staging manual* (7th ed). New York, NY: Springer; 2010.

146 Talari ACS, Movasaghi Z, Rehman S, urRehman I. Raman spectroscopy of biological tissues. *ApplSpectr Rev* 2015;50(1):46-111.

147 Li Z, Li C, Lin D, Huang Z, Pan J, Chen G, Lin J, Liu N, Yu Y, Feng S, Chen R. Surface-enhanced Raman spectroscopy for differentiation between benign and malignant thyroid tissues. *Laser Phys Lett* 2014;11:045602

148 Marshall CP, Leuko S, Coyle CM, Walter MR, Burns BP, Neilan BA. Carotenoid analysis of halophilic archaea by resonance Raman spectroscopy. *Astrobiology* 2007;7(4):631-43.

149 Jehlicka J, Edwards HG, Oren A. Bacterioruberin and salinixanthin carotenoids of extremely halophilic Archaea and Bacteria: a Raman spectroscopic study. *Spectrochim. Acta A Mol Biomol Spectrosc* 2013;106:99-103.

150 Macernis M, Galzerano D, Sulskus J, Kish E, Kim YH, Koo S, Valkunas L, Robert B. Resonance Raman Spectra of Carotenoid Molecules: Influence of Methyl Substitutions. *J Phys Chem A* 2015;119:56–66

151 Integrated genomic characterization of papillary thyroid carcinoma. The cancer genome atlas research network. *Cell* 2014;159:676–690

152 McClenahan P, Lin LL, Tan JM, Flewell-Smith R, Schaidler H, Jagirdar K, Atkinson V, Lambie D, Prow TW, Sturm RA, Soyer HP. BRAFV600E mutation status of involuting and stable nevi in dabrafenib therapy with or without trametinib. *JAMA Dermatol* 2014;150(10):1079-82.

153 Duraipandian S, Zheng W, Ng J, Low JJH, Ilancheran A, Huang Z. Simultaneous Fingerprint and High-Wavenumber Confocal Raman Spectroscopy Enhances Early Detection of Cervical Precancer In Vivo. *Anal Chem* 2012;84:5913–5919.

154 Puppels GJ, Garritsen HSP, Kummer JA, Greve J. Carotenoids located in human lymphocyte subpopulations and natural-killer-cells by Raman microspectroscopy. *Cytometry* 1993;14:251–256.

155 Mahadevan-Jansen A, Richards-Kortum R. Raman spectroscopy for cancer detection: a review. *Proceed 19th Intern Conf IEEE/EMBS Oct 30 – nov 2 1997 Chicago, IL USA*.

156 Macernis M, Galzerano D, Sulskus J, Kish E, Kim YH, Koo S, Valkunas L, Robert B. Resonance Raman Spectra of Carotenoid Molecules: Influence of Methyl Substitutions. *J Phys Chem A* 2015;119:56–66

157 Rimai L, Kilponen RG, Gill D. Excitation Profiles of Laser Raman Spectra in the Resonance Region of Two Carotenoid Pigments in Solution. *J Am Chem Soc* 1970;92:3824–3825.

158 Carotenoids. Volume 4: Natural Functions. Edited by Britton G, Liaaen-Jensen S, Pfander H. © 2008 Birkhäuser Verlag, P.O. Box 133, CH-4010 Basel, Switzerland. ISBN 3-7643-7498-3 Birkhäuser Verlag, Basel – Boston – Berlin, page 60

159 Andersson E, Vahlquist A, Rosdahl I. Beta-carotene uptake and bioconversion to retinol differ between human melanocytes and keratinocytes. *Nutr Cancer* 2001;39(2):300-306.

160 Chadwick D, Kinsman R, Walton P: The British Association of Endocrine & Thyroid Surgeons Fourth National Audit Report. Dendrite Clinical Systems Ltd, The Hub, Station Road, Henley-on-Thames, Oxfordshire RG9 1AY, United Kingdom. 2012.

161 Graev M, Panunzi CA: [Findings on one hundred cases of thyroid carcinoma; incidence, frequency of various histological types, prognosis on the basis of histology, survival]. *Arch De Vecchi Anat Patol*. 1957; 27(1): 31–63.

162 Zerey M, Prabhu AS, Newcomb WL, et al.: Short-term outcomes after unilateral versus complete thyroidectomy for malignancy: a national perspective. *Am Surg*. 2009; 75(1): 20–4.

163 Nixon IJ, Ganly I, Patel SG, et al.: Thyroid lobectomy for treatment of well differentiated intrathyroid malignancy. *Surgery*. 2012; 151(4): 571–9.

164 Zerey M, Prabhu AS, Newcomb WL, et al.: Short-term outcomes after unilateral versus complete thyroidectomy for malignancy: a national perspective. *Am Surg*. 2009; 75(1): 20–4.

165 Rosato L, Avenia N, Bernante P, et al.: Complications of thyroid surgery: analysis of a multicentric study on 14,934 patients operated on in Italy over 5 years. *World J Surg.* 2004; 28(3): 271–6.

166 Ezzat S, Sarti DA, Cain DR, et al.: Thyroid incidentalomas. Prevalence by palpation and ultrasonography. *Arch Intern Med.* 1994; 154(16): 1838–40.

167 Stack BC Jr, Ferris RL, Goldenberg D, et al.: American Thyroid Association consensus review and statement regarding the anatomy, terminology, and rationale for lateral neck dissection in differentiated thyroid cancer. *Thyroid.* 2012; 22(5): 501–8

168 American Thyroid Association (ATA) Guidelines Taskforce on Thyroid Nodules and Differentiated Thyroid Cancer, Cooper DS, Doherty GM, et al.: Revised American Thyroid Association management guidelines for patients with thyroid nodules and differentiated thyroid cancer. *Thyroid.* 2009; 19(11): 1167–214.

169 Stack BC Jr, Ferris RL, Goldenberg D, et al.: American Thyroid Association consensus review and statement regarding the anatomy, terminology, and rationale for lateral neck dissection in differentiated thyroid cancer. *Thyroid.* 2012; 22(5): 501–8

170 Hartl DM, Leboulleux S, Al Ghuzlan A, et al.: Optimization of staging of the neck with prophylactic central and lateral neck dissection for papillary thyroid carcinoma. *Ann Surg.* 2012; 255(4): 777–83.

171 Perros P, Boelaert K, Colley S, et al.: Guidelines for the management of thyroid cancer. *Clin Endocrinol (Oxf).* 2014; 81(Suppl 1): 1–122.

172 Clayman GL, Agarwal G, Edeiken BS, et al.: Long-term outcome of comprehensive central compartment dissection in patients with recurrent/ persistent papillary thyroid carcinoma. *Thyroid.* 2011; 21(12): 1309–16.

173 Kandil E, Krishnan B, Noureldine SI, Yao L, Tufano RP 2013 Hemithyroidectomy: a meta-analysis of postoperative need for hormone replacement and complications. *ORL J Otorhinolaryngol Relat Spec* 75:6–17.

174 Sosa JA, Bowman HM, Tielsch JM, Powe NR, Gordon TA, Udelsman R 1998 The importance of surgeon experience for clinical and economic outcomes from thyroidectomy. *Ann Surg* 228:320–330.

175 Loyo M, Tufano RP, Gourin CG 2013 National trends in thyroid surgery and the effect of volume on short-term outcomes. *Laryngoscope* 123:2056–2063.

176 Jeannon JP, Orabi AA, Bruch GA, Abdalsalam HA, Simo R. Diagnosis of recurrent laryngeal nerve palsy after thyroidectomy: a systematic review. *Int J Clin Pract.* 2009;63(4):624-629.

177 de Pedro Netto I, Fae A, Vartanian JG, et al. Voice and vocal selfassessment after thyroidectomy. *Head Neck.* 2006;28(12):1106- 1114.

178 Bergenfelz A, Jansson S, Kristoffersson A, et al. Complications to thyroid surgery: results as reported in a database from a multicenter audit comprising 3,660 patients. *Langenbecks Arch Surg.* 2008;393(5):667-673.

179 Scott-Coombes D. The British Association of Endocrine and Thyroid Surgeons—Third National Audit Report. Henley-on-Thames, UK: Dendrite Clinical Systems Ltd; 2009

180 Scott-Coombes D. The British Association of Endocrine and Thyroid Surgeons—Third National Audit Report. Henley-on-Thames, UK: Dendrite Clinical Systems Ltd; 2009

181 Hermann M, Alk G, Roka R, Glaser K, Freissmuth M 2002 Laryngeal recurrent nerve injury in surgery for benign thyroid diseases: effect of nerve dissection and impact of individual surgeon in more than 27,000 nerves at risk. *Ann Surg* 235:261–268

182 Kriskovich MD, Apfelbaum RI, Haller JR 2000 Vocal fold paralysis after anterior cervical spine surgery: incidence, mechanism, and prevention of injury. *Laryngoscope* 110:1467–1473.

183 Dralle H, Sekulla C, Haerting J, Timmermann W, Neumann HJ, Kruse E, Grond S, Muhligh HP, Richter C, Voss J, Thomusch O, Lippert H, Gastinger I, Brauckhoff M, Gimm O 2004 Risk factors of paralysis and functional outcome after recurrent laryngeal nerve monitoring in thyroid surgery. *Surgery* 136:1310–1322.

184 Randolph GW, Dralle H, Abdullah H, Barczynski M, Bellantone R, Brauckhoff M, Carnaille B, Cherenko S, Chiang FY, Dionigi G, Finck C, Hartl D, Kamani D, Lorenz K, Miccolli P, Mihai R, Miyauchi A, Orloff L, Perrier N, Poveda MD, Romanchishen A, Serpell J, Sitges-Serra A, Sloan T, Van SS, Snyder S, Takami H, Volpi E, Woodson G 2011 Electrophysiologic recurrent laryngeal nerve monitoring during thyroid and parathyroid surgery: international standards guideline statement. *Laryngoscope* 121(Suppl 1):S1–S16.

185 Pisanu A, Porceddu G, Podda M, Cois A, Uccheddu A 2014 Systematic review with meta-analysis of studies comparing intraoperative neuromonitoring of recurrent laryngeal nerves versus visualization alone during thyroidectomy. *J Surg Res* 188:152–161.

186 Sittel C, Stennert E, Thumfart WF, Dapunt U, Eckel HE. Prognostic value of laryngeal electromyography in vocal fold paralysis. *Arch Otolaryngol Head Neck Surg.* 2001;127(2):155-160.

187 Hassan-Smith ZK, Gopinath P, Mihaimed F. A UK-wide survey of life-threatening thyroidectomy complications. *J Thyroid Res.* 2011;2011:329620.

188 Rosato L, Carlevato MT, De Toma G, Avenia N. Recurrent laryngeal nerve damage and phonetic modifications after total thyroidectomy: surgical malpractice only or predictable sequence? *World J Surg.* 2005;29(6):780-784.

189 Musholt TJ, Musholt PB, Garm J, Napiontek U, Keilmann A. Changes of the speaking and singing voice after thyroid or parathyroid surgery. *Surgery.* 2006;140(6):978-988.

190 Page C, Zaatar R, Biet A, Strunski V. Subjective voice assessment after thyroid surgery: a prospective study of 395 patients. *Indian J Med Sci.* 2007;61(8):448-454.

191 Reeve T, Thompson NW. Complications of thyroid surgery: how to avoid them, how to manage them, and observations on their possible effect on the whole patient. *World J Surg.* 2000;24(8):971-975.

192 Pattou F, Combemale F, Fabre S, et al. Hypocalcemia following thyroid surgery: incidence and prediction of outcome. *World J Surg.* 1998;22(7):718-724.

193 . Shaha AR, Burnett C, Jaffe BM. Parathyroid autotransplantation during thyroid surgery. *J Surg Oncol.* 1991;46(1):21-24.

194 Randolph GW, Clark OH 2013 Principles in thyroid surgery. In: Randolph GW (ed) *Surgery of the Thyroid and Parathyroid Glands.* 2nd edition. Elsevier, Philadelphia, PA, pp 273–293.

195 Lorente-Poch L, Sancho JJ, Ruiz S, Sitges-Serra A 2015 Importance of in situ preservation of parathyroid glands during total thyroidectomy. *Br J Surg* 102:359–367.

196 Cusano, N. E. et al. PTH(1-84) is associated with improved quality of life in hypoparathyroidism through 5 years of therapy. *J. Clin. Endocrinol. Metab.* 99, 3694-3699 (2014).

197 Balasubramanian. Iatrogenic/post-surgical hypoparathyroidism: Where do we go from here? *Endocrine* 47, 357-359 (2014).

198 JP Bilezikian, A Khan, JT Potts Jr, ML Brandi, BL Clarke, D Shoback, H Juppner, P D Amour, J Fox, L Rejnmark, L Mosekilde, MR Rubin, D Dempster, R Gafni, M. & Collins. J Hypoparathyroidism in the Adult: Epidemiology, Diagnosis, Pathophysiology, Target Organ Involvement, Treatment, and Challenges for Future Research. *J Bone Min. Res* 26, 2317-2337 (2011).

199 See, A. C. & Soo, K. C. Hypocalcaemia following thyroidectomy for thyrotoxicosis. *Br J Surg* 84, 95-97 (1997).

200 Falk, S. A., Birken, E. A. & Baran, D. T. Temporary post-thyroidectomy hypocalcemia. *Arch. Otolaryngol. Head. Neck Surg.* 114, 168-174 (1988).

- 201 Percival RC, Hargreaves AW, K. J. The mechanism of hypocalcaemia following. *Acta endocrinol* 109, 220-6 (1985).
- 202 Edafe O, Antakia R, Laskar N, Uttley L, B. S. Systematic review and meta-analysis of predictors of post-thyroidectomy hypocalcaemia. *Br. J. Surg.* 101, 883 (2014).
- 203 Lorente-Poch, L., Sancho, J. J., Munoz-Nova, J. L., Sanchez-Velazquez, P. & Sitges-Serra, A. Defining the syndromes of parathyroid failure after total thyroidectomy. *Gland Surg.* 4, 82-90 (2015).
- 204 Baldassarre, R. L., Chang, D. C., Brumund, K. T. & Bouvet, M. Predictors of Hypocalcemia after Thyroidectomy: Results from the Nationwide Inpatient Sample. *ISRN Surg.* 2012, 1-7 (2012).
- 205 Morita H, Wu J, Z. D. The QT syndromes: long and short. *Lancet* 372, 750-63 (2008).
- 206 Shaha AR, J. B. Parathyroid preservation during thyroid surgery. *Am J Otolaryngol* 19, 113-7 (1998).
- 207 Lombardi CP1, Raffaelli M, Princi P, Santini S, Boscherini M, De Crea C, Traini E, D'Amore AM, Carrozza C, Zuppi C, B. R. Early prediction of postthyroidectomy hypocalcemia by one single iPTH measurement. *Surgery* 136, 1236-41 (2004).
- 208 Richards ML1, Bingener-Casey J, Pierce D, Strodel WE, S. K. Intraoperative parathyroid hormone assay: an accurate predictor of symptomatic hypocalcemia followingthyroidectomy. *Arch. Surg.* 138, 635-6 (2003).
- 209 Grodski S1, S. J. Evidence for the role of perioperative PTH measurement after total thyroidectomy as a predictor of hypocalcemia. *world J. surgery* 32, 1367-73 (2008).
- 210 Thomusch, O. et al. The impact of surgical technique on postoperative hypoparathyroidism in bilateral thyroid surgery: A multivariate analysis of 5846 consecutive patients. *Surgery* 133, 180-185 (2003).
- 211 Zarnegar, R., Brunaud, L. & Clark, O. H. Prevention, evaluation, and management of complications following thyroidectomy for thyroid carcinoma. *Endocrinol Metab Clin North Am* 32, 483-502 (2003).
- 212 Page, C. & Strunski, V. Parathyroid risk in total thyroidectomy for bilateral, benign, multinodular goitre: report of 351 surgical cases. *J. Laryngol. Otol.* 121, 237-41 (2007).

213 Reza Asari, MD; Christian Passler, MD; Klaus Kaczirek, MD; Christian Scheuba, MD; Bruno Niederle, M. & Hypoth. Hypoparathyroidism After Total Thyroidectomy. Arch. Surg. 143, 132-137 (2008).

214 Gao, L. Association between Decreased Serum Parathyroid Hormone after Total Thyroidectomy and Persistent Hypoparathyroidism. Med. Sci. Monit. 21, 1223-1231 (2015).

215 Shoback D. Hypoparathyroidism. N Engl J Med. 2008; 359:391-403. [PubMed: 18650515]

216 Reber PM, Heath H. Hypocalcemic emergencies. Med Clin North Am. 1995; 79:93-106. [PubMed: 7808098]

217 Tohme JF, Bilezikian JP. Hypocalcemic emergencies. Endocrinol Metab Clin North Am. 1993; 22:363-375. [PubMed: 8325292]

218 Murphy E, Williams GR. Hypocalcaemia. Medicine. 2009; 37:465-468.

219 Protocolli gestionali diagnosticoterapeutico- assistenziali in chirurgia tiroidea I Consensus Conference. Rosato L et Al. Chirurgia Italiana 2006 - vol. 58 n. 2 pp 141-150

220 Riek AE, T. DA. The pharmacological management of osteoporosis. Mo. Med. 108, 118-23 (2011).

221 Massachusetts, F. et al. Effect of Parathyroid Hormone (1-34) on Fractures and Bone Mineral Density in Postmenopausal Women With Osteoporosis. N. Engl. J. Med. 344, 1434- 1441 (2015).

222 Winer KK, Yanovski JA, C. G. J. Synthetic human parathyroid hormone 1-34 vs calcitriol and calcium in the treatment of hypoparathyroidism. JAMA 276, 631-6 (1996).

223 Winer, K. K. et al. Synthetic human parathyroid hormone 1-34 replacement therapy: a randomized crossover trial comparing pump versus injections in the treatment of chronic hypoparathyroidism. J. Clin. Endocrinol. Metab. 97, 391-9 (2012).

224 Winer KK, Fulton KA, Albert PS, C. G. J. Effects of pump versus twice-daily injection delivery of synthetic parathyroid hormone 1-34 in children with severe congenital hypoparathyroidism. J. pediatric 165, 556-63 (2014).

225 Winer, K. K., Yanovski, J. a, Sarani, B. & Cutler, G. B. A Randomized , Cross-Over Trial of Once-Daily Versus of Hypoparathyroidism. J. Clin. Endocrinol. Metab. 83, 3480-3486 (1998).

226 Shah M1, Bancos I1, Thompson GB2, Richards ML2, Kasperbauer JL3, Clarke BL1, Drake MT1, S. M. Teriparatide Therapy and Reduced Postoperative Hospitalization for Postsurgical Hypoparathyroidism. *JAMA Otolaryngol Head Neck Surg.* 1141, 822-7 (2015).

227 James MT, Zhang J, Lyon AW, Hemmelgarn BR. Derivation and internal validation of an equation for albumin-adjusted calcium. *BMC Clin Pathol.* 2008; 8:12

228 Hannan FM, Thakker R V. Investigating hypocalcaemia. *BMJ.* 2013; 346:f2213

229 Steele T, Kolamunnage-Dona R, Downey C, Toh C-H, Welters I. Assessment and clinical course of hypocalcemia in critical illness. *Crit Care.* 2013; 17:R106.

230 Schafer AL SD. Hypocalcemia: definition, etiology, pathogenesis, diagnosis and management. *Primer on the Metabolic Bone Diseases and Disorders of Mineral Metabolism.* 8th ed. Wiley-Blackwell. 2013: 572-580

231 Schafer AL SD. Hypocalcemia: definition, etiology, pathogenesis, diagnosis and management. *Primer on the Metabolic Bone Diseases and Disorders of Mineral Metabolism.* 8th ed. Wiley-Blackwell. 2013: 572-580

232 Raffaelli M, De Crea C, D'Amato G, Moscato U, Bellantone C, Carrozza C, Lombardi CP. Post thyroidectomy hypocalcemia is related to parathyroid dysfunction even in patients with normal parathyroid hormone concentrations early after surgery. *Surgery.* 2016; 159:78-84.

233 Santonati A, Palermo A, Maddaloni E, Bosco D, Spada A, Grimaldi F, Raggiunti B, Volpe R, Manfrini S, Vescini F, Hypoparathyroidism AME Group. PTH(1-34) for Surgical Hypoparathyroidism: A Prospective, Open-Label Investigation of Efficacy and Quality of Life. *J Clin Endocrinol Metab.* 2015; 100:3590-3597.

234 Mannstadt M, Clarke BL, Vokes T, Brandi ML, Ranganath L, Fraser WD, Lakatos P, Bajnok L, Garceau R, Mosekilde L, Lagast H, Shoback D, Bilezikian JP. Efficacy and safety of recombinant human parathyroid hormone (1-84) in hypoparathyroidism (REPLACE): a double-blind, placebo-controlled, randomised, phase 3 study. *Lancet Diabetes Endocrinol.* 2013; 1:275-283.

235 Rubin MR, Sliney J, McMahon DJ, Silverberg SJ, Bilezikian JP. Therapy of hypoparathyroidism with intact parathyroid hormone. *Osteoporos Int.* 2010; 21:1927-1934.

236 Cusano NE, Rubin MR, McMahon DJ, Irani D, Tulley A, Sliney J, Bilezikian JP. The effect of PTH(1-84) on quality of life in hypoparathyroidism. *J Clin Endocrinol Metab.* 2013; 98:2356-2361.